SCUOLA DI DOTTORATO
UNIVERSITÀ DEGLI STUDI DI MILANO-BICOCCA

Dipartimento di

SCIENZA DEI MATERIALI

Dottorato di Ricerca in SCIENZA E NANOTECNOLOGIA DEI MATERIALI

Ciclo XXXIII

PLASMA TECHNOLOGY APPLICATION ON TYRE REINFORCING MATERIALS

GAIFAMI CARLO MARIA

Matricola 721326

Tutor: PROFESSORESSA CLAUDIA RICCARDI

Supervisor: DOTTORESSA PAOLA CARACINO

Supervisor: DOTTORESSA BARBARA RAMPANA

Coordinatore: PROFESSOR MARCO BERNASCONI

ANNO ACCADEMICO 2019/2020

INDEX

CHAPTER 0

0-AIM

Plasma technology application on tyre reinforcing materials

This thesis is the result of three years of work carried out at the Università degli studi Milano-Bicocca and Pirelli Tyre, thanks to CORIMAV which permits a direct connection between these two institutions. The experiments were both performed at the university lab and at Pirelli, moreover some experiments on the adhesion were made at Sicrem, one of the most important textile suppliers of Pirelli. During the third year, I had the possibility to work at the Universidad Carlos III de Madrid where some studies on the effect of plasma treatments for the composite materials preparation were performed. The aim of the thesis is the application of plasma technology on tyre reinforcing materials. the project is focused on the investigation for an alternative method to guarantee the adhesion between textile reinforcements material and rubber. The need to find an alternative method is important because of the limitations that the actual chemical method will suffer from the future.

A plasma treatment on the textile reinforcing materials is proposed in the thesis, the treatment was performed on the textile material to improve the adhesion with the rubber matrix. One of the most important aspect about the composite materials is the good adhesion between the fiber and the matrix. A good adhesion is important for the integrity and the durability of the tyre. The chemical treatment with Resorcinol Formaldehyde Latex (RFL) is the most popular one, but the presence of the Formaldehyde and resorcinol could be restricted. Plasma treatment was chosen like an alternative method to guarantee the adhesion.

In the first year of thesis, the main reinforcement fibers were studied by classical characterization and alternative characterization. One of these characterizations was proposed to differentiate types of commingled yarns that differ by the producer, the analysis was carry out by the interlace evaluation (number of nodes in a yarn). A new method was proposed to count the number of nodes and becomes a new proceeding for the measurement of the interlacing in a commingled yarn; the characterization was

performed using the Rapid600v. The yarn number of nodes was related with the mechanical and thermal properties measured on cords built by commingled yarn. The cords characterization was performed with Zwick Z/10 tensile tester and by a shrinkage tester. The measurement of the hysteresis of different hybrid nylon constructions, mono and multifilament, was another alternative characterization which was presented as a poster at the International Textile Conference of Dresda. The friction between the filaments, in a multifilament yarn, creates an increase of hysteresis, the evaluation of the hysteresis was carried out with a tensile tester.

From the second year onwards, after the study of the fibers and a bibliography research on plasma treatment applied to fibers, the work was focused on the aim of the thesis: the investigation and the definition of a plasma treatment as an alternative method to guarantee the adhesion between fiber and matrix. A Plasma Enhanced Chemical Vapor Deposition (PE-CVD) was performed in vacuum system and the 2-isopropenyl-2-oxazoline was chosen like organic precursor. At first the treatment was performed on Polyester (PET) sheet, in order to optimize the Plasma treatment condition, and then on monofilament PET. PET monofilament is more challenging because of its geometry and its smooth surface. Therefore, the adhesion is more complicated compared to the same material in multifilament form (standard material) but it is easier to study. Different plasma conditions were tested to obtain the best treatment conditions, two strategies were followed: the continues plasma and pulsed plasma. The optimization of the plasma parameters was made by the study of the thin film deposited; on this purpose, the coatings were characterized by the measure of the contact angle to study the wettability and by the profilometer to estimate the thickness of the coatings. The Attenuated Total Reflection Infrared spectroscopy (ATR-IR) and the X-ray photoelectron spectroscopy (XPS) were used to recognize the different chemical species, which characterized the different films. The adhesion was evaluated by a peeling test, on the PET sheet, and with Cord Rubber Adhesion (CRA) test which were performed using a tensile tester. The amount of the rubber that remains on the fiber (coverage degree) after the CRA test was estimated by Optical Microscopy; TEM images were taken to compare the covering of the classical and the plasma treatment. The characterizations allow defining a plasma treatment that guarantees, on the PET monofilament, better adhesion than traditional RFL treatment. The results of the research were patented.

The researches carried out at Universidad Carlos III de Madrid were focused on the effect of the plasma treatment on the adhesion of fiber, used as reinforcement, and thermoplastic

matrices. The aim of the first project is the construction of more environmentally friendly materials, the evaluation of the composites was performed with the mechanical characterization (tensile tester) of three composites, which differed for layers of flax fiber instead of carbon fiber. Atmospheric pressure plasma torch (APPT) was utilised on flex fabric to modify the wettability with the polybutylene succinate (PBS), the APPT effect was estimated by the contact angle and the measure of the surface energies. The composite materials where prepared using a hot plates press. The reference material was a composite built with three layers of carbon fiber and four layers of PBS matrix. The tensile, bending and impact test indicated how the presence of the flax fibers, in the composites, has a positive effect in comparison with the reference materials. The second project was the study of the Low-Pressure Plasma treatment (LPP) on carbon fiber used for the preparation of composite materials where Polyamide 11 and Polyamide 12 are the matrices. The first step was the preparation of the composite materials, with the untreated carbon fibers, to measure the tensile properties to use as a reference. The tensile test allowed to define that the PA12_CF had better performance than PA11_CF, for this reason the LPP treated carbon fibers were used to prepare a new composite with the PA12. The effect of the LPP was evaluated by the measurement of the contact angle and the surface energy (SE). The plasma treatment increased the SE, but the increment was not enough to improve the adhesion with the matrix and the mechanical properties of the composite. SEM microscopy confirmed the low adhesion level between the reinforcement and the matrix. Due to the Covid-19 emergency, the experience at the Universidad Carlos III de Madrid was stopped prematurely.

CHAPTER 1

1- INTRODUCTION

1.1 Composite materials

Composite material is heterogeneous material formed at least by two component; each phase maintains its different chemical, physical and mechanical properties in the composite. Composite materials are not just artificial but also exist in nature, for example the wood is composed by two phases where the cellulose, in form of fiber, is a reinforcement for the lignin matrix [1]. The application of the synthetic composite materials is consistent and in expansion in many industrial sectors such as aerospace, automotive, marine, energy, infrastructure, biomedical and in sport application [2]. The advantages of these materials are many: they have high strength, stiffness and low density in comparison with the starting material without reinforcements, because are the reinforcement elements which provide to increase the tensile strength and the stiffness of the materials. The reinforcement could be in form of particles or fibers (figure 1). The particles have the same dimension in all of directions and have a regular geometric shape. The fibers are defined as such when they have a length much greater than the diameter, the smaller is the diameter the higher is the strength. Fibers could be continues, with a unidirectional orientation, or discontinues, with a random orientation[1].

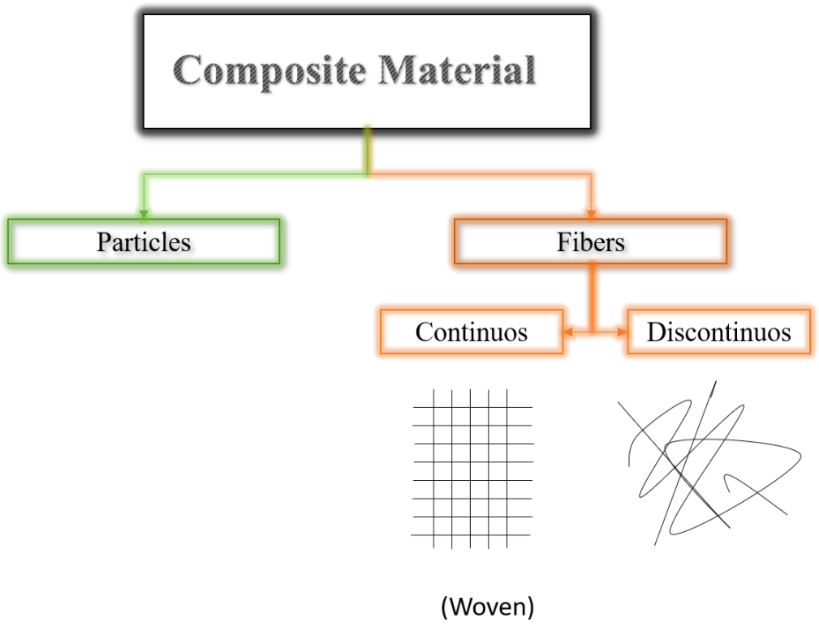

Figure 1 Composite Material (main reinforcement)

The thesis focuses on a particular composite material: Tyre. Tyre is a composite material where the rubber compound is reinforced by textile and steel reinforcements in form of cords. Elastomers (synthetic and natural rubber), fillers, chemicals products and oils constituted the rubber compound; the function of the reinforcements is to guarantee the the durability and the integrity of the tyre [3]. The pneumatic tyres were born in Great Britain at the end of the 19th century as evolution of the solid rubber tyre, in the 1920s "balloon" tires were used in the motor vehicle industry. From the mid- 20th century the tubeless tyres were introduced, and later the radial tyre, where the cord piles were positioned at 90° from the travel direction, to avoid the friction between the plies, became the most used in the world [4]. In a composite material the adhesion is a crucial aspect, for example in a tyre the adhesion between the reinforcement and matrix is guaranteed by Resorcinol- Formaldehyde-Latex, that acts like an interface between the rubber compound and the tyre reinforcement materials [5].

1.2 Rubber Matrix

Matrix has the function to keep the reinforcements and the additives together with the aim to maintaining the shape and to transmit the force in the composite material [6]. Tyre is a

rubber-cord composite where the rubber compound is the matrix, it is constituted for the most part by natural and synthetic rubber (figure 2). Natural rubber (NR) is obtained (UNI7703 standard) by the coagulation of the latex derived from the *Hevea brasiliensis* by the incision of the tree trunk. The natural rubber gives to the matrix its excellent mechanical properties, especially the elasticity, but the poor resistance to the temperature, atmospheric and chemical agents is a disadvantage [7]. To improve or adjust the mechanical properties the synthetic rubber is added, which is produced from unsaturated hydrocarbons generating by artificial latex polymerization and coagulation, the most used synthetic polymer is Styrene Butadiene Rubber (SBR) [8].

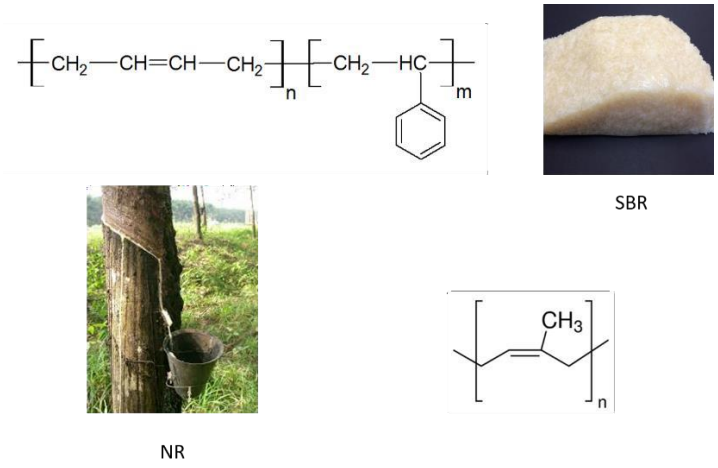

Figure 2 NR and SBR

The other components of the rubber compound, that are requested to improve the performance of the final product, are the fillers which increase abrasion resistance: carbon black and silica fall into this category. Silica guarantees an improvement of the braking distance in the final products. Furthermore, different chemical products are added in other to satisfy different requests, for example antioxidants and anti-degradants that have the function to preserve the compound. Chalk, oil, resins, catalyst, and sulphur are other ingredients that constitute the rubber compound, some of them are useful for the vulcanization [3].

1.3 Textile fibers for tyre reinforcement

There are five type of fibers that were used and are still used today in rubber industry as reinforcement. The cotton was the first yarn used in tyre industry but then was replaced by Rayon, the first manmade fiber with similar chemical structure to cotton. In 1935, in a Dupont laboratory in Delawere, the first polyamides were synthetized by Wallace Carothers; Nylon 6 and Nylon 6.6 (1937) were the first completely artificial yarn applied in tyre industry [9]. Polyester is another synthetic polymer, which was used as reinforcement, especially for its high Young's modulus. Aramid is the fifth yarn utilized in rubber industry, were patented by Stephanie Kwolek, a Dupont researcher, in 1965 [10]. This fiber is characterized by high strength and high Young's modulus. Other no-textile fibers are employed in tyre construction such as Glass and Steel [8]. In figure 3 a fibers classification is proposed.

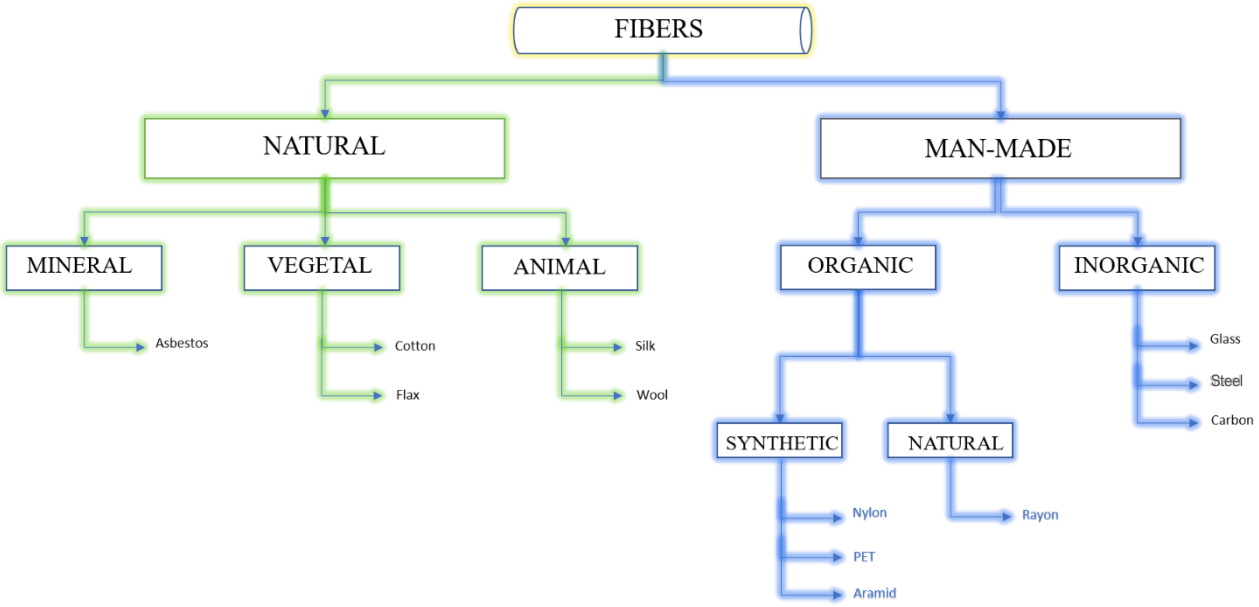

Figure 3 Fibers Classification

In tyre industry, one of the most important characterization is the stress vs strain curve where the slope of the curve represents the Young's Modulus, in the figure 4 the curves for the fibers that were mentioned before are highlighted.

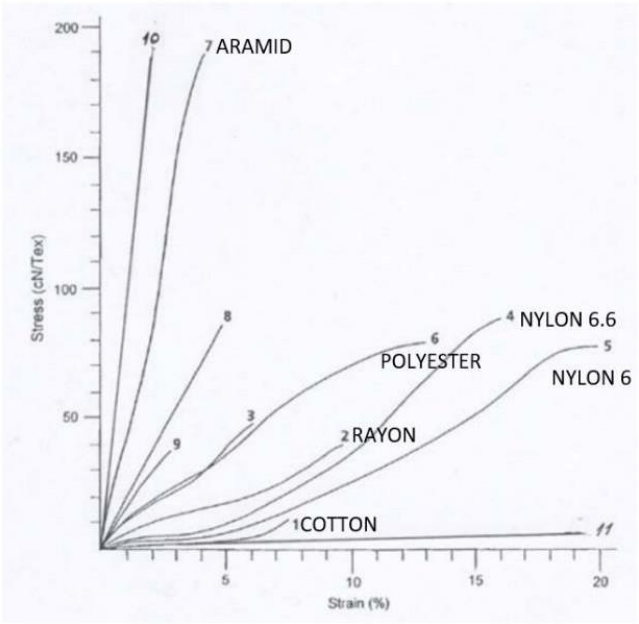

Figure 4 Stress vs Strain curves of some fibers [11]

1.3.1 Rayon

Rayon is synthetized starting from cotton or wood pulp, both have a high percentage of cellulose component. The final structure of Rayon is not so different from the starting cellulose structure because the process is a regeneration of the original polymer. The natural resources are steeped and boiled in sodic hydroxide, which takes away all that is not cellulose, giving pure cellulose soda. The product is treated by carbon disulphate to give sodium cellulose xanthate and then is dissolved again in caustic soda. The spinning solution is put in a coagulant bath, composed of sulphuric acid, sodium, zinc and a small percentage of glucose to give the regenerated cellulose (figure 5).

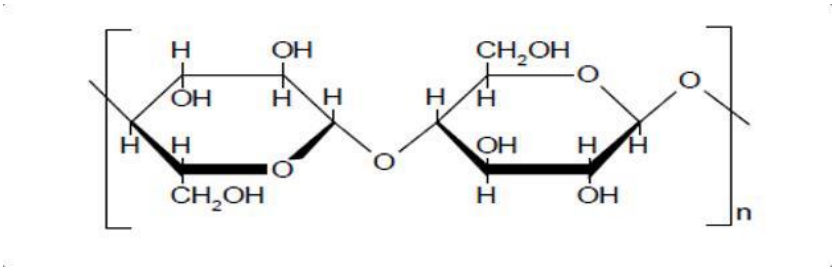

Figure 5 Rayon

Rayon has a good modulus and low elongation; it begin to lose strength at 150° C and is decomposed at 210° C such as other natural fibers [12]. An important disadvantage of Rayon is the high moisture regain, but in the tyre application, this is not a big problem because the influence of moisture on the structure is limited [8]. Rayon is used in the body ply or as belt reinforcement [13].

1.3.2 Nylon

Nylon is a linear aliphatic polyamide with similar chemical structure to some natural fibers such as wool. The difference is the starting monomer, which is amino carboxylic acids for the natural fiber, and the position of the amide groups. The different molecules, from which the synthesis starts, define two type of Nylon that are used in tyre industry: Nylon 6 and Nylon 6.6 (figure 6) [8]. Nylon 6 are synthetized from caprolactam that are heated in water in order to open the ring [14], Nylon 6 is a homopolymer. Nylon 6.6 are synthesised from benzene which is reduced and dehydrogenated until it is oxidized with nitric acid to obtain adipic acid. The adipic acid are mixed with hexamethylene diamine and both are dissolved in methanol to give a salt that are dissolved again in water to give Nylon 6.6 [8] [15].

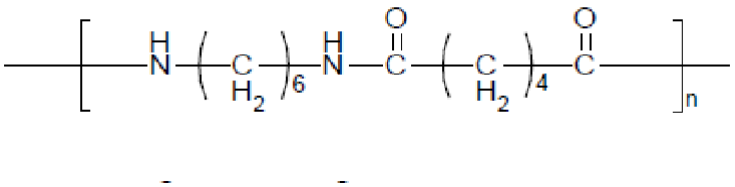

Figure 6 Nylon 6.6

The two type of polyamides have similar behaviour: they don't suffer the exposure to water and the moisture regain is 4,5 %; Nylon 6 and Nylon 6.6 are not sensitive to microbiological attacks and resist against the acid except when at high temperature the polyamide is attacked by concentrated acid [8]. They differ for the melting point: 250° C for Ny 6.6. and 225 for Ny 6. In comparison to the Rayon the polyamides have higher strength, lower modulus and consequently higher elongation. Nylon are thermoplastic material for this reason suffer the thermal shrinkage: when the temperature increases, the shrinkage increases [16]. The aliphatic polyamides are used in tyre industry as cap ply, belt edge cap and as body piles [13].

1.3.3 Polyester

Polyester (PET) fiber in tyre industry is polyethylene terephthalate, which derives from the condensation and the ester interchange starting form ethylene glycol and dimethyl terephthalate [17]. Ethylene glycol is a product of the oxidation of ethylene which are hydrolysed, dimethyl terephthalate is prepared from terephthalic acid. PET (figure 7) is less reactive than the other fibers, as was mentioned before, due to the less reactivity of the ester in comparison to the aliphatic ester [8].

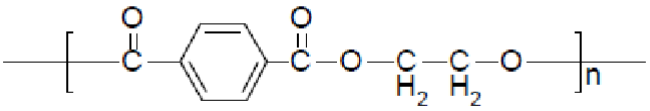

Figure 7 Polyethylene terephthalate

The water does not affect PET fibers, but at 100° C the water hydrolyses the material and causes a shrinkage that leads to a loss of strength. This behaviour is explained by the thermoplastic character of the Polyethylene terephthalate [18]. PET can withstand up to 180° C and the melting point is at 250° C, this fiber suffers from amine. The mechanical properties are a "mix" between Nylon and Rayon fibers, this thermoplastic fiber has the strength and the elongation of Nylon and modulus of Rayon. The low reactivity of the ester group of the PET results in adhesion problems that will be analysed in the next chapters.

1.3.4 Aramid

Aramid (figure 8) is a polyamide as Nylon but with aromatic group instead of aliphatic carbons, this leads to a low reactivity. The first Aramid was created by DuPont and names Nomex, which are used for the fireproof application because its non-flammable properties [8]. Kevlar (Dupont) [19] and Twaron (Akzo) were developed between 1970s and 1980s and derived from poly-p-phenylene [20]. Aniline is acetylated and nitrated, and the product is hydrolysed and reduced to give p-phenylene diamine that reacts with terephthalic acid chloride to obtain the polymer [8].

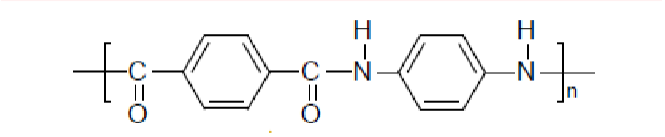

Figure 8 Aramid

The moisture regain of Aramid is 2,0%, in general this fiber doesn't suffer the effect of water and the alkali, resists to acid but is affected from boiling sulphuric acid. Aramid does not suffer the temperature up to 250° C and the melting point is at 500° C, the exposition to the UV causes a loss of strength. Aramid yarns are similar to inorganic filaments for the exceptional tensile strength (table 1), high modulus and low elongation, which causes some problem of flexion in some application [8]. Aramid is used for the fabrication of ballistic industry, in tyre industry the fiber is employ in the belt instead of steel cord as lightweight alternative [13].

Table 1 general physical properties of fibers[8] (initial modulus from 2% to 100% of elongation)

FIBER	Rayon	Nylon 6	Nylon 6.6	PET	Aramid
Specific gravity	1.52	1.14	1.14	1.38	1.44
Mean filament diameter (µm)	8	25	25	25	12
Mean decitex for filament	1.8	6.7	6.7	5.7	1.7
Tensile strength (Mpa)	685	850	950	1100	2750
Tenacity (cN/Tex)	40	80	85	80	190
Elongation at break (%)	10	19	16	13	4
Initial modulus (cN/tex)	600	300	500	850	4000
Shrinkage at 150° C (%)	0	6	5	11	0.2

1.4 From fiber to fabric

There are only few applications where the fibers are applied as they are, so a modification of the filaments is necessary to respond of purpose of the material. Fibers are used in materials as such single yarn or cord; in tyre industry the fibers, use like reinforcement, are in form of cord-fabric [8]. Yarns are an "assembly of substantial length and relativity small cross-section of fibers or filaments with or without twist" and they are obtained from fibers with a conversion process [21]. Depending on the type of fibers there are different spinning method to obtain the yarns: PET and Nylon (6/6.6) are obtained by melt spinning, Rayon and Aramid by solution spinning. In the melting spinning, the molten fibers are filtered and pumped into a spinneret with different fine holes. The semi-products are extruded and stretched many times being cooled in the same moment. The solidified product is lubricated, and the filaments are cold drawn over a godet. The drawing process stretch the filaments at the glass transition temperature in order to obtain high crystallinity and high molecules orientation to improve the mechanical properties. At the end, the yarns are collected on a bobbin with a light twisting. The solution spinning process is for the fibers that have not a define melting point, a dissolution is needed. Aramid, or Rayon, are pumped through the spinneret in a coagulant bath, and then the bath is air dried to evaporate the solvent. The filaments are dried under tension, but they are not elongated until to reach the crystallinity and the molecule orientation, cause high levels of these two characteristics is strictly related to mechanical properties. The resultant yarns are collected on bobbins. Three types of yarn exist: staple spun yarn, monofilament yarn and multifilament yarn made by two or more filaments. From the yarns is it possible to obtained cords, first the yarns are ply twists in Z direction and

then the cords are formed by the twist of two or more cords in the S direction. The twist influences the properties, the cord properties are different from both fibers and yarns properties. It is possible to increase the twist, this cause a reduction of strength, modulus and tension fatigue resistance but the elongation to break, the rupture energy and the compression fatigue increase [13]. Fabric is a flexible construction made by yarns or fibers, the most common process to produce fabric is the weaving, this technique was used by the ancient Egyptians 6000 years ago. Woven fabric is built by two perpendicular yarns: warp, which has a longitudinal direction, and the weft in the width direction. Warp needs different preparation as the winding, warping, sizing and drawing in; at the end of these process warp and weft are weaving together to form the fabric [21].

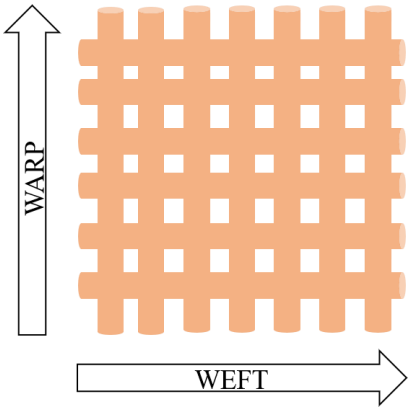

Figure 9 Warp and weft

1.5 Adhesion

The textile, in form of yarn, cord or fabric, before to be applied to the rubber matrix is treated to prevent some problems and to improve some properties. These processes are the heat-setting and the adhesion treatment, which will be mainly explored in this paragraph. Usually the two treatments are combined, the heat-setting treatments are particularly important for the thermoplastic fibers as Nylon and PET because prevent the shrinkage in the final product. To minimalize the changing of the fibers in the tyre, thermoplastic fibers are treated at high temperature and high tension in order to fix the

properties of the textile reinforcement, is possible to select the condition of this process to regulate the mechanical behaviour. During this heat-setting the fiber is stretched many times this process leads to create a new crystallinity and to improve mechanical properties, which could be regulated as mention before.

1.5.1 RFL

The adhesion between the reinforcement and the rubber matrix is a crucial aspect to ensures the integrity and durability of the tyre, nowadays the adhesion is guaranteed by Resorcinol/Formaldehyde/Latex adhesive system, which was used since the 1940s [13]. The low adhesion of the virgin fibers with the rubber is due to the differences in modulus, elongation, polarity and reactivity the aim of the adhesive is to reduce these contrasts acting as connection between the reinforcement and the matrix and to transmit the load stress from the elastomer to the fiber [22 23]. Synthetic yarns have a difficult adhesion with rubber because the smooth surface and the reactivity of the polymer that compose the fiber, in particular the reactivity, is low due to the lower polarity in comparison to the elastomeric matrix. The physical and chemical characteristics inhibit construction of a direct bond, an adhesive is necessary. The first adhesive system was developed for rayon and was composed by casein and natural rubber, later the employment of the synthetic fibres needed a different chemical cure for the purpose [24]. In figure 10 the basic resin condensation is show: the synthesis starts with the reaction of resorcinol and formaldehyde, than the resorcinol substituted forms the basic resin; depending on the catalyst the resin could be with a three-dimensional (alkali catalyst) structure or a linear system (acid catalyst) [8].

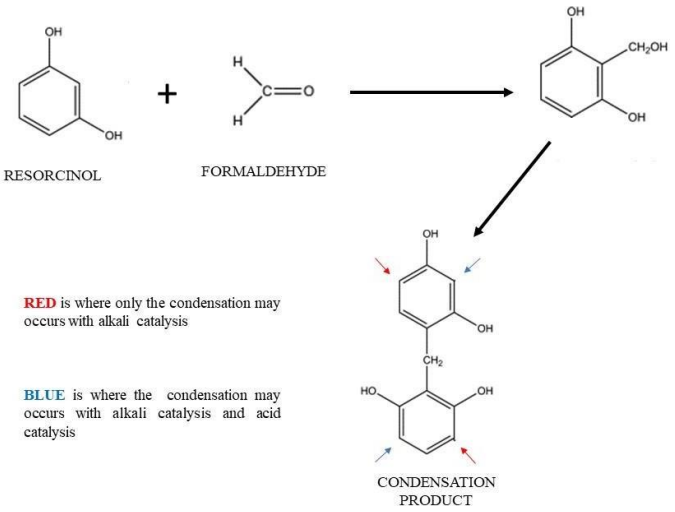

Figure 10 Basic condensation of RFL

1.5.2 Rayon and Nylon adhesion treatment

As was mentioned before Rayon fiber was the first reinforcement that was used in tyre industry and to improve the adhesion it was treated by a mixture of casein and natural/latex. Then, thanks to the arrival of new synthetic fibers on the market, a resorcinol/formaldehyde resin replaced the first treatment and even the natural latex was substituted by SBR latex. The new system, SBR/resorcinol/formaldehyde was improved by a new thermopolymer latex composed by styrene, butadiene and vinyl pyridine. In industrial process Rayon fabrics are immersed in a bath of the adhesive. The water, that is present in the dip, is dried at 100° C and the adhesive film is heated again at 140° C-160° C for one minute [8]. For Nylon cords the same process is used but a heat-setting is necessary for the thermoplastic characteristic of this polymer; for this reason, the temperature, for the dip application on the polyamide cords, is higher than the temperature used for the Rayon, 200° C [13]. The adhesion mechanism must be considerate both for the matrix and fiber, because the adhesive acts like interface [23] (figure 11).

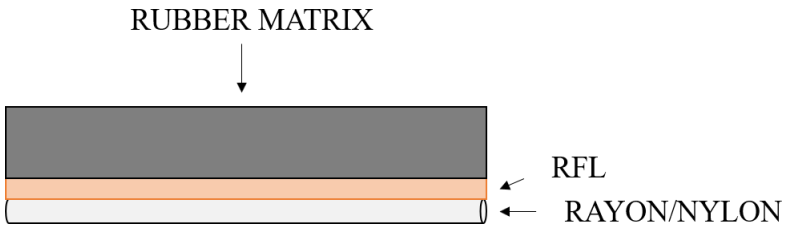

Figure 11 RFL interface

The RFL-elastomer matrix adhesion has a great contribution from the crosslinking of the rubber latex of the resin with the rubber matrix. This is due to the chemical agents, like sulphur, that migrate during the vulcanization (which will be highlighted in the next paragraph); is important to have a right level of sulphur: low quantity or high quantity doesn't permit the migration and even the time doesn't have to be short. There is even a strictly chemical contribution due to the active hydrogens of the rubber polymer chain. On the other side the adhesion between the dip and reinforcement is not so clear but in generally the major contribution is that provided by the RF resin. For the Rayon is supposed the RF resin spreads inside the yarn but not in a macro level but thanks to a microscopic diffusion inside the superficial pores of the cellulose fiber [25]. There is also a chemical contribution due to the formation of a covalent bond and hydrogen bond between the Rayon and the RF resin. For the Nylon the diffusion contribution is lower than the Rayon due to the surface structure of the polyamide, the major contribution is for the formation of a direct chemical bond between the methoxy group of the Resorcinol-Formaldehyde and the amide groups of the Nylon, figure 12. [23-8]

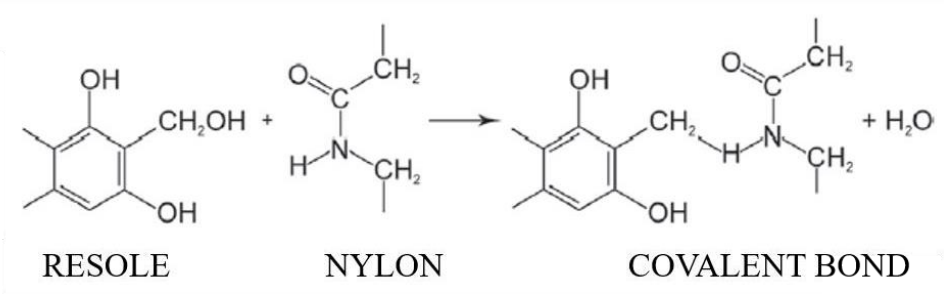

Figure 12 Covalent bond between Nylon and Resole [26]

1.5.3 Polyester and Aramid adhesion treatment

Both Polyester and Aramid are less reactive in comparison to the other fibers, that were mention before; for this reason, in order to rich a good adhesion level between the reinforcements and the elastomer matrix, is necessary to pre-treat the fibers. The first pre-adhesion system for PET was an application of isocyanate followed by RFL application, then different method to preactivated was developed as the addition of blocked isocyanate to the RFL [26] or different approach as aromatic urethane used like coating before the RFL application [27]. But the development of DuPont D417 is the most used, the pre-dip is prepared by a mix of water miscible epoxy to the blocked isocyanate, in the next table the formulation is shown, table 2 [28].

Table 2 Pre-dip DuPont D417 [29]

Ingredients	**Wet pre-dip DuPont D417 (parts by weight)**
Blocked isocyanate (40% dispersion)	180.0
Epoxy resin	27.2
Gum tragacahnt solution (2%)	25.0
Dispersant	0.6
Water	1767.2

Polyester is a thermoplastic for this reason suffers heat-setting process during the application of the dips which occurs at approximately 230-240° C. The scheme in figure 13 represents a simplify industrial process to apply the pre-dip and dip, the fiber (in form of yarns, cord or fabric) passes four different oven where was heated in order to dry the PET and stretched to work on and improve the mechanical properties, as was mention before, than the treated fiber is collected on a new bobbin.

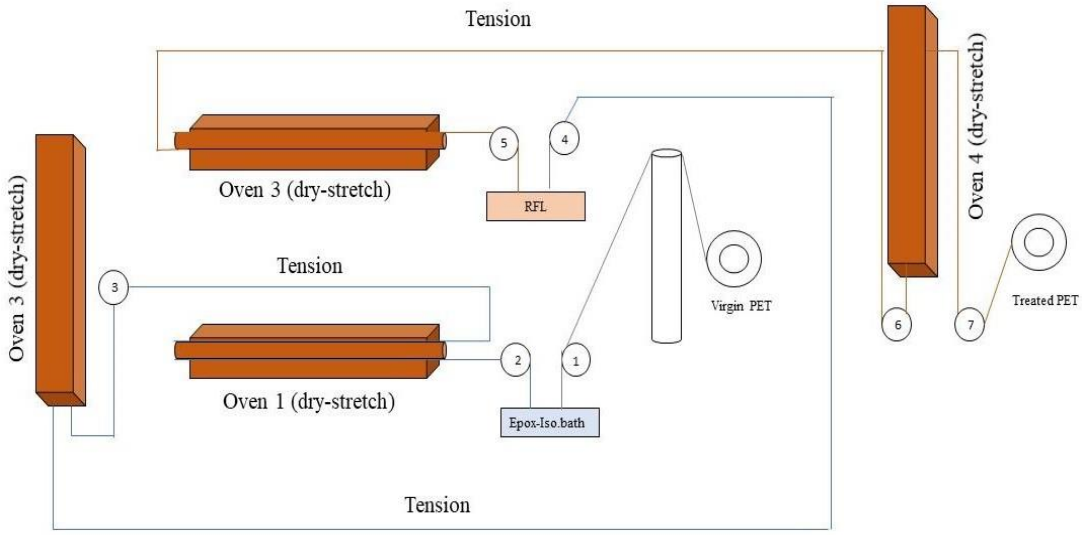

Figure 13 Schematic representation of dip application on PET

Some company uses different approaches where the pre-treatment components are applied in the spinning stage [8]. Even if Aramid is a polyamide, it hasn't the same reactivity of the Nylon, due to the aromatic nature of the molecular structure. This fiber is treated following the same strategy of PET with a pre-treatment into an epoxy bath, epichlorohydrin with glycerol, before the application of RFL [13]. Some approaches used to pre-treat the Aramid in the spinning stage [8]. For these two inert fibers the mechanism that rules the adhesion of the cords with the adhesive is even more complicated than the mechanism for Rayon and Nylon. There is more information about the PET adhesion and the reaction with the pre-dip, in particular with the epoxy component; between the end group of the PET and the epoxy is possible the formation of a covalent bond, figure 14 [23]. The pre-dip and the RFL react as was mention before by a crosslinking development with the rubber matrix.

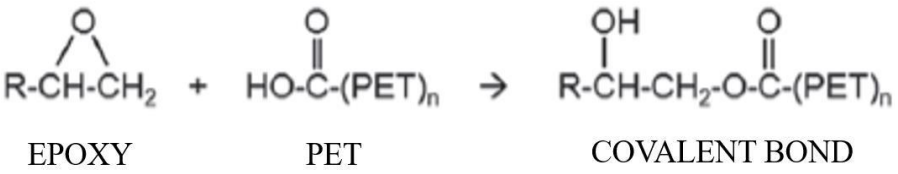

Figure 14 Pre-dip PET covalent bond [23]

1.5.4 Alternative methods

In the recent years the scientific research on the adhesion, between the fiber and elastomer, is focused on alternative for the Resorcinol/Formaldehyde/Latex system to guarantee the better performance of integrity and durability in a tyre. The main reason because is necessary to find new adhesion methods is due of the bad effect that the RFL has on the environment [30]. The use of formaldehyde and resorcinol will be probably limited because their toxicity, the formaldehyde is classified from the Committee of Risk Assessment as carcinogenic and mutagenic [31] and resorcinol in high dose could be cancerogenic too [32]. Even the use of some epoxy resin, to pre-treat the PET and Aramid, may present some toxicity problems. There are also less significant drawbacks as the multistep process and the difficulty to understand clearly the mechanism of reaction [23]. As was mentioned before the RFL treatment, despite some drawbacks, is the most used, but different approaches were developed in the past and recently. One of the strategies taken by the researchers was to reduce the amount of formaldehyde and resorcinol in the dip system, but the adhesion results were not the same [24]. In the recent years a formaldehyde-free adhesive was found, especially for the less reactive fibers, the system contains acrylic resin in latex and in an epoxy and polyisocyanate bath [33]. Another completely different approach to RFL system was the synthesis of an aramid-polydiene copolymer to treat the aramid or the use of silane promoters contain an amine group to react with the reinforcement and double bond on the other side that reacts with the matrix [34-35]. One of the first alternative methods to classic RFL system used was the inserting, into the rubber compound, of some adhesion promoters like methylene donor [36], or the insertion of blocked isocyanate in the matrix and surface treatment on the fibers[37]. The first fiber used in tyre industry was the cotton, the surface of this natural resource is not smooth but rough and this characteristic permit to have a good adhesion only by dry process. For this reason, the roughening of the fiber surface is one of the strategies which is more explored both by chemical and physical approaches. The chemical treatment by bromine to modify the morphology of the reinforcement is a chemical etching: after the cure by bromine the materials are inserted in ammonia solution and the movement of the nitrogen from the surface to the fiber creates the roughness [36]. Plasma technology is another technique which is used to modify the morphology of the surface ,without modify the bulk properties of the substrate, and to improve the adhesion properties of the fiber; with plasma is possible to make etching in different condition of pression, which could

be atmospheric or low pressure. The etching is performed thanks to a gas that, i.e. in a vacuum system, is insert in a chamber, the application of potential difference charges the gas, and the particles bomb the surface to create roughness [38]. Etching is not the only plasma application to improve the adhesion, the Plasma Enhanced Chemical Vapor Deposition (PE-CVD) is another alternative to RFL system. Thanks to this technique is possible to deposit, on the substrate surface, a coating made by organic or inorganic molecule with the features to promote the bond between the surface and the rubber matrix. The plasma treatments are favoured from an environmental point of view, because a less quantity of reagents is request and they don't need solvent to perform a reaction [39]. Plasma technology will be discussed in the next chapter.

1.6 Basic processes of Tyre manufacturing

In this paragraph the basic processes of tyre manufacturing are resumed form the mixture of the rubber matrix and compounds to the final assembly. The first step of the manufacturing is the mix of the natural and synthetic rubbers, the result of this process is roll and cut: this basic material is defined "sheet". In the second step the sheet is mixed with the compound, that were mentioned before (paragraph 1.2 Rubber matrix), depending on the role which will be performed: for the tread, the part of the tyre that is in contact with the ground, is requested carbon black and silica to resist against the abrasion and chemical additives are request for the longevity and anti-oxidative properties. The inner liner is constituted by a thin layers of butyl rubber in order to guarantee the no-permeability of the air. Usually two inner liner sheets are prepared, cut and mixed thanks to a calender, the final sheet has the purpose to maintain the air pressure into the tyre [3]. The textile reinforcing materials are present in the rubber in form of cords which constituted a sheet of fabric. Before the application, the reinforcements are treated by the adhesive system, as was mentioned in the paragraph 1.5, and then body plies are prepared: the fabric passes in a calender where is covered, on the both side, by a two thin layers of rubber mix [13], (figure 15).

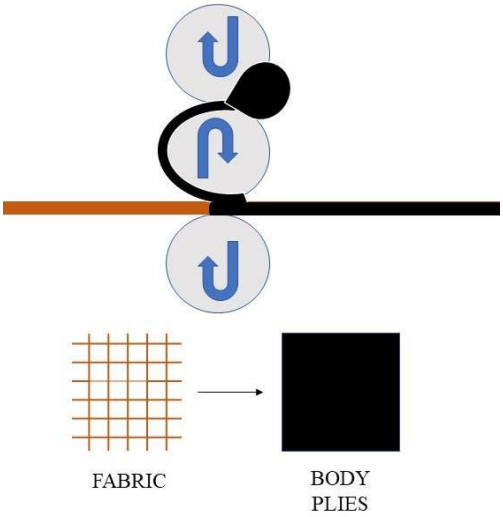

Figure 15 Schematic preparation of body plies

During the calendaring of the textile fabric is important to control three parameters: the first is the feed-rate at which the rubber is applied on the cords, the second is closely related to this and it is the thickness of the compound on the textile, from this parameter depend the properties of movement and strength of the body plies; the third parameter is the control of the temperature that rules the uniformity of the coverage and the smoothness [8]. In a radial tyre the plies are perpendicular to the rolling direction, in the bias tyre the plies are overlapped in a crisscross configuration. The body plies constituted the carcass that forms the resistance part. Metallic belts have the function to oppose to the expansion of the carcass in the rolling direction, and, they improve the strength of the tread. The belts are located between the carcass and the cap-ply and are constituted by steel cords that form a thin steel ply which is covered by rubber in a calender and then applies on the carcass. Nylon Zero degree or cap-ply covers the belts to limit the expansion of the centrifugal forces during the rolling. Cap-ply is parallel to the rolling direction. The steel is also present in the bead that has a crucial role because transfer the load from the rim to the tyre and absorbs the vibration. The bead owes its usefulness to the apex that is produced at the same time of the bead and is fixed on this. Before the assembly, the tread is cut with the requires dimensions, this sheet is responsible of the grip and the rolling resistance. The body-plies are positioned on the inner liner and the bead and the apex are mounted on the inner liner too, so the carcass is built; than the metallic belts are covered by the Ny cap-ply and by the tread, the assembly is assembled

on the mark with same dimension of the final tyre, this assembly is called green tyre and is ready for the vulcanization process, figure 16 [3-13].

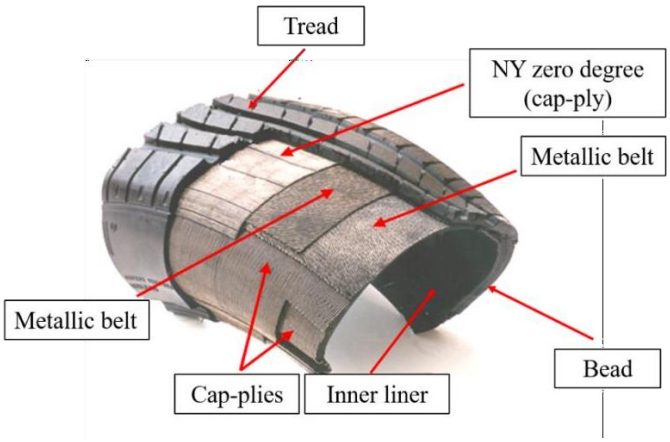

Figure 16 Green tyre

1.7 Characterization methods of textile-rubber adhesion

The reinforcing materials (textile and/or metallic) are present in the tyre to constitute the cap-plies in the carcass, the metallic belts and the NY zero-degree cap-ply; these materials are present in the tyre in form of cords and guarantee the tyre integrity and durability. Adhesion tests are performed in order to verify the adhesion and in this paragraph the most common tests are explained, these trials are pull-out and peel-test for the cords and peel-stripping for the fabrics. These experiments measure the adhesion as the strength that is necessary to separate the reinforcement from the matrix [40]. In some case, the tear resistance evaluated by the coverage can measure the adhesion: the rubber phase that remains on the cords after doing the trial. The pull-out test can be performed with different methods, the classical one measured the necessary strength to pull-off a cord incorporated in a rubber block. The H-Test (figure 17) is the most used type of pull-test, where each of the two ends of the cords are fixed in two rubber block that are blocked by clamps. In this adhesion test, the force required to pull-off the cord, from one of the blocks, is measured.

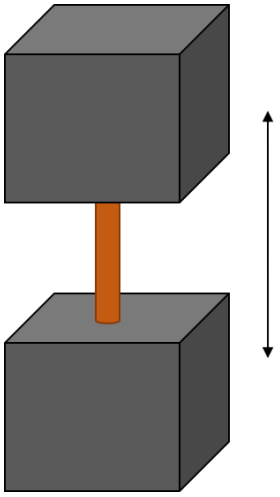

Figure 17 H-Test

The disadvantage of this test is the stress suffered by the samples due to the clumps that hold up the rubber blocks, which could be invalidate the trial. To bypass the problem the rubber blocks are reinforced by cotton, the cotton reduces the deformation. The T-test is an alternative made to resolve this problem; in this trial a bracket is added to support the rubber block. To measure the required strength to pull-off a cord from rubber, a load cell is necessary, the trial is performed with a dynamometer and the force values are expressed in Newton [N]. More than one cord side by side are tested by the peel test (figure 18), the preparation of the sample is important because is necessary that adhesion does not extend along the whole sample: a release paper placed at the end of the sample guarantees the separation between the reinforcement and the matrix. The paper is used during the application off the rubber on the textile material before the curing. The two separated ends of the samples are put in the grips and the dynamometer measure the force required to separate the component of the composite material due a load cell. To test the adhesion on the fabric a peel test is performed, following the ISO 36. The probe for this adhesion test is built by two or more plies of fabric reinforcement which are embedded with the rubber matrix, the sample is thicker than the sample prepared to test the cords [8].

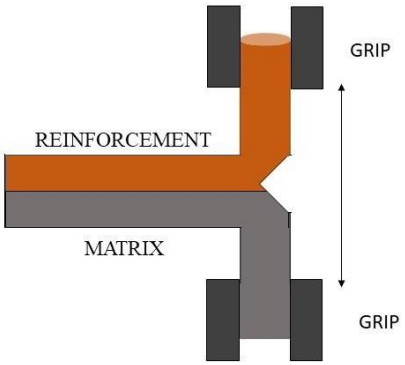

Figure 18 Peel-test

1.8 Vulcanization

The last process to complete the production of tyre is the vulcanization. The green tyre, which is assembled as mentioned in the paragraph 1.7, is collocated in a baking mold hermetically sealed where an air jets pushes the tyre against the mark giving to the assembly the tyre shape. Hot steam or hot water heats the system up to a temperature of 170° C for 12 or 15 minutes, the chemical reaction begin when the temperature increase and rubber compound passes from a plastic to an elastic state [3-13]. Historically the term of vulcanization is referred to the heating process of rubber with sulphur and white lead, the term is not only related to the tyre production. At the end of the 19th century, Charles Goodyear introduced the vulcanization, for the tyre industry, as a process to chemically bonding rubber to sulphur. Thanks to this chemical process at high temperature, also called curing, the rubber passes from plastic polymer (high molecular weight) to elastic substance by chancing the macromolecular arrangement and architecture; this change not also modify the elasticity but improve the tensile strength and eliminate some disadvantages as the abrasion and the stickiness [41]. The vulcanization leads to the formation of thioether bonds, sulphur acts as a cross-linked bridge with the polymer chains at both intermolecular and intramolecular levels [42]. The principal bonding site is the carbon of the group -CH_2- close to the carbon of the double bond, even the carbons of the methylene groups and the carbons that form the double bond are involved in the formation of the sulphur bridges (figure 19). The mechanism of the vulcanization is complex, and it could follow ionic or radical way [43].

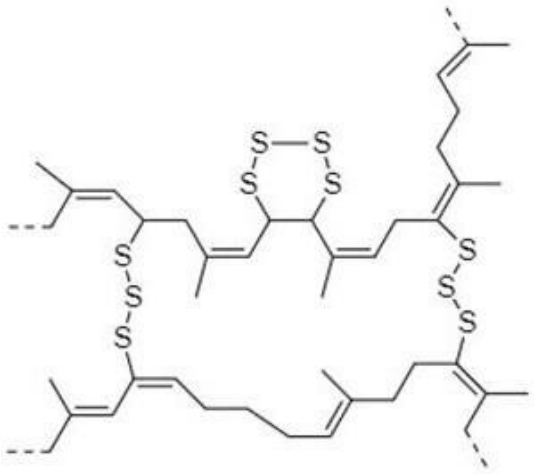

Figure 19 Crosslinking

Sulphur could be added as Sulphur (S_8), as sulphur donating group like S_2Cl_2 or as polymers, which contain sulphur group [41]. In order to lower the energy necessary to start the vulcanization some accelerants are inserted in the curing system; there are 5 basic groups that form the structures of the activators: Benzothiazole (mercapto- and sulphonamides accelerators); Thio Carbanalide (with Zinc or or Sulphur to replace Carbon); Guanidines; Morpholines; Xanthates. Other additives with cover a critical role in the curing process are the activators, which improves the efficiency of the sulphur vulcanization. The activators are metal oxides but the most used is zinc oxide (ZnO), this oxide has an influence on the nature and the number of the crosslinking between the polymer chains [44].

References

[1] Structural Composite Materials. (2010). http://search.ebscohost.com/login.aspx?direct=true&db=nlebk&AN=395920&site=eds-live

[2] Daniel, Isaac M.; Ishai, Ori. Engineering Mechanics of Composite Materials. Second ed. New York: Oxford University Press, 2006.

[3] Leister, G. (2018). Passenger Car Tires and Wheels [electronic resource]: Development - Manufacturing - Application / by Günter Leister. In Springer eBooks.

[4] Woods, E. C. (1952). Pneumatic Tyre Design. W. Heffer. https://books.google.es/books?id=j27QAAAAMAAJ

5 Wennekes, W., Datta, R., & Noordermeer, J. (2007). Mechanistic Investigations into the Adhesion between RFL-Treated Cords and Rubber. Part II: The Influence of the Vinyl-Pyridine Content of the RFL-Latex. Rubber Chemistry and Technology, 80, 565–579. https://doi.org/10.5254/1.3548181

6 D. Hull, T. W. Clyne; An introduction to composite materials, 2nd; Cambridge University Press; 2012; ISBN: 9781139170130

[7] Mark S. Dennis, David Richard Light; Rubber elongation factor from Hevea Brasiliensis. Identification, characterization, and role in rubber biosynthesis. The journal of biological chemistry, vol. 264, No 31, Issue of November, pp 18608-18617, 1989

[8] David B. Wootton, The Application of Textiles in Rubber, 2001, Rapra Technology LTD.

[9] Klaus Weissermel, Hans-Jürgen Arpe, Charlet R. Lindley, Industrial organic chemistry, 4ª ed., Wiley-VCH, 2003, pp. 239-266, ISBN 3-527-30578-5.

[10] Stephanie Kwolek, Hiroshi Mera e Tadahiko Takata, “High-Performance Fibers”, in Ullmann's Encyclopedia of Industrial Chemistry, Wiley-VCH, Weinheim, 2002. DOI: 10.1002/14356007.a13_001

[11]Reinforcing material in Rubber Product, Nokian tyres plc; 2015 www.lovorket.com/wp-content/uploads/2015/03/reinforcing_materials.pdf

[12] K. L. Pickering, M. G. A. Efendy, and T. M. Le, “A review of recent developments in natural fibre composites and their mechanical performance,” Composites Part A: Applied Science and Manufacturing, vol. 83. pp. 98–112, 2016

[13] A.N. Gent and J.D. Walter; The pneumatic tyre; published by the National Highway Traffic Saefty, Administration, 2005.

[14] US2071253A; 1935-01-021937-02-16; Du Pont Linear condensation polymers

[15] Palmer, R. J. (2001). Polyamides, Plastics. In Encyclopedia of Polymer Science and Technology.

[16] Simal, A. L., & Martin, A. R. (1998). Structure of heat-treated Nylon 6 and 6.6 fibers. I. The shrinkage mechanism. Journal of Applied Polymer Science, 68(3), 441–452.

[17] US2534028A United States (1948); Du Pont Izard Emmette Farr; Production of polyethylene terephthalate

[18] Thermoplastic Composites: Emerging Technology, Uses and Prospects. (2016).

[19] US 3819587 A, 25-jun-1974 – Ei Dupont De Nemours and CO. – Kwoleck

[20] Aramid Fiber Formed of Poly Para-Phenylene Terephthalamide From the Netherlands, U.S. International Trade Commission, Robert A. Rogowsky Director of Operations, August 1993.

[21] Textile Engineering : An Introduction. (2016). http://search.ebscohost.com/login.aspx?direct=true&db=nlebk&AN=1289660&site=eds-live

[22] Wennekes, W. B., & Noordermeer, J. W. M. (2007). Mechanistic investigations into the adhesion between RFL-treated cords and rubber. Part I: the influence of rubber curatives. In Rubber Chemistry (Vol. 80, Issue 4, pp. 545–564). http://search.ebscohost.com/login.aspx?direct=true&db=&AN=28162289&site=eds-live

[23] Louis, A., Noordermeer, J., Dierkes, W. K., & Blume, A. (2016). Technologies for polymeric cord/rubber adhesion in applications. KGK Kautschuk Gummi Kunststoffe, 69, 30–36.

[24] Resorcinol Formaldehyde Latex (RFL) Adhesives and Applications (2205). In: Resorcinol. Springer, Berlin, Heidelberg

[25] J.E. Ford, Transactions of the institution of the rubber industry, 1963, 39.

[26] Meyrick and Wootton, inventors; Imperial Chemical Industries; GB patent 1,902,908, 1967.

[27] Yankowsky, Stanhope, Hicks; Celanese Corporation, 4,462,855, 1984.

[28] Shoaf, inventor; E.I. DuPont De Nemours & Co. assignee, 3,307,1967.

[29] Handbook of RubberBonding, Bryan Crowther (edition); Rapra Technology, 2001.

[30] Jaššo, M., Krump, H., Hudec, I., St'ahel', P., Kováčik, D., & Šíra, M. (2006). Coating of PET cords at atmospheric pressure plasma discharge in the presence of butadiene/nitrogen gas mixtures. In Surface (Vol. 201, Issue 1, pp. 57–62).

[31] RAC, European Chemicals Agency (2012); Helsinki, December 2012.

[32] Toxicology and Carcinogenesis Studies of Resorcinol (CAS No. 108-46-3) in F344 Rats and B6C3F1 Mice (Gavage Studies). National Toxicology Program Natl Toxicol Program Tech Rep Ser. 1992 Jul; 403(NaN): 1–234

[33] WO Pat. 091376A1 (2014) to Kordsa Global Industry, Istanbul, Turkey, inv.: A.F. Mahallesi, S. Caddesi.

[34] D.J. Burlett and R.G. Bauer; Goodyear, 1991; EP0445484

[35] S. Li and D.F.M. Michiels, Milliken, 2003; US0092340

[36] Wennekes, W. (2008). Adhesion of RFL-treated cords to rubber: new insights into interfacial phenomena. Integrated Assessment.

[37] Process to produced reinforced tire cords with plasma treated fibers incorporated into a rubber/blocked isocyanate composition; Dane K. Parker, Derek Shuttleworth; The goodyear Tire & rubber company; 1994, US50501880.

[38] Donnelly, V. M., & Kornblit, A. (2013). Plasma etching: Yesterday, today, and tomorrow. In Journal of Vacuum Science (Vol. 31, Issue 5, pp. 50825–50872).

[39] Morent, R., De Geyter, N., Verschuren, J., De Clerck, K., Kiekens, P., & Leys, C. (2008). Non-thermal plasma treatment of textiles. In Surface (Vol. 202, Issue 14, pp. 3427–3449).

[40] ISO 36; 2017

[41] M. Akibà and A. S. Hashim. Vulcanization and crosslinking in elastomers. Prog. Polym. Sci., Vol. 22,475521, 1997. Published by Elsevier Science Ltd Printed in Great Britain.

[42] James E. Mark, Burak Erman (eds.) (2005). Science and technology of rubber. p. 768. ISBN 978-0-12-464786-2.

[43] Nasir, M.; Teh, G.K. (January 1988). "The effects of various types of crosslinks on the physical properties of natural rubber". European Polymer Journal. 24 (8): 733– 736. doi:10.1016/0014-3057(88)90007-9.

[44] Joseph, A., George, B., Madhusoodanan, K., & Alex, R. (2015). Current status of sulphur vulcanization and devulcanization chemistry: process of vulcanization. Rubber Science, 28, 82.

CHAPTER 2

2-INNOVATIVE CHARACTERIZATIONS

The first year of the thesis was dedicated to the study of the main textile fibers used as reinforcement in tyre. During this period, spent at the PIRELLI TYRE laboratories, two new characterizations on innovative materials were developed to study different types of yarns. These experiments are part of the study of the prior art, which was necessary to understand the reinforcement behaviour and the yarns properties for different constructions: multifilament, monofilament commingled and cords. In the first innovative characterization four different types of Nylon 6 cords were analysed. The cords are made of both mono and multifilament ends and differ for the percentage of one respect to the other: 0% (pure multifilament ends) and 100% (pure monofilament ends). Two characterizations were performed: mechanical tests and hysteresis cycles. All the greige cords were characterized at different temperatures: 1) at 22°C; 2) at 70°C, greige cords were compared to RFL dipped one at 22°C. In the mechanical characterization the variation of cord properties, as breaking load and modulus, were studied as a function of the different percentage of monofilament and for the different conditions which were considered. The second part of the experiment was focused on hysteresis Cycle performed with Zwick z/10 dynamometer at low frequency. This kind of characterization is increasingly important to study the stress that the tyre cords suffer under working conditions. The data that were used to characterize the cords were the dissipated energy that is the difference between positive work and negative work. Hysteresis tests were performed at the same conditions considered for the mechanical characterization. The evaluation of the mechanical properties shows the influence of the multifilament ends on the cord breaking load. The results of the hysteresis cycle show a reduction of dissipated energy for the cords with high percentage of monofilament ends.

The dissipated energy is also lower on raw Nylon cords than on RFL treated cords, due to the lower filament/filament friction that is more relevant in samples with high percentage of multifilament ends and also in RFL samples, because the adhesive increases the friction among the filament. The second innovative characterization is divided in two parts: the first part was focused to find and alternative method to distinguish commingled of PET/Aramid (2200 dtex) developed from different producers; in the second part hybrid yarns (commingled), which was created thanks to Sicrem (one of the most important textile reinforcement supplier of Pirelli), with different parameters of the texturizing process were characterized. The parameters which were changed in the texturizing process were: speed, pressure and the overfeeding of the incoming yarns. The variation of the texturizing process is closely related with the variation of the number of nodes (interlace) in the hybrid yarn. In this trial the relationship between number of nodes per meter of the yarns and the mechanical properties of the cords, built from the different commingled yarns, were demonstrated. The new method to discriminate different commingled yarns were developed by Rapid 600v. All the characterizations of the interlace were performed by Rapid600v, the mechanical properties were measured by dynamometer Zwick to measure the mechanical properties.

2.1 Thermomechanical characterization of Nylon cords made with mono and multifilament ends

The work is focused on the characterization of different types of Nylon cords which differ from each other for the percentage of monofilament in their composition, with approximately the same linear density (2800 dtex). The second aim of the work is the characterization of the dynamic properties of the cords with the dissipated energy expressed like work loss, measure after hysteresis cycles performed with Zwick dynamometer [1-2]. The evaluation of dynamic properties is increasingly important, in the recent years the research and development in tyre technology focuses the studies on the rolling loss, high-speed performance, and ride and handle characteristics of tire. “Rolling loss” is the mechanical energy converted into heat by a tire moving for a unit distance on the roadway [3-4-5]. The lost energy is due to the damp of tyre, this property causes an increase of the temperature, the mechanical energy is converted in thermal energy, and a

reduction of rolling resistance which contributes to the deterioration of the tyre [6], (figure 1).

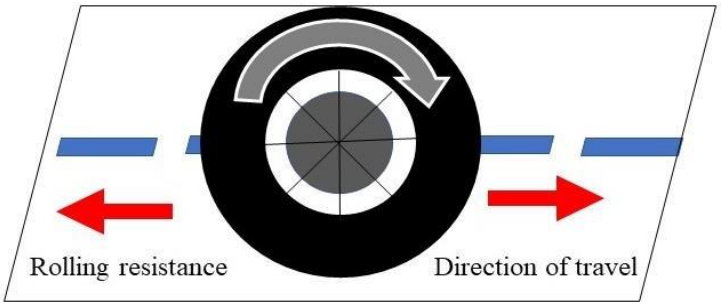

Figure 1 Rolling resistance

The necessity to characterize the dynamic properties is important to study the stress imposes by the air pressure in the tyre. The stress on the cords changes when the tyre is in running condition or not. The stress increase with the air pressure. This phenomenon is also called Flatspotting [4]. The hysteresis cycles were created in order to simulate the deformation that occurs between a low and high strain [7-8-9]. The mechanical properties and the work loss were measured for the raw nylon cords (at different temperature, 20° and 70°) and for the Nylon cords after the treatment with RFL. The mechanical properties evaluation was estimated on the following parameters:

- Breaking load [N] is the force required to break a cord [10];
- Tenacity[cN/Tex] measure the strength of the cords;
- Elongation at break [%] is the elongation deformation until the break of the cord;
- E45N [%] is the elongation at 45N;
- LASE [3%] is the load at specific elongation;
- Free Shrinkage [%] is the percentage value of the shrink due to heat;
- Shrinkage Force [cN] is the opposite force to the shrink;
- Stiffness [cN] is the ability that a material has in opposition to the elastic deformation due to a force [11].

2.1.1 Materials

In the first chapter (paragraph 1.4) mono and multifilament yarns construction (figure 2) were mentioned, in this work different combination of mono and multifilament were characterized. To build a monofilament a polymer is extruded to fabricate a single, flexible, and extra thin, yarn which is characterized by a high tensile strenght and durability but with low flexibility [12]. Thanks to its corrosion resistance, to its ability against the vibration, uniformity and relativity low cost the monofilament construction is used in many chemical and food, medical and automotive industries [13]. Multifilament are built form extruded polymer which is spun out of many spinnerets to form thin filaments [14]. Multifilament is a conjunction of extremely thin monofilaments; this form of yarn is more flexible than a monofilament and is strong and durable [13-15].

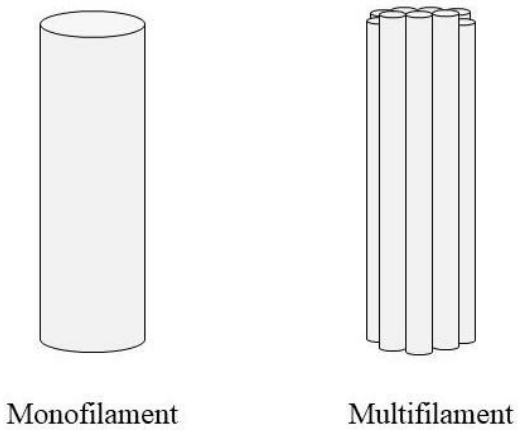

Figure 2 Mono-Multifilament construction

Monofilament and multifilament can be twisted together to form a cord, the materials, tested in this experiment, were four different Nylon 6 cords with the same linear density (2800 dtex) but with different geometry due to a different percentage of monofilament:

- NY-149 (1400 dtex) x 2 (0% monofilament)
- NY-150 (0,23 mm + 940 dtex) x 2
- NY-151 (0,21 mm) x 3 + 1400 dtex
- NY-152 (0,28 mm) x 4 (100% monofilament)

These cords were tested at room temperature, at 70°C and also tested after the classical adhesive treatment using RFL, described in the paragraph 1.5.2.. The dynamometer used to collect all the measures was Zwick Z/10 and all experiments were performed in PIRELLI TYRE laboratories.

2.1.2 Instruments and experimental procedure

To perform the trials on the samples a proline Zwick Z010 [16] (Zwick Roell group, Germany) dynamometer was used, the instrument must be in a conditioned laboratory (20° C, 65 % U.R. ±2). Through the dynamometer was possible to measure the mechanical properties and, thanks to a particular software, the hysteresis cycles were simulated on nylon cords in order to evaluate the work loss. The motor of the tensile machine is a servo motor that works in AC, the 10kN load cell works in compression and the main frequency (power) is between 50 and 60 Hz. Depending on the material and the type of characterization, the choice of the grips is important and the international bureau for the standardisation of man-made fibres (BISFA) gives the rules to follow. The grips to characterize PET/NYLON and RAYON differ from those to measure the mechanical properties on the ARAMID and HYBRID YARNS which contains Aramid, figure 2.

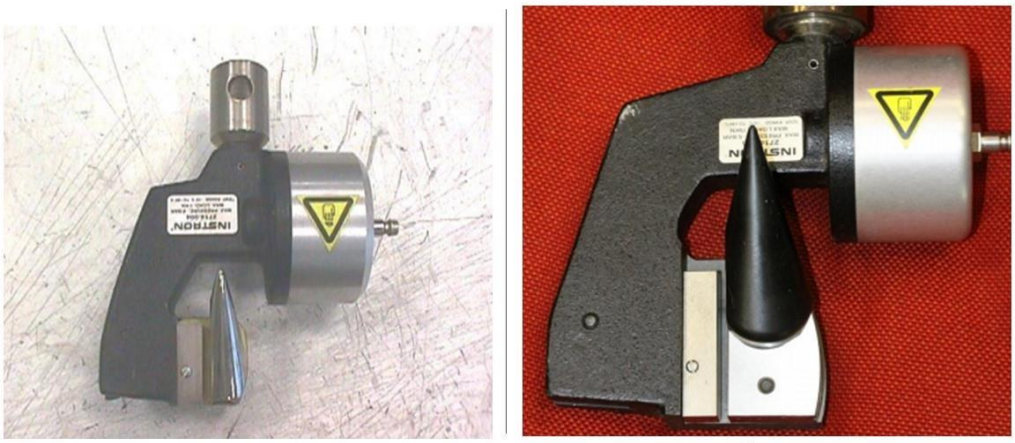

Figure 3 Instrom[17] grips (BISFA)

In this experiment Nylon cords with a different percentage of mono and multifilament were tested, the parameters to prepare the experiment in standard condition were the grips distance, the crosshead speed and the pre-load, table 1.

Table 1 Dynamometer parameters for Nylon

Grips distance	400 mm
Crosshead Section	500 mm/min
Preload	0.5 cN/dtex

The measurement of the mechanical properties at 70° C was possible thanks to an oven which was applicated at the tensile instrument, to perform this characterization at high temperature the preparation of nylon is critical because its thermoplastic characteristics: the grips were inserted in the oven and the thermoplastic sample was blocked in the grips but using a lower pre-load because the shrinkage of the material. The load cell permits to measure the mechanical properties reporting in a graph the load-elongation curves. The same instrument was used to perform the hysteresis cycle, which were also made for the four greige Nylon cord at room temperature, at 70°C and after RFL treatment. Due to the software of the Zwick Roell instrument was possible to create a particular program by

setting the distance of the grips, the crosshead section, the elongation and the number of cycles, table 2.

Table 2 Hysteresis cycles parameters

Grips distance	400 mm
Speed	500 mm/min
Elongation	1%-3%
Cycles	100

The values of elongation were set as minimum and maximum, the cycle starts at 1% of elongation up to 3 % then a new cycle begins for 100 cycles. The shrinkage characterization was carried out through TST 510/250 built by Lenzing Instrument (Austria) [18]. The measure of the free shrinkage and the shrinkage force are possible due to the oven and the 10 measurement channels where the cords is inserted, following ASTM D4974; the percentage and the force are measure thanks to some weights which are hung at the ends of the cords to keep the samples tensioned.

2.1.3 Mechanical characterization and shrinkage measure

The mechanical properties and thermal shrinkage were measured on the Nylon cords, as was mention before the mechanical characterization were performed on four cords at room temperature, at 70°C and after the RFL treatment to evaluate the effect of the temperature and the effect of the RFL treatment; the shrinkage was measured only for the greige cords before and after adhesive treatment. The samples differ for the construction and for the percentage of monofilament and multifilament: the sample NY-152 was composed by four monofilaments (pure monofilament cord), the sample NY-149 was a pure multifilament cords, table 3.

Table 3 Cords composition

NY-152	NY-151	NY-150	NY-149
0.28 mm x 4	0.21 mm x 3 + 1400 dtex	(0.23 mm + 940 dtex) x 2	1400 x 2 dtex

The first step was the characterization of the greige cords with the dynamometer and the thermal shrinkage tester; in each instrument ten measurements were made for each mono/multifilament construction, the parameters of the mechanicals characterization are reported in the paragraph 2.1.2 the TST was set following the ASTM D4974 rules. The table 4 collects both the mechanical and thermal characteristic of the raw Nylon cords.

Table 4 Greige NY cords characterization

NY (RAW)	**NY-152**	**NY-151**	**NY-150**	**NY-149**
Break.load [N]	152 ± 4	178 ± 5	199 ± 4	221 ± 5
Tenacity (cN/tex)	55	66	69	76
Elong.break [%]	19.8 ± 0.8	20.7 ± 0.9	20.2 ± 0.4	22.6 ± 1.0
E 45N [%]	7.7 ± 0.0	7.6 ± 0.0	6.4 ± 0.0	7.2 ± 0.1
LASE 3% [N]	17.8 ± 0.1	17.8 ± 0.1	21.2 ± 0.2	19.1 ± 0.1
LASE 5 % [N]	26.5 ± 0.1	26.9 ± 0.1	33.1 ± 0.2	28.5 ± 0.3
Free Shrink. [%]	6.4 ± 2.3	6.2 ± 0.1	6.4 ± 0.1	7.0 ± 0.1
Shrink.force [cN]	594 ± 10	585 ± 10	667 ± 10	582 ± 16
Stiffness [cN]	55.8 ± 15.9	27.0 ± 8.6	17.2 ± 3.0	12.8 ± 1.5

The analysis on the four Nylon cords show the increase of the breaking load and the elongation at break with the increase of the presence of the multifilament in the yarn's constructions, the behaviour of this mechanical properties is explained by the "Griffith's theory" were is explained the influence of the diameter of a fiber: the larger is the fiber diameter, the lower is the breaking load [19]; the multifilament cords are made up by many small fibers which determinate the high breaking load value. The load at specific elongation (LASE), which evaluate the modulus, is higher for the sample that contains multifilament, in particular the highest value is for the NY-150 made up by two

monofilaments and two multifilament, this means that not only the percentage of mono/multifilament but even the construction of the cord has an influence on the mechanical properties. The free shrinkage is higher for the 100% multifilament construction and is lower for the cord composed by monofilament; the shrinkage force is higher fort the NY-150 this is a confirmation that the construction not only influences the mechanical properties but even the thermal properties. The stiffness is higher for the pure monofilament cord due to the large diameter of the monofilament in comparison to that of multifilament, NY-152 is less flexible [20].

2.1.4 The mechanical behaviour of Nylon cords at 70° C and after RFL treatment

The mechanical properties measured on the greige Nylon cords were evaluated even for the same cord at 70° C and after RFL treatment. For the measure of the properties of the Nylon cords at 70° C some precautions were taken: a lower pre-load, in comparison to the analysis at room temperature, were set; the results are collected in Table 5.

Table 5 Ny cords characterization at 70°

NY (RAW)	NY-152	NY-151	NY-150	NY-149
Break.load [N]	131 ± 2	164 ± 4	174 ± 4	209 ± 4
Δ BL (70°/20° C)	-16 %	-10 %	- 11 %	-8 %
Elong.break [%]	22.0 ± 0.7	23.6 ± 0.6	21.8 ± 0.5	24.2 ± 0.9
LASE 3% [N]	10.3 ± 0.1	13.7 ± 0.1	16.2 ± 0.1	18.5 ± 0.1
Δ LASE 3% (70°/20°) [N]	- 46 %	-24 %	-17%	-5 %
LASE 5 % [N}	17.4 ± 0.1	21.5 ± 0.2	24.6 ± 0.1	27.0 ± 0.2

The values that express some mechanical properties of the cord at 70° C decrease because the thermoplastic characteristics of the polyamide fiber, with an increase of temperature the Nylon cords become more softer and the bonds weaken. The trend of the values is the same of the greige cords at room temperature (table 4). The deltas, calculated between

the breaking load and LASE at 3% at the different temperatures, show how the decrease of the properties is higher for the sample which contains the monofilament. The same properties, which were measured on the un-treated cords, were also made for the cords that underwent the adhesion treatment. The adhesion treatment of the Nylon cords was performed as explain in the paragraph 1.5.2. The results of the dynamometer test are showed in the table 6.

Table 6 Ny + RFL characterization

NY (RAW)	NY-152	NY-151	NY-150	NY-149
Break.load [N]	126 ± 3	117 ± 2	185 ± 2	219 ± 3
Tenacity (cN/tex)	46	41	62	75
Elong.break [%]	15.2 ± 0.2	16.4 ± 1.5	16.9 ± 0.3	21.4 ± 0.3
E 45N [%]	6.8 ± 0.1	6.3 ± 0.0	5.8 ± 0.0	6.2 ± 0.0
LASE 3% [N]	18.9 ± 0.2	20.1 ± 0.1	22.3 ± 0.1	21.2 ± 0.2
LASE 5 % [N]	30.1 ± 0.3	33.0 ± 0.2	37.1 ± 0.3	33.9 ± 0.3
Free Shrink. [%]	4.0 ± 0.1	4.3 ± 0.1	4.3 ± 0.2	4.4 ± 0.2
Shrink.force [cN]	482 ± 20	603 ± 13	566 ± 8	563 ± 1
Stiffness [cN]	83.2 ± 20.0	49.5 ± 17.3	39 ± 11.0	26.0 ± 7.0

The values of the breaking load decrease in the same way of the Ny-cords at 70°, but the values of the LASE are similar than the greige cords at room temperature due to the thermoset process that happened during the RFL treatment. For the same reason the free shrinkage and the shrinkage force decrease, especially for the pure monofilament. The increase of the stiffness is a result of the treatment by Resorcinol-Formaldehyde-Latex [21].

2.1.5 The variation of force with number of cycles

After the mechanical and thermal characterization the four Nylon cords, with the same linear density (2800 dtex) but with different percentage of mono/multifilament, were underwent to hysteresis cycles to measure the work loss (paragraph 2.1) suffered during

a dynamic elongation: the cycle starts at 1% of elongation up to 3 % then a new cycle begins for 100 cycles (table 2). The cycles were simulated thanks a Zwick Z/10 dynamometer and its software that provides the results of the experiment in a graph (figure 4), where the force and elongation are showed concurrently on ordinate axis and the number of cycles is expressed on the abscissa axis. The Nylon construction which was took as example in the graph was NY-150 (0,23 mm + 940 dtex) x 2 cord.

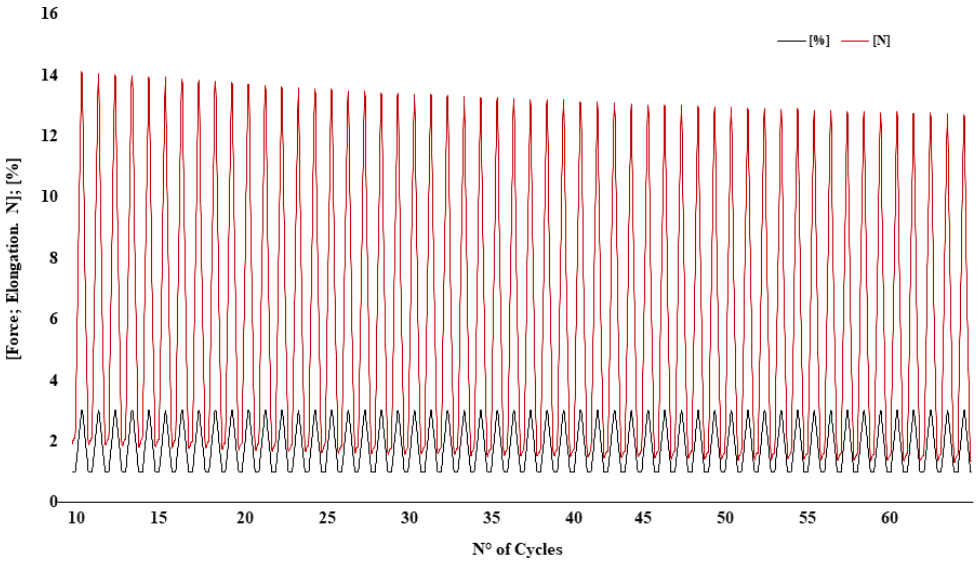

Figure 4 Force/elongation vs N° of cycles NY-150

The force correlated to the elongation decreases with the increase of the number of cycles at the maximum elongation of 3%, the minimum force is pre-set as the elongation. The Nylon 150 shows a good elasticity, but the material is not completely elastic. To evaluate the elastic behaviour of each material the maximum force was measured after 10, 20, 30, 40, 50, 60 ,70 ,80 ,90 cycle (figure 5). The percentage variation of the maximum force, at 3% of elongation, was calculated for the four Nylon cords (table 7), each cord suffered the hysteresis cycles three times.

Table 7 Percentage loss with the increase of cycles

N°of cycles	10	20	30	40	50	60	70	80	90
NY-149	11.02	10.61	10.37	10.19	10.06	9.84	9.67	9.51	9.32
% loss	0 %	4 %	6 %	8 %	9 %	11 %	12 %	14 %	16 %
NY-150	10.42	10.21	10.16	10.09	10.09	10.06	10.05	10.02	9.98
% loss	0 %	2 %	3 %	3 %	3 %	3 %	4 %	4 %	4 %
NY-151	9.79	9.58	9.42	9.31	9.22	9.18	9.12	9.07	9.06
% loss	0 %	2 %	4 %	5 %	6 %	6 %	7 %	7 %	7 %
NY-152	10.25	9.97	9.79	9.67	9.55	9.51	9.45	9.27	9.25
% loss	0 %	3 %	4 %	6 %	7 %	7 %	8 %	10 %	10 %

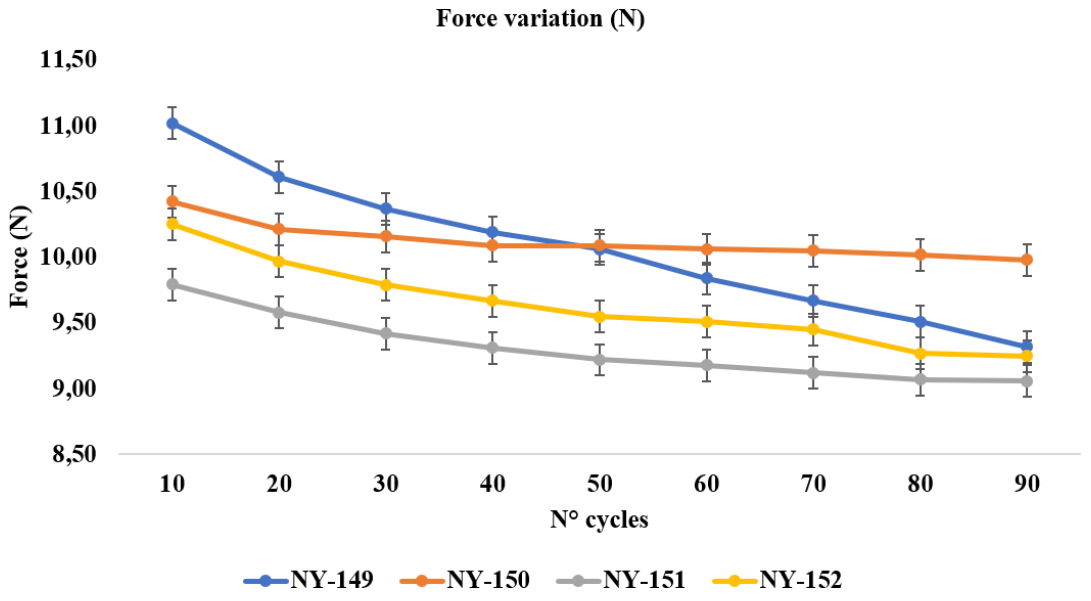

Figure 5 Max force variation vs n° cycles

The pure monofilament and the pure multifilament seem to be the constructions that lose more force with the increase of the cycles, on the other hand the cords which were built both with monofilament and with multifilament seem to lose less force with the increase of the cycle. The cord NY-150 (0.23 mm + 940 dtex) x 2 shows a minimal loss of force. The maximum force for every cycle was measured even after the adhesion treatment (table 8), in particular for the NY-149 1400 x 2 dtex which showed the greatest loss of force (figure 6).

Table 8 NY-149 vs NY-149 RFL force loss

N°of cycles	10	20	30	50	60	80	90
NY-149	11.02	10.61	10.37	10.06	9.84	9.51	9.32
% loss	0 %	4 %	6 %	9 %	11 %	14 %	16 %
NY_149 rfl	9.86	9.78	9.45	9.40	9.37	9.28	9.07
% loss	0 %	2 %	5 %	6 %	6 %	7 %	9 %

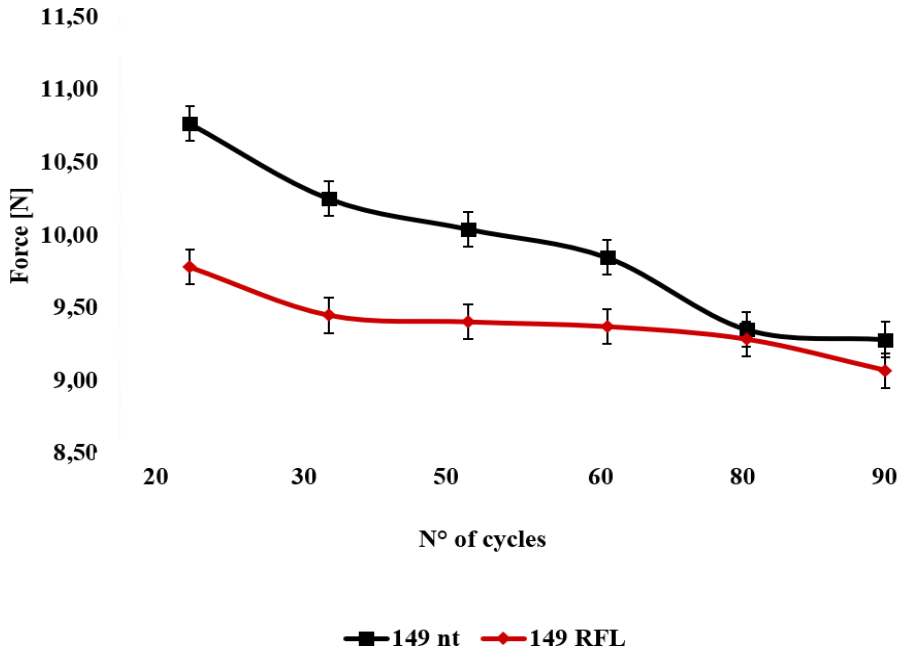

Figure 6 Max Force nt vs RFL

The maximum values of force after the RFL treatment are lower than the NY-149 greige cord tested at room temperature, but the percentage of loss is higher for the greige NY-149. The least loss is probably due to the heat setting treatments that happened during the application of RFL adhesive, during the application of the dip the cord is kept in tension, as was explained in paragraph 1.5.2..

2.1.6 Hysteresis

The variation over time of the force and elongation could be also represented as a graph with the force on axis x and the fixed elongation on the axis y (figure 7). In this kind of graph is possible to identify the cycles and their positive and negative work difference: the hysteresis which quantifies the work loss.

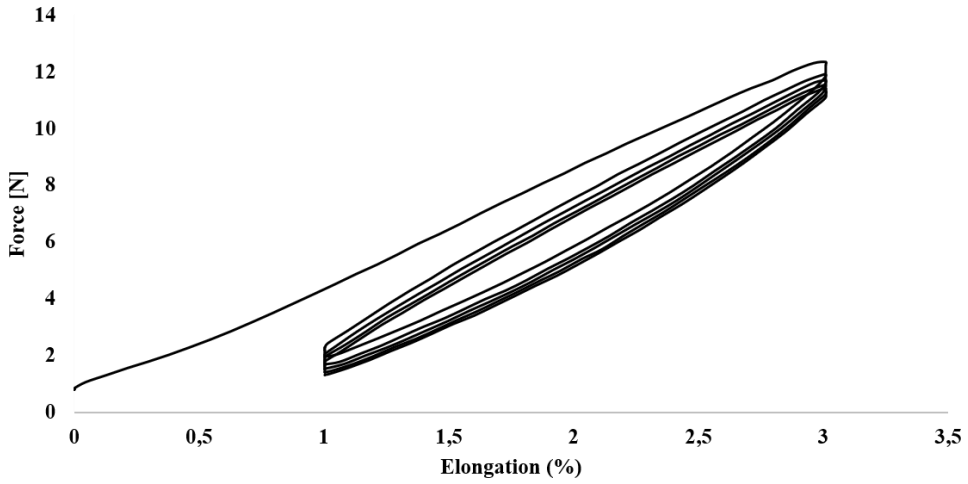

Figure 7 Hysteresis cycles of NY-149

The “positive work” is defined as the integral of the subtended area of the loading phase, while the “negative work” as the integral of the subtended area of the unloading phase. The hysteresis is the resulting area, which was calculated as the difference between “positive work” and “negative work” (figure 8).

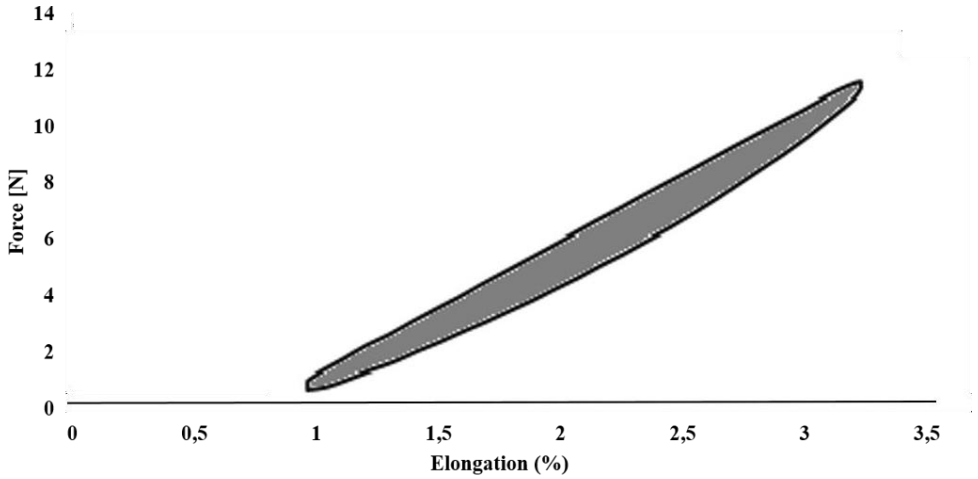

Figure 8 Hysteresis (positive work-negative work)

The "work loss" was calculated for the four cords, each cord suffered the hysteresis cycles three times (table 9). The values are an average of the hysteresis of the three measure of each cords measured in a range of ten cycles.

Table 9 Hysteresis (mJ)

Cycles	NY-149	NY-150	NY-151	NY-152
20-30	**2.45 (±0.10)**	**2.34 (±0.06)**	**2.13 (± 0.05)**	**1.77 (± 0.02)**
50-60	**2.42 (± 0.08)**	**2.23 (± 0.04)**	**2.05 (± 0.06)**	**1.74 (± 0.01)**
70-80	**2.41 (±0.03)**	**2.19 (± 0.03)**	**2.02 (± 0.02)**	**1.67 (± 0.03)**
80-90	**2.39 (±0.02)**	**2.17 (±0.03)**	**2.01 (± 0.04)**	**1.67 (± 0.02)**

The cord construction NY-152 (100%) has the lower hysteresis, NY-149 on the contrary has the highest value of work loss; the other two cords have hysteresis values included between the two extremities. The trend of the hysteresis is due to the reduced extension of friction between the filaments, for this reason the pure monofilament is characterized by a lower work loss. The hysteresis cycles were also made on the other two conditions, which were tested to measure the mechanical properties: at 70° C and after the RFL

treatment; the hysteresis cycles were performed by Zwick z/10. Every type of cord, built with different percentage of multi/monofilament, was tested three times; the resulting trend was collected in a graph, figure 9, with the values of hysteresis on the axis x and the n° of cycles on the axis y. The values of hysteresis are an average between 10 cycles and was measured for three ranges: 10-20, 50-60, 80-90 cycle.

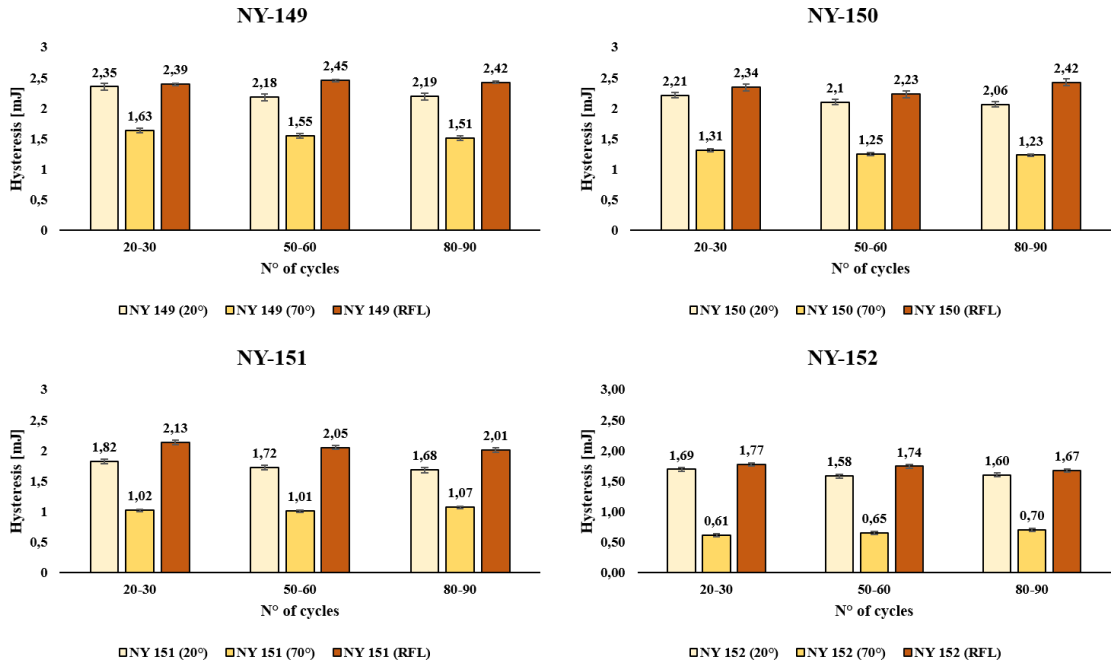

Figure 9 Hysteresis under three different conditions

The values of the hysteresis show how with an increase of temperature the work loss decreases, this is due to the reduction of the modulus as a consequence of the thermoplastic characteristic of the Nylon. The hysteresis is higher for the samples after the adhesion treatment with RFL, because the adhesive acts generates a friction between the filament; for this reason, the hysteresis measured on the sample NY-152 (100% monofilament) suffers less than the other Nylon cords. The general trend of the work loss observed for the Nylon at room temperature is confirmed for the other two conditions (at 70° C and after RFL adhesive treatment).

2.1.7 Conclusion

In these paragraphs, a thermomechanical characterization of four different Nylon cords was introduced and the trials were described. The cords differ for the ratio between the monofilament and multifilament composition, the sample composed by 100% of monofilament (NY 152) and composed by the 100% of multifilament (NY 149) are the extreme constructions; the four cords were tested at 70° C and after RFL treatment. The first part of the experiment was a static measure of the mechanical and the shrinkage properties performed by Zwick Z/10. The breaking load is the highest for the NY 149 and is the lowest for the NY 152 but the pure monofilament has the maximum value of stiffness. The other two sample have intermediate characteristic between the pure constructions. NY 150 is characterized by the highest value of LASE and by a high value of the shrinkage force, this means that with a combination of the monofilament and multifilament is possible to improve some properties and the two extreme conditions not always have the maximum or minimum values of the thermomechanical properties. The properties trend was confirmed even for the cords at 70° C, the changes of the single values is predictable because the thermoplastic characteristic of the synthetic polyamide. The characterization of the samples after the RFL treatment confirm the trend. The adhesive treatment was able to fix same properties, as the LASE values, thanks to the thermoset process that characterized the adhesion treatment for the Nylon; the stiffness is higher for the treated cord than the greige one. The hysteresis of the samples with high percentage of monofilament is lower than the samples with high percentage of multifilament, this is due to reduced extension of friction between the filaments. The dissipated energy of the nylon greige cord at 20° C is higher than nylon cords at 70° C, due to reduction of cords modulus. After RFL treatment the values of hysteresis is greater, due to the increase of friction as a consequence of the applied adhesive.

2.2 The relationship between the interlace and the mechanical properties in hybrid yarns and hybrid cords.

In these paragraphs the second innovative characterization is presented. The work is divided in two parts: in the first part a method to measure the interlace were optimized to discriminated different commingled yarn from different producers. An ASTM method

already exist for the measure of the nodes in a yarn, but the Rapid600v, used for the characterization, is usually used for intermingling yarns formed by less nodes: During the experiment the parameters were optimized for the work purpose and a new method was developed. Then different types of commingled yarn constituted by Aramid/PET were characterized by the measure of the n° of nodes (interlace), the new hybrid yarns differ from each other for the commingling parameters process. New cords were built from the different commingled which were produced from different process parameters, then the mechanical properties of the cords where measured to investigate the relationship with the interlace.

2.2.1 Commingled yarns

Commingled yarn can be defined as a hybrid construction consisting by two different materials (i.e Aramid and Polyester) with a certain linear density. Thanks to an air jet is possible to construct the hybrid yarn, the fibers are mixed to form a continuous filament [22]. The production of commingled yarns is an important resource to develop new thermoplastic composites, these kinds of yarns show significant advantages over thermoset composites in several applications including aerospace, marine, sporting, and automotive industries. The research on this innovative material is focused on the stability and homogeneity of the material [23]. The properties of this hybrid yarn are a middle ground between the two fibers which constitute the yarn. To generate commingled yarns is necessary to produce entanglements between the two different filaments, in the intermingling process is the movement of air, due to an air jet, that produce entanglements or nodes [24]. In the intermingling process two types of filaments enter in the device in two different input points, compress air pushes the filaments up to a mix-chamber where the fibres are opened by an orthogonal air jet. In the mix-chamber happened the creation of nodes between the two fibres that permit the creation of a new hybrid yarn, which is recollected in a new bobbin, figure 10. The parameters of this process are the air pressure, the degree of overfeeding and the production speed [25]; during the experiment the parameters of the process will be changed to studying the relationship between the interlace of commingled, made by Aramid and Polyester, and the properties of the cords constructed from the hybrid yarns. In this work the interlace is defined as the number of

nodes among the commingled yarns, the procedure to construct a cord from a yarn is described in the paragraph 1.4..

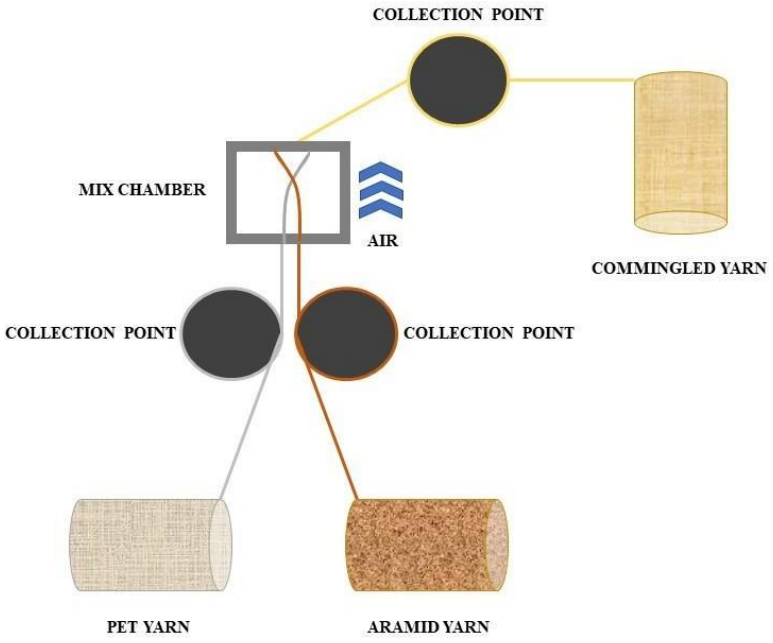

Figure 10 Mingling process

2.2.2 Materials and instruments

In the first part of this work four (PET1100 dTex + ARAMID1100 dTex) commingled yarns built by different producers were used to optimize the measure of the interlacing by the RAPID600v (Lenzing Instrument GMBH & co.) [26]. The RAPID600v permits to measure the number of nodes in a yarn thanks to a needle, which reveals the presence of nodes in the sample, figure 11.

Figure 11 Rapid 600v and the needle

The Commingled enter in the device thanks to compress air jet, which gives the right direction to the yarn, the computer collect the output. It is possible to setting up different input parameters:

- Speed
- Pretension
- Trip-Force (threshold force which permit to locate the nodes)
- Inter-trip (60% of the threshold force which permit to locate the "weak nodes")
- Skip-distance (portion of thread that passes between the exit and the entry of the needle)
- Measure count (n° of cycle)

The output is as follows:

- SP [n/m] the number of nodes for meter
- SPD [cm] the distance between each node
- IT [n/m] the number of nodes which opposed an 60% of Inter-trip force to the needle

ASTM method [27] already exist for the measure of the nodes in a yarn (Table 10), but this equipment is usually used for intermingling yarns formed by less nodes, during the experiment it was decided to optimize the method for the work purpose.

Table 10 ASTM input

SPEED	**2 m/min**
PRETENSION	**32.8 cN**
TRIP-FORCE	**48.9 cN**
INTER-TRIP	**60 % of IT**
SKIPE DISTANCE	**0.5 cm**
N° OF CYCLE	**3**

To investigate the differences between the hybrid yarns the input parameters were changed. After the first part of the experiment, 10 different (PET1100dTex +AR1000dTex) commingled yarn were prepared (table 11). The bobbins were created by changing the parameters of the commingling construction in order to study the relation between the parameters of constructions and the interlace:

- Production speed
- Overfeeding degree
- Air pressure

The new bobbins (figure 11) were created at Sicrem laboratories at Pizzighettone (CR).

Table 11 Variation of the parameters in commingling process

	Production Speed (m/min)	**Air Pressure (bar)**	**Overfeed (%)**	
0	Standard	Standard	Standard	**standard**
1	Low	Standard	standard	**low speed**
2	High	Standard	Standard	**high speed**
3	Standard	Low	Standard	**low Pressure**
4	Standard	High	Standard	**high Pressure**
5	Standard	Standard	Low	**low overfeed**
6	Standard	Standard	High	**high overfeed**
7	Low	High	Low	**Maximum Interlace**
8	High	Low	High	**Minimum interlace**
9	Standard	Low	High	**low P + High Overfeed**
10	Standard	High	Low	**high P+ Low Overfeed**

(The values of the parameters are not explicated due to confidentiality reason)

The 10 different commingled yarns were used to build 10 different cords in order to measure the mechanical properties by Zwick Z/10 dynamometer. The mechanical properties were compared with the measure of interlace measured with the Rapid600v.

2.2.3 Interlace measure

The interlace (n° of nodes) of 4 different (PET1100dTex+AR1100dTex) Commingled yarns built by different producers were measured by ASTM input [27]. The results of the measure by ASTM method give the results which are collected in Table 12 and in figure 12.

Table 12 Interlace measure using ASTM input

(PET1100+AR1100)	SP [n/m]	ST.DEV.
TEST A	70.7	1,9
TEST B	88,5	3,3
TEST C	72,4	1,6
TEST D	70,1	1,9

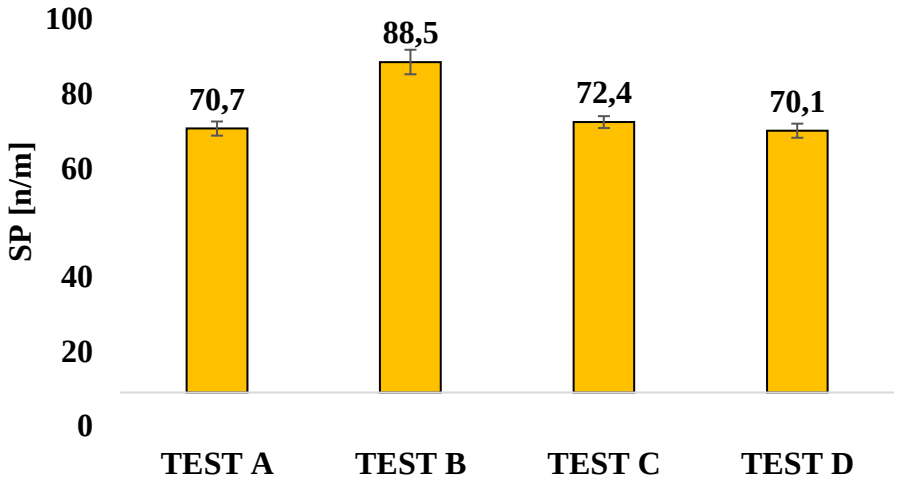

Figure 12 n° nodes for meter

All the commingled yarns were built by the same filament (PET1100 dTex+ Aramid1100dTex) but by different producers, which used different process. As it shown in Figure 12, the Test B presents a high number of nodes, but the other commingled yarns have same number of nodes for meter, to investigate the existence of possible other differences a new input was created to characterize the samples. To create a new method all the parameter of the input was modified, the study focused on the TEST A, then the TEST A (70.7 n/m) were compared with the TEST C (72.4 n/m) these commingled were built by the same producer but using different mixing chamber.

2.2.4 New Input

The first parameter which was analysed was the yarn entry speed, to analyse this parameter the distribution of the distance of nodes was taken into consideration (figure 13): SPD, the distance between nodes expressed in cm. The ASTM input was changed only for the speed value from 2m/min to 1m/min. Test A was taken as reference material.

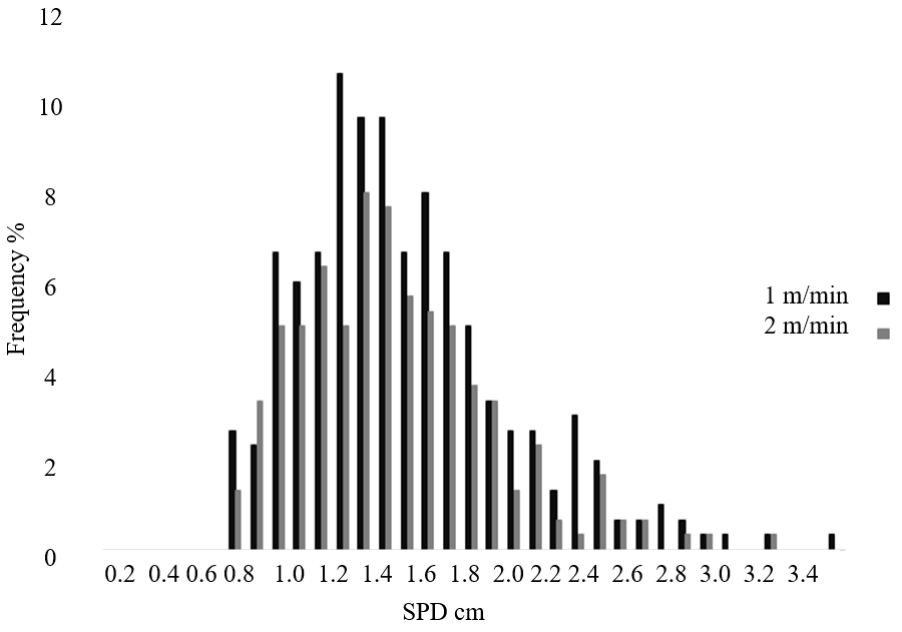

Figure 13 SPD distribution Test A

At the trip-force of 48.9 cN the distribution of the SPD does not change with the two entry speeds tested, but with high values of trip force a slowdown is useful. Two different Trip-force were tested: 15 cN (low trip-force) and 200 cN (high trip-force). With the use of different Trip-force a new output was developed:

- Strong Nodes [n/m]
- Weak Nodes [n/m] the number of nodes which opposed an 60% of Inter-trip force to the needle
- WN/SP the ratio between the weak nodes and the strong nodes

The number of strong nodes and weak nodes for the TEST A are collected in the table 13.

Table 13 Strong nodes and weak nodes for the TEST A

Trip-force	Speed	SN [n/m]	WN [n/m]	WN/SN %
15 cN	1 m/min	91.7 (±1.8)	37.3 (±2.5)	40 %
15 cN	2 m/min	98.1 (±4.4)	27.3 (±11.3)	28 %
48.9 cN	1 m/min	68.8 (±1.8)	8.1 (±1.5)	12 %
48.9 cN	2 m/min	70.7 (±1.9)	6.6 (±2.7)	9 %
200 cN	1 m/min	60.5 (±2.2)	9.7 (±2.2)	16 %
200 cN	2 m/min	60.9 (±2.5)	7.7 (±1.7)	13 %

The data collected in table 13 indicate that, with the entry speed of 1 m/min, the standard deviation is lower than the standard deviation for the other entry-speed tested. The 15 cN trip-force gives many information: the overestimation of the strong nodes and weak nodes is a consequence of the low Trip-force which was used, for this reason the development of the new input will focus on the other two trip-force. The last parameter of the input tested was the skip distance which is define as the portion of thread that passes between the exit and the entry of the needle, every time the needle recognizes the knot it comes out from the filament. Three different skip distances were tested: 0.3 cm, 0.5 cm and 1.0 cm; the larger is the skip distance the lower is the number of nodes for meter (table 14).

Table 14 Skip-distance at 1 m/min

Trip-force	Skip-distance	SN [n/m]	WN [n/m]	WN/SN %
48.9 cN	0.3 cm	89.1 (±2.9)	11.8 (±3.3)	13 %
48.9 cN	0.5 cm	68.9 (±3.7)	8.1 (±2.7)	12 %
48.9 cN	1.0 cm	55.0 (±1.8)	7.5 (±0.8)	14 %

The diminution of the weak nodes is more evident between 0.3 cm and 0.5 cm, the ratio WN/SN % does not change for the skip-distance tested. The standard deviation is lower for the skip-distance of 1.0 cm. In order to define the better skip-distance for the purpose, two tests were compared: Test A (reference material) and Test C which were built by the same producer but with different mix chamber.

Table 15 sk.dist. Test A vs Test B (T.F. 48.9 cN, speed 1m/min)

1.0 cm	SN [n/m]	WN [n/m]	WN/SN
Test C	46,5 (0,6)	6,3 (1,9)	13 %
Test A	48,3 (2,4)	2,9 (1,1)	6 %
0.5 cm	**SN [n/m]**	**WN [n/m]**	**WN/SN**
Test C	63,5 (3,2)	7,1 (1,5)	11 %
Test A	55,2 (2,4)	4,1 (1.3)	7 %

The ratio WN/SN % is higher for Test C in comparison to Test A and this result is the same for both skip distance tested. The skip distance of 0.5 cm permits to distinguish not only the weak nodes but even the strong nodes. After evaluating of the main parameters that characterize the nodes count, the new input was defined (table 16).

Table 16 New input

SPEED	**1 m/min**
PRETENSION	**32.8 Cn**
TRIP-FORCE	**200 Cn**
INTER-TRIP	**60 % of TF**
SKIPE DISTANCE	**0.5 cm**
N° OF CYCLE	**3**

The new input will be used in the second part of experiment to characterize the commingled cords built in Sicrem laboratories using different mingling construction parameters.

2.2.5 Interlace and mechanical properties

The new input and the new output were used to investigate the relationship between interlace (n° of nodes for meter) and the mechanical properties of cords built form the commingled yarns (PET1100dTex+AR1000dTex). As was shown in table 11 ten different bobbins of commingled were prepared in Sicrem laboratories, using different mingling parameters. The Rapid600v measured the number of strong nodes and weak nodes for each bobbin (Table 17).

Table 17 SN and WN for ten different Bobbins

		High speed		Low speed		High pressure		Low pressure		High over feed	
Strong nodes [n/m]		59.4	*1.30*	59.4	*0.8*	63.7	*1.3*	57.4	*0.3*	54.8	*0.5*
Weak nodes [n/m]		5.4	*0.80*	6.3	*0.6*	5.7	*0.8*	5.7	*0.4*	4.9	*1.6*
Weak nodes/Strong nodes %		9%		11%		9%		10%		9%	
		Low over feed		High P – Low over feed		Low P – High over feed		Min Interlace		High Interlace	
Strong nodes [n/m]		66.7	*1.4*	55.6	*0.5*	62.0	*1.3*	52.1	*0.8*	74.7	*0.5*
Weak nodes [n/m]		4.1	*1.1*	5.4	*0.5*	6.9	*0.2*	6.4	*0.3*	5.2	*0.7*
Weak nodes/Strong nodes %		6%		10%		11%		12%		7%	

The bobbin “High Interlace” is characterized by a low speed, high pressure and low overfeed while the “Min Interlace” bobbins is characterized by high speed, low pressure and high overfeed. The commingled yarn that contains a low number of strong nodes has high ratio WN/SN. The mingling parameters which have an influence on the interlace are the pressure (in the mix-chamber) and the overfeed. Ten different cords were built, from the ten different commingled, changing the mingling process, the mechanical properties were measured by dynamometer Zwick Z/10 (table 18). (The cords were built as was described in the chapter 1 paragraph 4.)

Table 18 Mechanical properties

	High Speed		**Low Speed**		**High Pressure**		**Low Pressure**		**High Overfeed**		**STD**	
	X	***Dev.st***	***X***	***Dev.st***	***x***	***Dev.st***	***x***	***Dev.st***	***x***	***Dev.st***	***x***	***Dev.st***
Break. Load [N]	248	*9*	249	*9*	240	*9*	254	*8*	**221**	*11*	245	*8*
Elong at break [%]	3.9	*0.12*	3,9	*0,10*	3,8	*0,12*	4,0	*0,09*	3,8	*0,14*	3,9	*0,12*
Elong.at 45N [%]	0.8	*0.02*	0,8	*0,02*	0,8	*0,02*	0,8	*0,02*	**1,0**	*0,03*	0,8	*0,02*
Elong.at 90N [%]	1.6	*0.03*	1,6	*0,03*	1,6	*0,03*	1,6	*0,03*	1,7	*0,04*	1,6	*0,03*
LASE 1% [N]	54,9	*1,30*	55,7	*1,35*	54,6	*1,21*	56,0	*1,48*	**47,8**	*1,75*	55,5	*1,33*
LASE 3% [N]	182,0	*2,18*	183,6	*2,94*	180,9	*3,04*	183,8	*3,00*	**169,0**	*3,43*	182,9	*2,81*
Free Shrinkage [%]	4,0	*0,1*	4,0	*0,1*	3,9	*0,2*	**4,1**	*0,2*	**3,7**	*0,2*	3,9	*0,1*
Shrinkage Force [cN]	321	*17*	341	*18*	318	*19*	329	*18*	**284**	*18*	328	*18*
	Low Overfeed		**High Pressure-Low Overfeed**		**Low Pressure-High Overfeed**		**Minimum Interlace**		**Maximum Interlace**		**STD**	
	X	***Dev.st***	***X***	***Dev.st***	***x***	***Dev.st***	***x***	***Dev.st***	***x***	***Dev.st***	***x***	***Dev.st***
Break. Load [N]	256	*5*	253	*7*	**228**	*11*	**261**	*6*	**206**	*10*	245	*8*
Elong at break [%]	4,0	*0,08*	4,0	*0,09*	**3,7**	*0,14*	4,0	*0,08*	**3,7**	*0,13*	3,9	*0,12*
Elong.at 45N [%]	0,8	*0,02*	0,8	*0,01*	0,9	*0,04*	0,8	*0,01*	**1,0**	*0,05*	0,8	*0,02*
Elong.at 90N [%]	1,5	*0,02*	1,5	*0,02*	1,7	*0,05*	1,5	*0,02*	**1,8**	*0,06*	1,6	*0,03*
LASE 1% [N]	57,5	*1,00*	58,0	*0,91*	51,3	*2,60*	58,4	*1,02*	**44,5**	*2,41*	55,5	*1,33*
LASE 3% [N]	185,9	*2,00*	185,1	*1,76*	176,9	*4,89*	188,4	*2,74*	**162,3**	*4,22*	182,9	*2,81*
Free Shrinkage [%]	4,0	*0,1*	4,0	*0,1*	3,9	*0,2*	4,0	*11,0*	**3,6**	*0,2*	3,9	*0,1*
Shrinkage Force [cN]	338	*13*	335	*16*	293	*18*	**353**	*13*	**263**	*16*	328	*18*

The mechanical characterization measures different values of some mechanical properties for the ten (PET1100+AR1100) commingled bobbins. For the bobbins which were built to obtain the maximum interlace and minimum interlace the differences are clear, especially for the values of breaking load and the shrinkage force. The parameter that seems to influence most on the mechanical properties is the overfeed: the differences between the bobbins built with low or high overfeed is clear.

2.2.6 Conclusion

A new input was defined in the first part of the experiment, thanks to the new method it's possible to distinguish different constructions of commingled, the four hybrid yarns were built by different parameters process of the commingling process. A new definition for the output was given: Strong nodes, Weak nodes and Weak nodes/ Strong nodes %. Then ten bobbins, which differ from each other for the commingling parameters, were produced. The characterization with Rapid600v gives some information (table 8.):

- The overfeed have a big influence during the production
- The speed production (in the range of values that were taken) doesn't affect the production.
- Due a combination of the commingling parameters is possible to create different condition of interlace: Maximum and Minimum.

From the different bobbins of (PET1100+AR1100) hybrid yarns ten different cords were built and the mechanical properties were measured. The data collected by the zwick Z/10 dynamometer give information about the relationship between the number of nodes and the mechanical properties (table 9.):

- With high overfeed (high number of nodes) condition the breaking load, the modulus and the shrinkage force decrease in comparison with the standard bobbin, built under standard conditions of process.
- With the minimum interlace condition (low number of nodes): the breaking load and the shrinkage force increase, the other parameters remain the same in comparison with the reference bobbin.
- With the maximum interlace condition (high number of nodes): the mechanical properties of the bobbin are completely different in comparison to the standard bobbin. The decrease of the breaking load, modulus and on the thermal properties is evident.

The new input and the new output permit to discriminate different type of commingled yarns built from different producers, which use different parameters. The ratio between the number of weak nodes and the strong nodes is used to distinguish the different commingled yarns. In the second part of the experiment is demonstrated that is possible to predict the mechanical properties of the cord, built from different

commingled yarns. The overfeed is the most influential parameter which determines some mechanical properties of the cords.

References

[1] Barun Kumar Samui, M. P. (2011). Hysteresis characteristics of high modulus low shrinkage polyester tire yarn and cord. Rubber Chemistry and Technology, 84(4), pp. 565-579.

[2] Honold, H. W. (1946). Hysteresis and Related Elastic Properties of Tire Cords. Journal of Apllied Physics 17, 698.

[3] S. Futamura (1987) Effect of Material Properties on Tire Performance Characteristics—Part I. Tire Cords. Tire Science and Technology: July 1987, Vol. 15, No. 3, pp. 198-206.

[4] P.V. Papero, E. K. (1967). Fundamental Property Considerations in Tailoring a New Fiber, 37, 823. Textile research Journal.

[5] Yamamoto, Y. Z. (2007). Tire Sci. Technol. 35, 317

6 Leister, G. (2018). Passenger Car Tires and Wheels [electronic resource]: Development - Manufacturing - Application / by Günter Leister. In Springer eBooks.

[7] Intyre, M. (2005). Nylon, Polyester, Acrylic, Polyolefin. Polyester, acrylic, polyolefin. Material Science

[8] Herbert L. Davis, Michael L. Jaffe, L. LaNieve, III, Edward J. Powers, inventors; Celanese Corporation; Polyester yarn of high strength possessing an unusually stable internal structure. US4101525. 1976 Oct. 26

[9] Howard, W., Williams, W. H. (1967). RUBBER CHEM. TECHNOL. 40, 1139 (1967)

[10] A.N. Gent and J.D. Walter; The pneumatic tyre; published by the National Highway Traffic Saefty, Administration, 2005

[11] Baumgart F. (2000). "Stiffness--an unknown world of mechanical science?". Injury. Elsevier. 31: 14–84. doi:10.1016/S0020-1383(00)80040-6

[12] Textile Engineering: An Introduction. (2016). http://search.ebscohost.com/login.aspx?direct=true&db=nlebk&AN=1289660&site=eds-live

[13] Trevor Sparks, George Chase, in Filters and Filtration Handbook (Sixth Edition), 2016

[14] R. Alagirusamy, A. Das, in Fibrous and Composite Materials for Civil Engineering Applications, 2011

[15] M. Tausif, I. Butcher, in High-Performance Apparel, 2018

[16] Z005 and Z010 materials testing machine; https://www.zwickroell.com

[17] Tensile grips; https://instrom.us

[18] Tst 510/250; https://lenzing-instruments.com/product/tst-510-250/

[19] McGarrigle, Cormac; Rodgers, I; McIlhagger, Alistair; Harkin-Jones, Eileen; Major, I; Devine, D; Archer, Edward. / Extruded Monofilament and Multifilament Thermoplastic Stitching Yarns. In: Fibres. 2017; Vol. 5, No. 45

[20] Metal Matrix Composites T.W. CLYNE, in Comprehensive Composite Materials, 20008

[21] Durairaj, Raj B., Resorcinol Chemistry, Technology and Applications, 2005

[22] T. Gries, M. Raina, T. Quadflieg, O. Stolyarov, 1 - Manufacturing of textiles for civil engineering applications, Thanasis Triantafillou, Textile Fibre Composites in Civil Engineering, Woodhead Publishing, 2016, Pages 3-24, ISBN: 9781782424468

[23] Alagirusamy, R., & Ogale, V. (2005). Development and Characterization of GF/PET, GF/Nylon, and GF/PP Commingled Yarns for Thermoplastic Composites. Journal of Thermoplastic Composite Materials, 18(3), 269–285. https://doi.org/10.1177/0892705705049557

[24] Alagirusamy, R., & Ogale, V. (2004). Commingled and Air Jet-textured Hybrid Yarns for Thermoplastic Composites. Journal of Industrial Textiles, 33(4), 223–243. https://doi.org/10.1177/1528083704044360

[25] Kravaev, P., Stolyarov, O., Seide, G., Gries, T., 2014. Influence of process parameters on filament distribution and blending quality in commingled yarns used for thermoplastic composites. J. Thermoplast. Compos. Mater. 27, 350–363.

[26] https://lenzing-instruments.com/product/rapid-600-v/

[27] https://www.astm.org/Standards/D4724.htm

CHAPTER 3

3-PLASMA TECHNOLOGY APPLICATION ON TYRE REINFORCING MATERIALS

After the first year, which was focused on the study of the different fibers used as reinforcement and the study of adhesion process, from the second year the work is centred on the plasma technology application on tyre reinforcing material. Before to describe the experimental results, which will be shown in the next chapter, a theoretical introduction about the plasma definition and its interaction with the surface are presented. As was mentioned the aim of the thesis is to find an alternative method to guarantee the adhesion between the fiber and the rubber matrix. Today the adhesion is guaranteed by RFL which

gives the requires properties, but the presence of formaldehyde and resorcinol can be a problem because in the future the use of these two chemicals could be limited. For this reason, in the last paragraph the study of the prior art highlights the new methods of adhesion between reinforcement and tyre.

3.1 Definition of Plasma

Plasma are very present in the nature, most of the matter in the universe is constituted by this ionized gas: the surface region of the sun, interstellar gas and the magnetosphere; the lightning is plasma that exist naturally in earth, is due to the creation of potential difference between the cloud and the earth's surface, the air acts as dielectric (figure 1). Plasma is an ionized gas, is generated by heating a gas. Each gas is ionized to a small extent, when a gas is heated the neutral particles collide the charge particles, ion and electron, and plasma is generated. The plasma is defined as the fourth state of matter. [1]

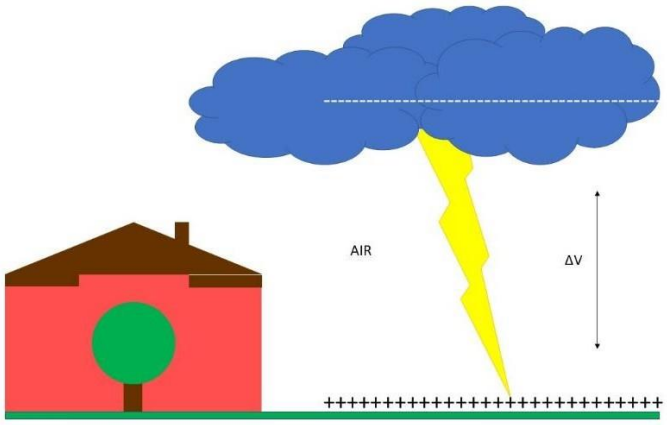

Figure 1 Lightning is a plasma

Plasma is not a classic ionized gas, there are two particular properties that characterize the fourth state of matter: quasineutrality and the plasma parameter. The quasineutrality defines that in a plasma every perturbation of the neutrality must be screenedin a small radius of action, Debye length. The radius is small in comparison with the dimension of the system, which contains the plasma. The plasma parameter means that the number of

the charge particles contain in a sphere with a radius equal to the length of Debay must be >>1 [2]. The typical physical quantities to define a plasma are the Power (W), the electric charge (e) which is the elementary charge of the electron, the energy expressed in eV, the pression (atm, mbar) and the temperature. The temperature is expressed in eV (1 eV = 11600 K), the expression of the temperature in energy derives from the product of the temperature with the Boltzmann constant [3]. Plasma can be divided in Thermal Equilibrium Plasma and in Not thermal Equilibrium Plasma, for the first type of plasma the temperatures are included between 4000 K and 20000 K [4]. In NTEP the temperatures of the different species are not the same, the temperature of the electron is higher than the other particles contain in the gas, the difficulty of energy transfers leads to a no equilibrium; non thermal equilibrium plasma is also called cold plasma (figure 2) [5].

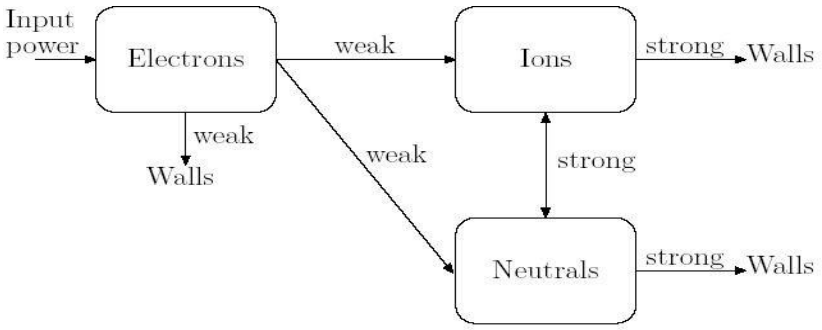

Figure 2 Energy transfer in a cold plasma (NTEP) [6]

From a physical point of view, the equilibrium of particles is defined as the condition for which the speed of the particles is distributed on a curve that is determinated by the temperature, Maxwell-Boltzmann distribution [1]. In figure 3 the electronic temperature of a cold plasma is shown.

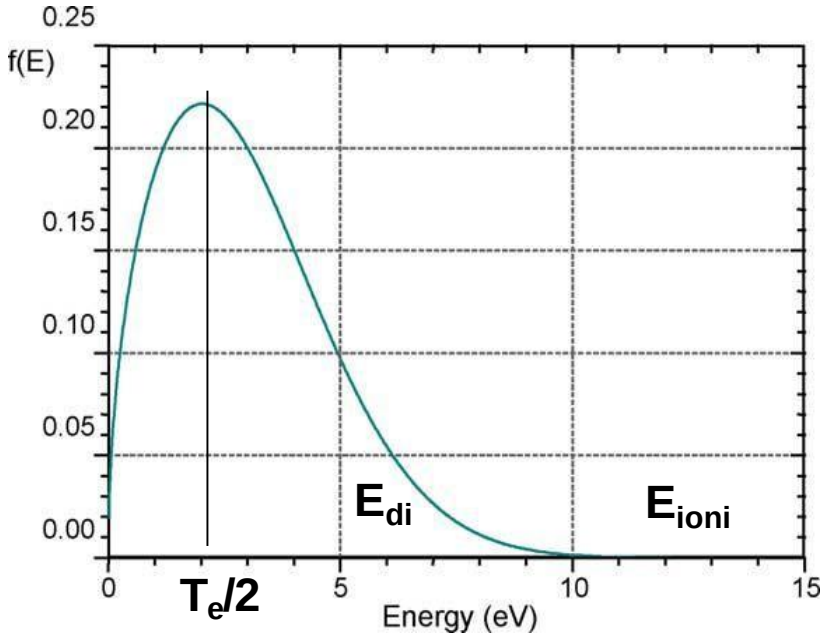

Figure 3 Maxwell-Boltzmann, electronic temperature [6]

3.2 How to create Plasma in a laboratory

Cold (NTEP) and hot (TEP) plasma can be created in laboratory, TEP discharge is used when high temperature is request i.e. cutting, spraying or for evaporation of an analyte, NTEP discharge is used when high temperatures are not required i.e. etching and thin film deposition [5]. In this project cold plasma was created in laboratory, providing energy using a frequency generator; plasma discharge can be happened inside a reactor. The frequency source kicks off the breakdown: every gas has a little percentage of charge particles as a result of the cosmic radiation, when a potential different is applied to the gas the small particles (ions and electrons) collide against the neutral particles which in turn will be charged [7] [8]. The breakdown turns the gas in an ionized gas (plasma). The effects of the process that trigger the collision between the electrons and the heavy particles are resumed in the following equations:

Electron impact dissociation: e + AB -> A + B + e [radical production]

Ionization: e + AB -> AB^+ + 2e [ion production]

Dissociative Ionization: e + AB -> A^- + B^+ + 2e [ions production]

Dissociative recombination: $e + AB^+ \rightarrow A + B^*$ [ions loss]

Dissociative electron attachment: $e + AB \rightarrow A + B^-$ [negative ions production]

The electronic energies involved in the plasma discharge could lead to the breakdown of bonds, table 1.

Table 1 Dissociation energy [9]

Bond	Dissociation Energy (eV)
C-H	4.3
C-O	3.7
C-C	3.7
C=C	6.5
O=O	5.2
H-H	4.5
O-H	4.8
N≡N	9.8

The ionizations process is triggered by the temperature, the ionization energy of some elements is shown in table 2.

Table 2 Ionization Energy

Bond	Ei (eV)
H	13.6
He	24.6
Ar	15.8
O	13.6
C	11.3
N	14.5
F	17.4

3.3 The Plasma-Surface interaction

As was mentioned in the prior paragraph, NTEP could be generated in laboratory in a reactor. In this system a sample could be insert and the new charge particles of the plasma bombs the surface of the sample and, depending on different parameters, gives rise to different interactions, figure 4.

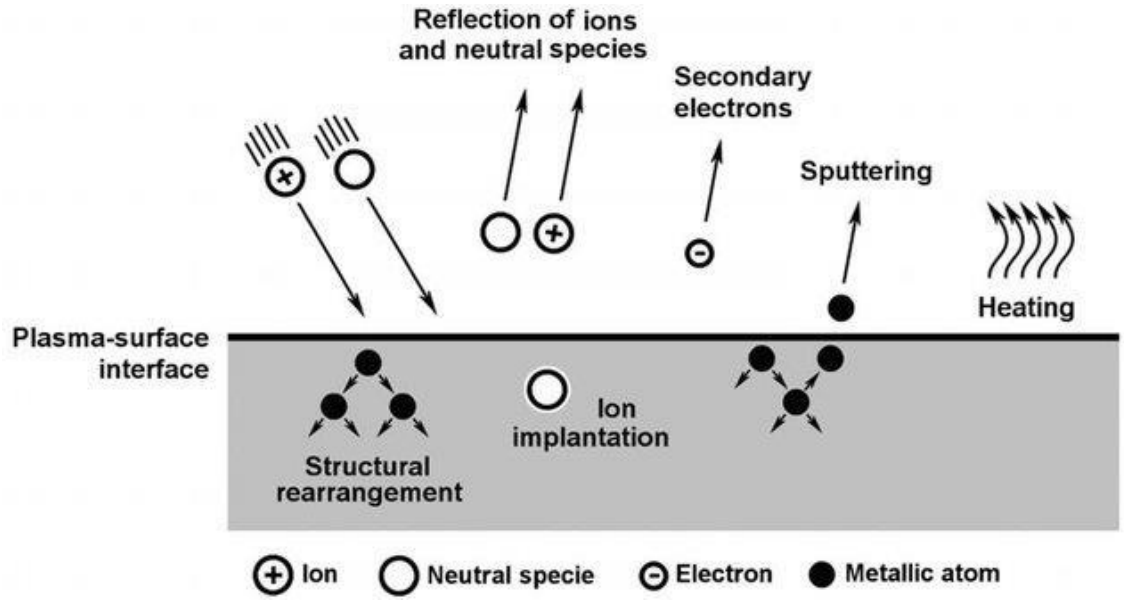

Figure 4 Plasma surface interaction [10]

The interaction of the ionized gas and the substrate are specified by different process:

Electronic bombartment: the collision of the electrons on the surface, the temperature reach values close to 10 eV;

Surface neutralization: is the recombination of ions and electrons that leads to energy production (exothermic process) which conducts in turn to the breaking of superficial bonds;

Formation of radical species

Radiations: plasma emits radiations in the whole spectra region.

Ion bombardment: because of the ionic bombing, the surface loses more electrons than ions; the potential of the surface are lower than the plasma potential, for this reason the surface of the sample attracts ions and rejects electrons [6 8].

The interaction between the plasma and the surface of material makes that this method is a good one to modify the surface properties, i.e. polymer surface to improve the reactivity. Different surface modifications can be made thanks to the interaction between plasma and the surface:

Activation: homolytic rupture of chemical bonds on the surface of the substrate that leads to the formation of radical species.

Cleaning: removal of organic contaminations on the surface, is usually performed with oxygen plasma which is able to remove organic contamination on the inorganic samples but is critical to use when the surface is a polymer.

Etching: as the cleaning, the etching is a removal of surface layers of inorganic or organic material; unlike cleaning, removal is more penetrating and change the surface morphology. The morphology is important because is related to the reactivity, the greater the roughness the more surface area will be available. [11]

Grafting: is the insertion of specific functional groups. Usually the grafting is performed in two different steps: the first step is the plasma activation of the surface; in the second step the activated surface is immersed into the solution which contains the desired functional groups. [12]

PE-CVD: plasma enhanced chemical vapor deposition is a deposition of organic or inorganic thin film, from a gas state, on the surface. [13]

All of these surface treatments don't change the bulk properties of the materials, the treatments are clean because they need only small doses of reagents and don't need solvent. [8]

3.4 Prior art on the application of Plasma on reinforcing materials

During the first year of Ph.D. a bibliography research was completed. The research was focused on the application of plasma technology to improve the adhesion of natural and synthetic fibers. In this paragraph some articles are resumed. In 1984 "The General Tire & Rubber Company" patented a plasma treatment to improve the adhesion of aramid cord, the treatment consisted in the activation using Nitrogen or Argon before a grafting with vinyl pyridine. Plasma treatment was performed in a vacuum system, and in order to have the adhesion the treated cords has to be dipped in RFL after the plasma treatment [14]. In 1990 another patent regarding the improvement of adhesion was registered by Goodyear. In this project two LPPT were applied, the first was a Plasma cleaning, using a mixture of CF_4/O_2 or H_2O/air, followed by a polymerization of CS_2 in order to develop a network that could interact with the RFL [15]. Six years later Michelin propose a plasma treatment which was patented even for the atmospheric condition of the pressure, the power was high, and the treatment time could vary, after the treatment RFL bath is needed [16]. Another strategy to improve the adhesion of the fiber was proposed by Goodyear, in the patent registered in 1996 not only the plasma treatment on the tyre cord was applied but even the rubber suffered modification: the fibers were incorporated in a rubber/blocked isocyanate composition. The plasma treatment was an activation using gas that contains Nitrogen in order to exploit the reaction of the active Hydrogen, of the amine or carboxylic acid, with the isocyanate in the rubber [17]. Carlotti at al. [18] treated PET, a pretty inert polymer, using Ar/O_2 in order to activate the surface for the grafting with RFL. Another interesting work on PET cords was made in 2004 in Slovak technical University [19] : the plasma treatment was performed in a water solution (KOH/NaCl) and the adhesion results were good without the RFL application, moreover the treatment was at atmospheric temperature. One of the conclusions of the cited paper was the importance of the polar group on the surface to reach satisfactory levels of adhesion. The presence of amines also play an important role for the improvement of the polymers surface reactivity [20], an activation or the treatment using a species which contains Nitrogen promote the development of amine species on the surface. The grafting with maleic acid after surface activation (N2) also give good results, the adhesion values are comparable with RFL values [21]. In the paper, which was mentioned before, not only the grafting was experienced but even the plasma enhanced chemical vapor deposition (PECVD) with the same acid,

the thin film has good adhesion values. Goodyear in 2014 registered a patent were metallic cords were treated by plasma using PECVD [22]. PECVD seems to be promising technique, for the number of molecules which could be used to create a reactive thin film and cleanliness of the treatment, in addition being a rather unexplored technique the space to act and find something innovative is wide. For these reasons, to reach the aim of the thesis PECVD was chosen. In the next chapter the molecule choose as precursors and experimental procedures will be presented.

3.5 Plasma polymer

Plasma enhanced chemical vapor deposition is a chemical deposition of a gas, the result of the deposition is a thin film, if the precursor is an organic molecule the coating will be organic. Plasma polymers (PPOL) are materials resulted from the interaction between an electric discharge and organic molecule in form of gas. These polymers are new materials, they differ from the classical polymer with the structural unit, PPOL the chains are short and is difficult to identify a repeating unit: the degree of crosslinking is high [23]. The high level of crosslinking is due to the presence of many free radical (result of the discharge) trapped between chains; but not all of free radicals reacts with the chains of the molecule , some of these reacts, after the plasma treatment, with the oxygen and the water of the atmosphere. The rapid interaction between the free radicals and the atmosphere contributes to the formation of a disordered structure and is a reason why is difficult to perform a PECVD by APP. The mechanism of plasma polymerization is carried on by the reactions between plasma species, plasma-surface species and surface-surface species [24].

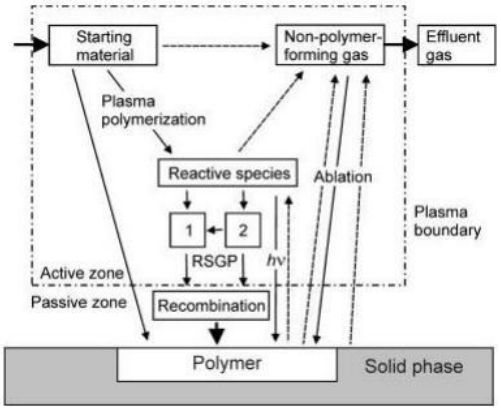

Figure 5 Plasma Polymerization Mechanism [8]

The plasma-polymerization consists in two phases (figure 5): the fragmentation and re-combination process, if the discharge is pulsed during the phase off the molecule is deposited on the surface without fragmentation [25]. Plasma polymerization is governed by amount of energy consumed for units of monomer; the following equation defines R, a parameter that rules the PECVD with organic precursor (equation 1).

$$R = \frac{W\tau act}{pVact}$$

(W = absorbed power; Ƭ = residence time in the active zone; p = atmospheric pressure; V = volume of the active zone)

Equation 1

The fragmentation of the monomer increases with the power density (W/Vact) and the time (Ƭact) density, on the other hand decreases with an increment of power [8]. The R parameter is also defined Yasuda Factor and could be simplify in equation 2.

$$R = \frac{W}{F}$$

W = absorbed power; F = volumetric flow) Equation 2

Depending on the value of R is possible to define two different condition as monomer defect and monomer excess (figure 6).

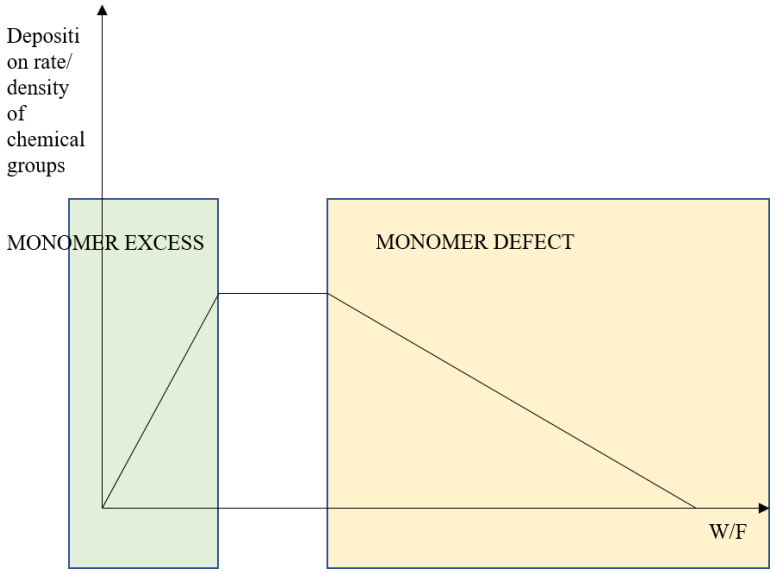

Figure 6 Yasuda Factor

Whit monomer excess the ratio W/F is low as the fragmentation; in this case the plasma polymer deposited has a similar structure to the original precursor. When the monomer is in defect, the ratio W/F is high as the fragmentation, in this case the plasma polymer has a different structure to the original precursor and many functional groups are deposited on the substrate [26].

References

[1] Introduction to Plasma Physics R. J. Goldston, Paul Harding Rutherford; Institute of Physics Pub., 1 gen 1995 - 491

[2] Chen, Francis F. (1984). Introduction to Plasma Physics and controlled fusion. Springer International Publishing. pp. 2–3. ISBN 9781475755954. Archived from the original on 15 January 2018

[3] Gould, R. J. (1972). Boltzmann equation for a photon gas interacting with a plasma. Annals of Physics, 69(2), 321–348. https://doi.org/10.1016/0003-4916(72)90179-0

[4] M.A. Lieberman, A.J. Lichtenberg, Principles of Plasma Discharges and Materials Processing, Wiley, New York, 1994.

[5] Bogaerts, A., Neyts, E.C., Gijbels, R., & Mullen, J.V. (2002). Gas discharge plasmas and their applications.

[6] Carlo Gaifami, Polimerizzazione a plasma di 2-etil-2-ossazolina e 2-isopropenil-2-ossazzolina; 2016

[7] Piel, Alexander, Plasma Physics: An Introduction to Laboratory, Space, and Fusion Plasmas; 2010

[8] Stefano Zanini, Introduzione alla tecnologia del vuoto; 2015

[9] T. L. Cottrell, The Strengths of Chemical Bonds, 2d ed., Butterworth, London, 1958; B. deB. Darwent, National Standard Reference Data Series, NationalBureau of Standards, no. 31, Washington, 1970; S. W. Benson, J. Chem. Educ. 42:502 (1965); and J. A. Kerr, Chem. Rev. 66:465 (1966).

[10] Klein, A. N., Cardoso, R. P., Pavanati, H. C., Binder, C., Maliska, A. M., Hammes, G., Fusao, D., Seeber, A., Brunatto, S. F., & Muzart, J. L. R. (2013). DC Plasma Technology Applied to Powder Metallurgy: an Overview. Plasma Science and Technology, 15(1), 70–81. https://doi.org/10.1088/1009-0630/15/1/12

[11] Hegemann, D., Brunner, H., & Oehr, C. (2003). Plasma treatment of polymers for surface and adhesion improvement. Nuclear Instruments and Methods in Physics Research Section B: Beam Interactions with Materials and Atoms, 208, 281–286. https://doi.org/https://doi.org/10.1016/S0168-583X(03)00644-X

[12] Oehr, C., Müller, M., Elkin, B., Hegemann, D., & Vohrer, U. (1999). Plasma grafting — a method to obtain monofunctional surfaces. Surface and Coatings Technology, 116–119, 25–35. https://doi.org/https://doi.org/10.1016/S0257-8972(99)00201-7

[13] Yasaman Hamedani, Prathyushakrishna Macha, Timothy J. Bunning, Rajesh R. Naik and Milana C. Vasudev; Plasma-Enhanced Chemical Vapor Deposition: Where we are and the Outlook for the Future; November 9th 2015Reviewed: June 20th2016Published: August 31st 2016 DOI: 10.5772/64654

[14] Satish C. Sharma, Mogadore, Ohio; The General Tire & Rubber Company,1984; US4469748

[15] Shuttleworth, Derek Munroe Falls, The Goodyear Tire & Rubber Company, 1980; EP0451425B1

[16] Dennis Bernard, Jean-Luc Cornillon; Compagnie Generale Des Establissments Michelin-Michelin & Cie, 1990; US005411638A

[17] Dane K. Parker, Derek Shuttleworth; The Goodyear Tire & Rubber Company, 1996; US5501880

[18] Stephane Carlotti, Andre Mas, Universite´ Montpellier II, Improvement of adhesion of PET fibers to rubber by AR-OXYGEN plasma; Journal of Applied Polymer Science, Vol. 69, 2321–2330, 1997

[19] M. Simor, H. Krump et al; Atmospheric pressure H_2O plasma treatment of polyester cord thread; Sacta physica slovaca vol. 54 No. 1, 43 – 48, 2004

[20] J. Janca, P. Stahel et al.; Plasma Surface Treatment of Polyester Textile Fabrics Used for Reinforcement of Car Tires; Plasmas and Polymers, Vol. 6, Nos. 1/2, June 2001

[21] Hudec, I., Jaššo, M., Černák, M., Krump, H., Dayss, E., & Šuriová, V. (2005). Plasma treatment and polymerization-method for adhesion strength improvement of textile cord to rubber. KGK Kautschuk Gummi Kunststoffe, 58, 525–528.

[22] Samy Mzabi et al.; The Goodyear Tire & Rubber Company, 2014; US2014/0374009 A1

[23] Biederman, H.: Plasma polymer films. London: Imperial College Press, 2004. ISBN: 1-86094-467-1

[24] Biederman H., Osada Y. (1990) Plasma chemistry of polymers. In: Polymer Physics. Advances in Polymer Science, vol 95. Springer, Berlin, Heidelberg. https://doi.org/10.1007/3-540-52159-3_6

[25] Friedrich, J. (2011), Mechanisms of Plasma Polymerization – Reviewed from a Chemical Point of View. Plasma Processes Polym., 8: 783–802. doi:10.1002/ppap.201100038

[26] Siow, K., Britcher, L., Kumar, S., & Griesser, H.J. (2006). Plasma Methods for the Generation of Chemically Reactive Surfaces for Biomolecule Immobilization and Cell Colonization - A Review. Plasma Processes and Polymers, 3, 392-418.

CHAPTER 4

4-PE-CVD of 2-IOX ON PET MONOFILAMENT TO PROMOTE THE ADHESION

PE-CVD was chosen to improve the adhesion between PET textile cords and the rubber to find an alternative to the Resorcinol Formaldehyde Latex. 2-isopropenyl-2-oxazoline (2-iox) was the organic precursor, which was used for our purpose, the plasma discharge was created in a reactor where two pumps lowered the pressure. Two different strategy were used to treat the PET cord: plasma in continues and pulsed plasma. At first the treatments were performed on polyester sheets, because this surface in easier to characterize than the “target material” (PET monofilament). To evaluate the difference between two discharges the coatings were characterized by the measure of the contact angle, the measure of the thickness and by ATR-IR. After the characterizations of the surface, the adhesion between the PET sheets and the rubber was tested by peeling test. The adhesion test allowed to identify the best treatment which was later done on the PET

monofilament. The comparison between the monofilament covered by plasma coating and the monofilament dipped by RFL was evaluated by the coverage degree, with optical microscopy, after the CRA. In the second phase of experiment, to strengthen the stability of the monofilament and the coating, two different pre-activation were tested: chemical epoxy activation and plasma activation by argon. Plasma activation followed by 2-iox coating gives comparable results to the adhesive treatment with RFL. To complete the characterization an XPS analysis and TEM were made during the experiment. In this chapter the experimental procedures and the results were collected.

4.1 Monomer: 2-isopropenyl-2-oxazoline

The molecule used for the PE-CVD was 2-isopropenyl-2-oxazoline characterized by the presence of oxazole, a heterocyclic organic compound, and the isopropenyl in position 2, figure 1.

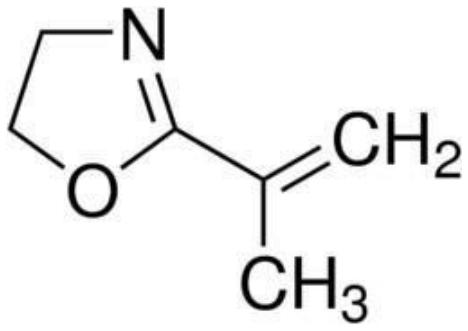

Figure 1 2-iox

The presence of the oxazoline ring guarantees high reactivity, during the fragmentation the presence of nitrogen and oxygen can lead to training new functional groups which could contains nitrogen and oxygen groups and polar group. All of the species which were mentioned seem to be important for the promotion of the adhesion according to the authors mentioned in the paragraph 3.4. As said previously, the presence of the isopropenyl group is also mandatory, the doble bond has an important role during the plasma discharge because the reactivity of this kind of bond with the radical active species, which was created on the surface by the particles bombing [1-2]. The 2-iox, as other

derivates of oxazoline (i.e. 2-ethyl-2-oxazoline), are stable polymer, water soluble, biocompatible and no-toxic. Thanks to these peculiar characteristics they have many uses for different application as pharmaceutical, medical application and the conservation of cultural heritage (as the pigment binder) [2-3]. Oxazoline derivates (in a water solution) was used to promote the adhesion, of textile fiber and rubber, as a subcoat before the application of the RFL [4].

4.2 Materials

The material, used as the subject for the increase of adhesion, was PET polyethylene terephthalate, 1.3.3. This material is characterized by a low reactivity due to the position of the ester group, which is not aliphatic, the mechanical behaviour of PET is a combination between the characteristic of Nylon (high strength and elongation) and the Rayon (modulus) [5]. PET is pretty inert and even in the classical chemical treatment a pre-dip is necessary to activate the surface of the polymer, for this reason polyethylene terephthalate is more challenging. The aim of this work is to improve the adhesion between a cord of PET, in form of monofilament, and the rubber with the use of plasma technology. Monofilament is also a challenging construction due to its geometry and smooth surface, which makes it even more difficult the adhesion. To simplify the study of the treatment parameters, at first the thin films were deposited on a PET sheet because it's easier to handle during the preparation and the characterization. The sheets (figure 2) were built with the same polymer used for the construction of the "target material" with the following dimension: 127.0 mm x 12.5 mm x 3.00 mm.

Figure 2 PET sheet

To treat the monofilament, diameter 0.44 mm, was necessary to construct a frame (180 x 250 mm), as a sample holder (figure 3). The monofilament is framed in the sample holder, which was inserted in the reactor where the plasma discharge happened.

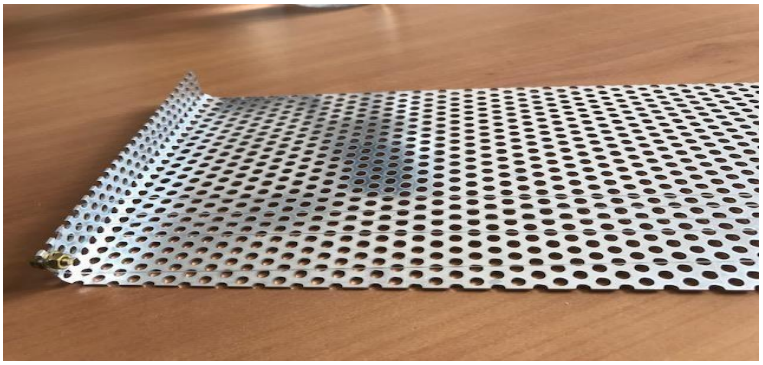

Figure 3 Frame

In a single treatment is possible to treat 180 cm of monofilament cord.

4.3 Plasma reactor

The plasma was created in laboratory in a reactor, figure 4. The reactor is composed by a stainless-steel chamber (diameter 30 cm) that contains parallel plates which work as electrodes.

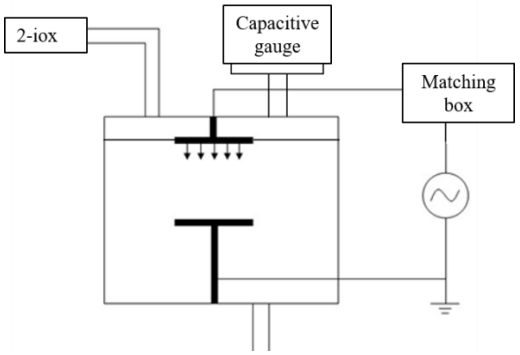

Figure 4 Reactor

The upper electrode is fixed to the plasma antenna that connects the reactor with the radiofrequency generator, 13.56 MHz. The lower electrode also works as sample holder, the sheets and the frame are place on top. Before to apply the plasma discharge, is necessary to reduce the internal pressure of the chamber, where the gas is fragmented. The pressure is reduced thanks to two pumps: rotary vane pump and turbomolecular pump. The rotary pump is a mechanical type pump that provides cyclical operation where the zone in which is desired to create the vacuum is put in communication with a low pressure zone filled with the gas to be expelled, thanks to the pump is possible to reach 10^{-3} Pa. Turbomolecular pump is able to reach the pressure inside the chamber up to 10^{-8} Pa, the pump is composed by a rotor and stator which have inclined vanes. The vanes spin and hit the gas until its compression [6-1]. When the precursor of the PE-CVD is organic, is necessary to place a liquid nitrogen trump before the rotative pump, this component is important to prevent the contamination of the oil with the monomer. In this experiment the treatments were made using 2-isopropenyl-2-oxazoline with variable parameters of power and duty cycle, time and flow were kept constant (these two parameters were optimized in the MSc thesis [1]). The 2-iox vapour is introduced in the system by a micrometric valve, the flow of the 2-iox is measured, before and after treatment, with weighing (equation 1).

$$F = \left(\frac{g}{PM}\right)\frac{22400cm^3}{t}$$

Equation 1 (F= 2-iox flow; g= 2-iox consumed during the treatment; PM=molecular weight of 2-iox; t= is the treatment time in minutes)

During the experiment another gas is inserted in the chamber: Argon, an inert gas necessary to activate the surface. The flow of Ar is regulated by a flow meter managed by a computer connected to the chamber.

4.4 Deposition of 2-iox strategy

Two different strategies were followed to treat the PET monofilament. The coating was deposited in a continuous plasma regimen and in a pulsed plasma regimen, the variables of these treatments were the power (W), for the continuous one, and the duty cycle for the pulsed discharge. In this paragraph the two strategies were described, as was mentioned in the previous paragraph the flow (of 2-iox and Ar) and the time treatment

were kept constant following the results of MSc thesis:

Ø(2-iox) = 3 sccm; Ø(Argon) = 2.3 mln/min; time treatment = 20 min

4.4.1 Continuous PE-CVD

To find the better condition to improve the adhesion of PET, five different plasma treatments were performed on the polyester sheets in continuous plasma regimen. The 2-iox was fragmented and recombined using different power condition: from 20 W to 175 W (table 1). To activate the surface before each PE-CVD a pre-activation using plasma Argon was completed.

Table 1. Tested power

Sample	Tested power (W)	Plasma Act.
PC-1	20	60 s 100 W Argon
PC-2	50	60 s 100 W Argon
PC-3	90	60 s 100 W Argon
PC-4	130	60 s 100 W Argon
PC-5	175	60 s 100 W Argon

During the plasma discharge in continuous regimen the 2-isopropenyl-2-oxazoline is constantly fragmented in the "middle zone" the recombination occurs in the area close to the sample [7]. The flow of 2-iox is kept constant, following the Yasuda Factor rules (paragraph 3.5) with low values of power the thin film should have a similar structure to the 2-iox, with high values of power the molecule is completely fragmented so the structure should have different from the monomer.

4.4.2 Pulsed PE-CVD

The second strategy followed to find the better condition to improve the reactivity of PET was a pulsed plasma discharge. The most important parameter is the duty cycle: the fraction of time a system goes from active to inactive; the phase on and the phase off are alternated with a defined frequency: 100 Hz in our experiment (figure 5). The variable of the PE-CVD, as was mentioned, is the duty cycle and in the trials varies from 10 % to 75 %. The percentage indicates the phase on [1].

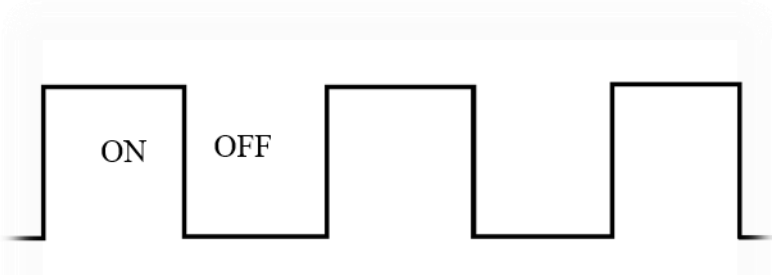

Figure 5 D.c. phase on and phase off

During the phase-on the molecule is fragmented and recombined, as was described for the continuous plasma discharge, during the phase-off is expected that the retention of the molecules happened. Four different treatments were tested (table 2), the 2-iox flows at the same time of Argon, used to help the activation of the surface the power was kept constant for each treatment (175 W)

Ø(2-iox) = 3 sccm; Ø(Argon) = 2.3 mln/min; time treatment = 20 min

Table 2 Tested d.c.

Sample	Tested D.C. (%)	Power
PC-6	10 %	175 W (2-iox+Ar)
PC-7	30 %	175 W (2-iox+Ar)
PC-8	50 %	175 W (2-iox+Ar)
PC-9	70 %	175 W (2-iox+Ar)

With low values of d.c., low effective power, is desirable that the structure of the plasma polymer could be similar to the structure of 2-iox, on the other hand using high values of d.c. high fragmentation is expected [8].

4.5 Coating characterization

In this paragraph the theorical aspects of the surface characterizations are explained, all of these are performed on the polyester sheets. The wettability was measure by the contact angle with water, the functional group and the species on the surface are investigated by ATR-IR, another surface characterization was performed using XPS and the thickness of the coating was measured by the profilometer.

4.5.1 Contact angle

The contact angle (c.a.) is a thermodynamic quantity, which describes the angle between two phase, liquid-solid or liquid-vapour or liquid-liquid. The c.a. defines the wettability of the surface with a liquid, the adhesion forces and the cohesion forces determine the degree of wettability. The degree of wettability of a surface is also defined by the Young relation (equation 2) [9-10].

$$0 = \Upsilon_s - \Upsilon_{sl} - \Upsilon_l \cos\Theta_{sl}$$

Equation 2 Young-relation solid-liquid

θ_{sl} is the static contact angle between the two dimension of tension solid-liquid and liquid-vapor and is represented by the tangent line to the outer surface of the drop; the vertex of the angle is identify in the three-phase point (figure 6). From a thermodynamic point of view θ_{sl} is the quantity that minimize the surface free energy of the system: the

balance of the horizontal force acting on the drop [1].

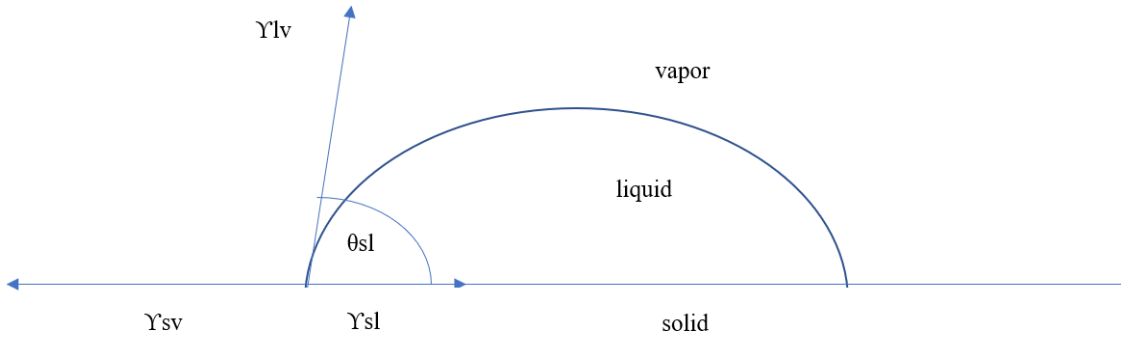

Figure 6 Static contact angle

On the basis of the measure of the contact angle with water, is possible to define surfaces hydrophobic or hydrophilic; if the value of the c.a. is greater than 90° the surface is hydrophilic if is less of 90° is hydrophobic. Two other definition of surface exist depending on the contact angle: if the contact angle measures more than 150° the surface is superhydrophobic, if the value is close to 0° the surface can be defined as superhydrophilic [11]. In order to measure the wettability of the coating the c.a. was measured, after the application on the surface of 3 µl, by Dataphysics OCA 20 instrument at room temperature. The result of this characterization will be presented in the next paragraphs, the c.a. values considered are the average of 5 measures.

4.5.2 Profilometer

To study the relationship between the variation of power or d.c. and the thickness, a profilometer Bruker DektakXT was used. The thickness characterization was carried out on silicon wafers, treated at the same time with the PET sheets, thanks to a mask that permits to locate the "step" (figure 7).

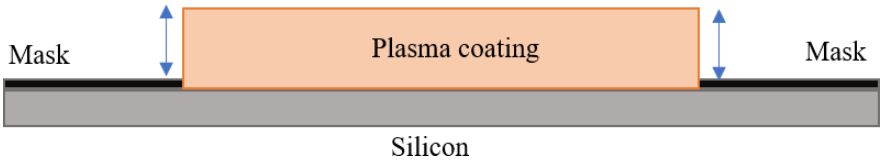

Figure 7 The step for the measure of thickness

The characterization is possible thanks to a diamond-tip that runs over the sample, the movement is both in vertical and horizontal directions. A camera allows to choose where to start the measure of thickness, the camera is assembled on the tip and is possible to rule the movement by a "joystick". The thickness variations are analysed by a software and the values are returned on a graph.

4.5.3 ATR-IR

The IR spectroscopy was used to characterize the coating in order to understand the chemical structure and the functional group located on the surface. This vibrational spectroscopy depends on the vibrational energy provided by an infrared radiation to a molecule, the IR supplies information at molecular level [12]. Molecules have different vibration modes: stretching and bending (figure 8).

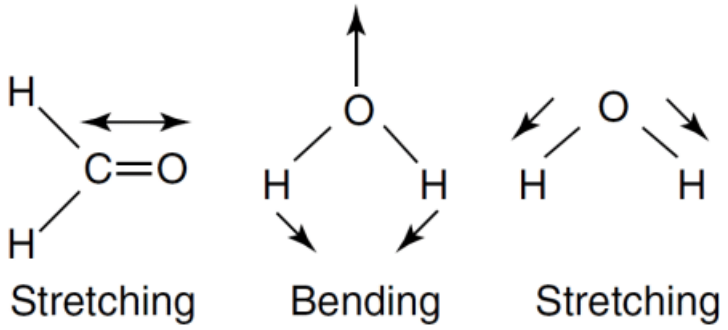

Figure 8 stretching and bending[13]

The stretching is the change in length along the bond, this vibrational mode could be symmetrical or asymmetrical; the bending vibrational mode is due to the variation of the bond angle. Thanks to IR spectroscopy is possible identify the different functional groups which are deposited on the surface with the PE-CVD; each functional group vibrates at specific frequencies the IR active modes are identifiable in infrared spectra (700 nm- 1 mm). The sampling approach used was the Attenuated Total Reflectance (ATR), this technique allows to examine the sample in solid and liquid phase. The sample is in contact with a crystal, the signal of the source is reflected on the surface and evanescent field is generated. The oscillating field is projected on the sample and penetrates it with a thickness in the order of nanometres, a part of the energy is absorbed by the sample and the reflected radiation reaches the detector which generates the reflectance spectrum [14-15]. For the experiments Infrared Nicolet Avatar 360 FTIR equipped with PIKE Miracle ATR, the analysis range is between 4000 and 650 cm^{-1} and the spectras were acquired using different scans depending on the material; 16 scans were used to characterized PET surface and 32 scans for the aluminium, to limit the noise. The resolution was maintained

constant at 2 cm^{-1}. This characterization was used to study the variation of the chemical species on the surface depending on the variation of power and duty cycle.

4.5.4 XPS

X-ray photoelectron spectroscopy (XPS) was used to identify the elements that cover the surface of the treated PET sheet, with this technique is also possible to identify the chemical state and bond state; XPS exploits the photoelectric effect to identify the elements. The surface of the sample is irradiated by the monochromatic x-ray source, the photons interact and create interactions on the surface this effect is called photoelectric effect. The final result of the interaction between the source and the surface is the ejection of an electron with a certain kinetic energy which is correlated with bond energy (equation 3) [15-16].

$$Eb = hv - (Ek + \phi)$$

(E_b is the binding energy, hv is the photon energy, E_k is the kinetic energy and Φ is the work function)

Equation 3 photoelectric effect, Binding energy

The source is an x-ray tube, composed of a filament crossed by a current with a lower potential than the grid in front of it. The filaments produced electrons which are accelerated towards the anode and collide thanks to an aluminium sheet, the electrons that penetrate the sheet lose energy and emit x-ray. The x-ray emission creates electron vacancy, the vacancy is covered by another electron radiative transition correlated to the release of a photon with the same energy of the atomic levels involved [15]. XPS was used in our experiment to evaluate the 2-iox ring opening in different duty cycle situations. The analysis was performed by a Perkin-ElmerΦ5600-ci spectrometer using Al Kα radiation (1486.6 eV). The sample analysis area was 800 □m in diameter. Survey scans were obtained in the 0−1350 eV range (187.8 eV pass energy, 0.8 eV step-1, 0.05 sec step-1). Detailed scans were recorded for the C1s, O1s and N1s (23.5 eV pass energy, 0.1 eV step-1, 0.1 sec step-1).

4.6 Adhesion characterization

The adhesion characterization was performed both on sheets and on monofilament of PET using two different method: for the sheets was a Peeling test, which was built specially for these samples, for the monofilament a CRA test was performed. The reference adhesion values were that of sheets and monofilaments treated in classical chemical way (epoxy bath + RFL), these samples were prepared at Sicrem (Glanzstoff group) the most important supplier of Pirelli. In the preliminary phase the adhesion was measured with and without RFL to study the coating also as a pre-dip and to define the best treatment to apply on the "target material". The optical microscopy was used to evaluate the coverage of the monofilament after the CRA test. In order to compare the uniformity of the coating and the adhesive, TEM images were acquired.

4.6.1 Peel test

The test is performed by tension machine, dynamometer, and measures the peel resistance of adhesive bonds between flexible adherends by means of a T-type specimen (paragraph 1.7). The Peel strength is the average load per unit width of bond line required to separate progressively a flexible member from a rigid member or another flexible member [17-18]. The peel test was carried out exclusively on the PET sheets:

- PET untreated
- PET soluble polyfunctional epoxides blocked with isocyanate (pre-dip) + RFL
- PET treated by plasma using different duty cycle + RFL
- PET treated by plasma using different power + RFL
- PET treated by plasma using different duty cycle

The preparation of the samples for the test was made in Sicrem, three sheets were prepared for each plasma treatment to study the 2-iox coating as a pre-dip (figure 9).

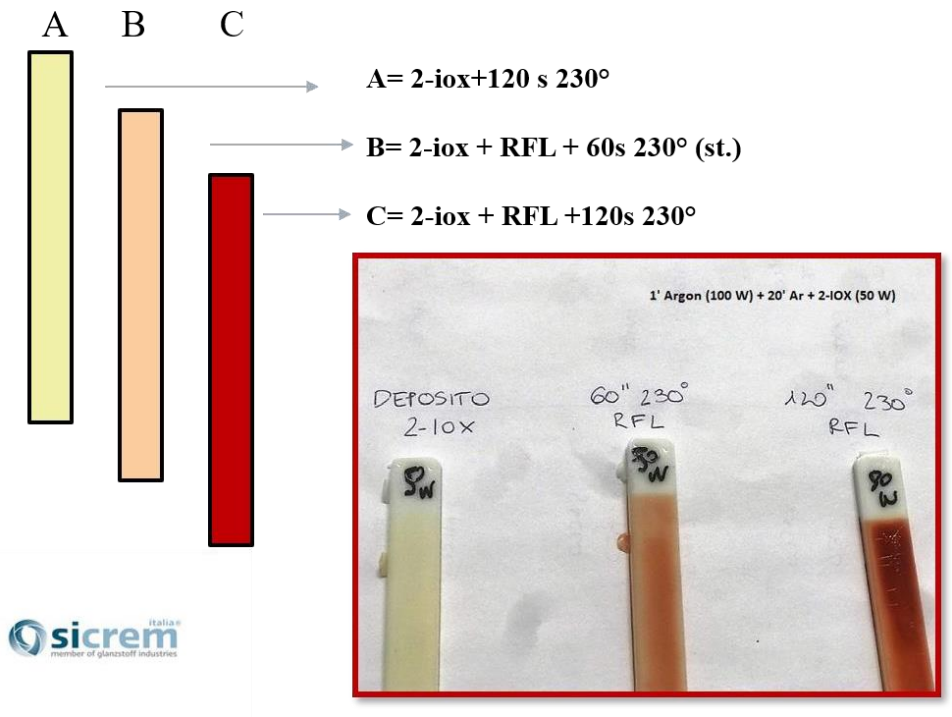

Figure 9 Sample preparation

The plasma treated sheet was put in the oven in order to study the influence of the annealing on the adhesion (A), the procedure B was made using the classical chemical treatment for the fiber, but using plasma treatment as pre-dip; the procedure C was longer and warmer because the size of the sheets. In order to study the plasma coating as adhesive, and not as pre-dip, no other preparations are needed and, after the plasma treatment, the sample is ready to be vulcanized for the test. All of the samples prepared was vulcanized using the standard compound which is used to perform the same test on the fibers (FZG), the pressure (8 bar) and temperature (151° C) were maintained for 40 minutes. After cooling the samples, the peel test was carried out using ZwickRoell Z/10 with the following parameters (table 3):

Table 3 Peel test parameters

Sample Height	100 mm
Grips Distance	122.3 mm
Test Speed	100 mm

4.6.2 CRA

To evaluate the adhesion on the PET monofilament treated by PE-CVD of 2-iox, CRA test was performed. The treated fibers are arranged and fixed in a mold as shown in figure 10, the white fibers are the untreated PET the “yellow” are the 2-iox treatment fibers.

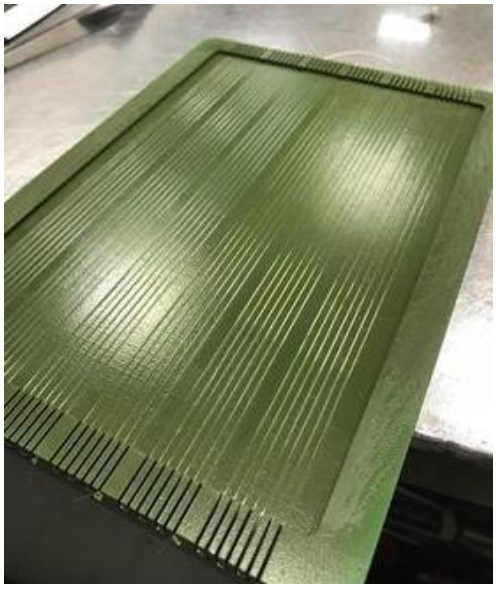

Figure 10 Monofilaments in the mold

After the arrangement of the monofilaments, the mold is covered with a sheet of compound (30% poly 1,3-butadiene and 70% synthetic rubber cis-1,4-polisoprene) which is covered in turn with a Mylar; the covered mold is put in a press, to proceed with vulcanization, using the same parameters used for the peel test preparation (4.6.2). After the cooling of the compound the samples were prepared and tested using ZwickRoell Z/10. The adhesion is evaluated with the maximum extraction strength between the compound and the treated monofilament and with the coverage, the rubber residue on the yarn after the treatment; the degree of coverage is estimated with the following scores (table 4):

Table 4 degree of coverage

Score	Degree of coverage
5	≤ 100%
4	≤ 75 %
3	≤ 50 %
2	≤ 25%
1	≤ 15%
0	= 0%

.

The maximum score indicates excellent adhesion: after the extraction the compound residues completely cover the monofilament. The lower score indicates that no residues remained on the yarn. The CRA test was performed on the monofilament which suffers the best adhesion plasma treatment, identified after the study on the PET sheet. The reference sample (PETmono + epoxy + RFL) and other monofilaments, which were activated in different way, were tested using CRA.

4.6.3 TEM

The transition electron microscope (TEM) is an electronic microscopy, in the project TEM was used to evaluate the uniformity of the coating in comparison to the adhesive. The electrons of the beam crossed vacuum section and the pass through the sample, the sample has to be very thin, between 50 nm – 500 nm [19]. The resolution of the TEM is greater than that the SEM. The equipment consists in three essential systems: the source of electrons which is an electron gun; the lens, the movable sample holder and the intermediate and projector lens are the image-producing system; the last system is the image-recording, which consist in fluorescent screen that permits the permanent records [20]. The transition electron microscopy used in our experiments is JEOL JEM 2100 Plus with a LaB_6 source and can work at acceleration voltages between 80 e 200 kV. The technology was exploited to collect the images of the PETmono untreated, PETmono treated by chemical classical way and PETmono treated using plasma.

4.7 Results - Coating

In this paragraph the results, the values collected after characterizations and the images that were taken are collected. The 4.7 paragraph has the same structure of the previous

paragraph: at first the coating characterization are presented and then the adhesion results are presented too; contact angle measure, thickness, ATR-IR and XPS were performed on the PET sheets, which were also characterized by Peel test.

4.7.1 a Contact angle, continuous 2-iox Plasma Enhanced Chemical Vapor Deposition

Different sheets which were treated in continuous plasma regime were characterized by Dataphysics OCA 20 instrument at room temperature, following the procedure described in the paragraph 4.5.1. The sheets were preactivated in the same way (60 s at 100 W of plasma Argon) but suffered the PE-CVD at different condition of power, from 20 to 175. The time treatment and the flow of 2-iox and Argon was kept constant: time treatment 20 min, Ar Ø 2.23 mln/min, 2-iox Ø 3 sccm. The values of the contact angle are the average of 5 values collected for each sample (table 5), three sheets were prepared for each coating. The contact angle of the 2-isopropenyl-2-oxazoline was experimentally measured with the same instrument.

Table 5 C.A° continuous Plasma (Ar+2-iox)

Power (W)	Contact Angle (°)	St.Dev.
PET untreated	86.9	± 1.2
20	71.2	± 2.1
50	71.1	± 0.9
90	67.8	± 1.4
130	72.6	± 3.2
175	81.2	± 3.4
2-IOX (Monomer)	18.7	± 0.7

The values of the measured contact angles indicate that the coating increases the hydrophilicity of the PET sheets, except for the values at 175 W, the C.A. values are included in a range from 60° and 70°. At 90 W the contact angle shows the maximum hydforphilicity due to the high fragmentation, which allows the formation of polar groups that modify the surface energy. The high angles measured in comparison to the c.a. of the monomer informs that the plasma fragmentation already occurs at low power,

and even at 20 W (low power) the retention does not occur. To evaluate the stability of the coatings in continuous regime the wettability was measured again after five days and after rinsing it in water (table 6).

Table 6 ageing and rinsing

Power (W)	Contact Angle (°)	St. Dev.
20	67.4	2.2
50	65.4	2.3
90	60.5	2.7
130	70.0	3.8
175	82.2	3.5

The ageing and the rinsing do not significantly modify the wettability, coating created in continuous regime seems to be stable.

4.7.1 b Contact angle, pulsed 2-iox Plasma Enhanced Chemical Vapor Deposition

Different sheets treated in pulsed plasma regime were characterized measuring the wettability, estimated with the measure of the contact angle. The instrument used was Dataphysics OCA 20 and the values were collected at room temperature with the procedure described in the paragraph 4.5.1. The variable of the treatments in pulsed plasma is the duty cycle; power was maintained constant at 175 W, the time treatment and the flows of the gas were the same used in continuous regime. Three sheets of each different coating were prepared in order to measure the contact angle (table 7).

Table 7 C.A pulsed plasma (mix AR+2-iox)

Duty Cycle	Contact Angle (°)	St.Dev.
PET untreated	86.9	± 1.2
10 %	22.8	± 1.8
30 %	62.9	± 0.6
50 %	65.5	± 1.9
70 %	66.9	± 0.5
175 W (100 %)	81.2	± 3.4
2-IOX (Monomer)	18.7	± 0.7

The values of the C.A increase up to 70% of d.c., the coatings increase the wettability of the sheets, the values are included between 60° and 68° except for the coating at 10 % (Weff= 17.5 W). The plasma polymer obtained at 10% of d.c. has values very similar to the monomer, that indicates that the power combinated with the low d.c. is not enough to open the oxazoline ring and fragment the molecule and, thanks to the high phase-off, the retention is favourited. The ageing and the rinsing were studied in the same way applied to the samples obtained in continuous regime (4.7.1a) the C.A values are collected in the table 8.

Table 8 ageing and rinsing (pulsed plasma)

Duty Cycle	Contact Angle (°)	St.Dev.
10 %	31.2	± 3.2
30 %	66.1	± 1.2
50 %	65.6	± 1.0
70 %	67.7	± 2.1
175 W (100 %)	82.2	± 3.5

The ageing and the rinsing do not have great influence on the coating, the low increment of the C.A. for the lower duty cycle tested is probably due to a partial hydrolysis of the oxazoline ring [2].

4.7.2 Thickness

The Bruker DektakXT instrument was used to measure the thickness of the coatings deposited on the silicon wafers which suffered the same treatment of the PET sheets. Three silicon wafers of each coatings were characterize measuring the thickness (table 9).

Table 9 thickness of continuous coatings

Power (W)	Thickness (nm)	St.Dev.
20	235	± 14
50	357	± 15
90	364	± 10
130	503	± 10
175	448	± 20

The values indicate how the increment of the power increases also the thickness, the tabled values, compared with those collected in table 7, show that the increment is also related to the fragmentation: at high power the active species are more and higher is the thickness. The same conclusion can be done with the values collected for the coatings obtained with a pulsed PE-CVD (table 10).

Table 10 Thickness of pulsed coatings

Duty Cycle	Thickness (nm)	St.Dev.
10 %	202	± 10
30 %	334	± 15
50 %	417	± 10
70 %	426	± 15

4.7.3 ATR-IR

The coatings were characterized by IR spectroscopy using Infrared Nicolet Avatar 360 FTIR equipped with PIKE Miracle ATR. To identify the characteristic peaks of 2-isopropenyl-2-oxazoline, IR profile of the monomer was collected [1]. The spectrum of the 2-iox (monomer) was compared with the spectrum of the coating obtained at 10% of d.c. (figure 11), because the values of the c.a (table 7) indicated similarity. Both spectras were collected on aluminium sheets in order to avoid the overlapping of the 2-iox peaks with them of the PET. At 1662 cm^{-1} is possible to recognize the characteristic peak of the doble bond Carbon-Nitrogen, and at 3000 cm^{-1} the peaks of the stretching of the CH_x, these two peaks are clearly identifiable in both spectra. At 1182 cm^{-1} is the peak of the bending of CO [21] which characterizes the oxazoline ring, this peak is recognizable even in the spectra of the coating of 2-iox, the plasma polymer obtained at 10% of d.c. maintains in its structure the oxazoline ring. The peak relative to the doble bond C=C is not identifiable because the reaction of the doble bond with the radical species formed during the discharge.

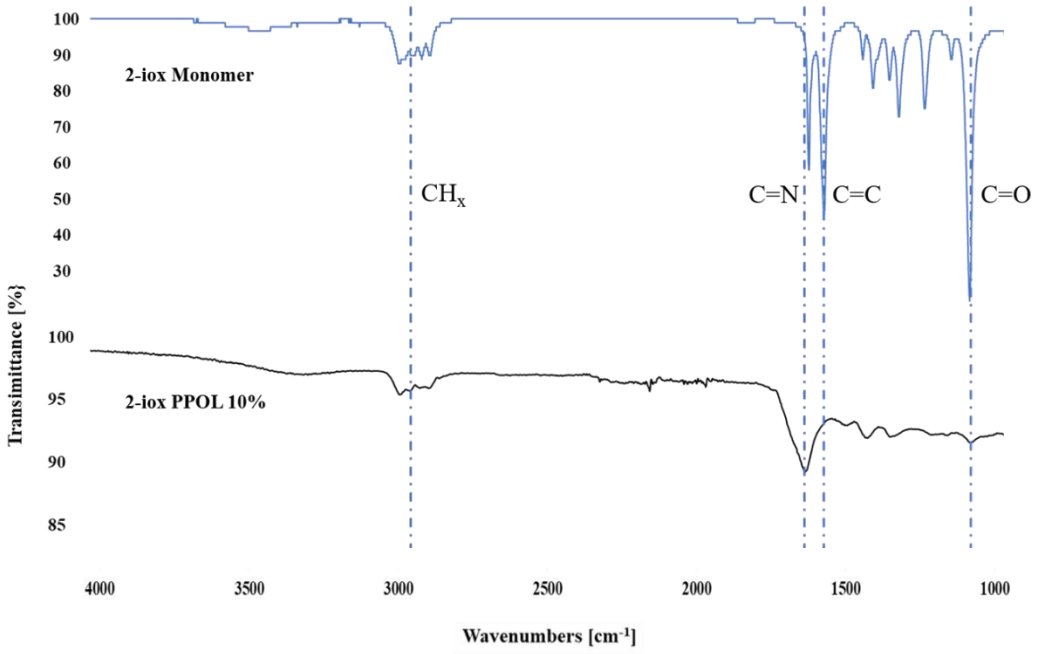

Figure 11 ATR-IR 2-IOX vs 10% d.c. plasma

Increasing the duty cycle the spectra of coating changes, as expected after the contact angle measurement (table 7). In the figure 12 the spectra of the coating obtained at 50%, in pulsed plasma regime, is shown. The 50% d.c. spectra is representative for all coating obtained in pulsed regime with a duty cycle bigger than 10%. The first indication is the lost of the characteristic peak of the CO, this means that the oxazoline ring is open. Small peaks appear in the zone between 2300-2200 (isocyanate area) and a swelling of the profile is recognizable in the region of 3100-3800 cm^{-1} (-OH and -NH stretching), these groups, as reported by authors [22-23], improve the adhesion. A little shift occurs in the zone of the C=N, the neighbourhood changes. The peaks relative to the C=N and CH_x, characteristic of the 2-isopropenyl-2oxazoline monomer, remain recognizable [21].

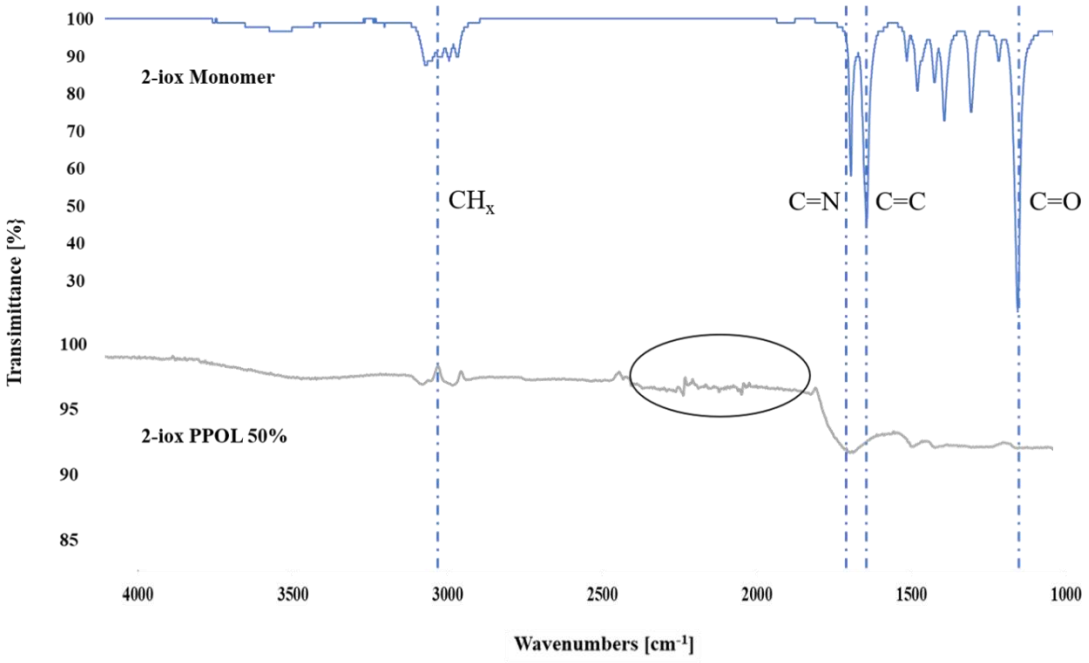

Figure 12 ATR-IR 2-IOX vs 50% d.c. plasma

The surface analysis was also performed on aluminium sheet covered by coating obtained in continuous plasma regime. The ATR-IR spectra indicates a high level of fragmentation of the molecule, the transmittance is intense, and the background noise is not negligible. In the figure 13 the spectra of the coating deposited at 90 W (series in green), in

continuous regime, is taken as an example and is compared with the monomer and the coating obtained with a plasma deposition at 10% (series in red) of duty cycle. Some of the characteristic peaks of 2-iox are recognizable as the swelling in the area of -OH and -NH (3100-3800 cm^{-1}) and the peaks of the CH_x stretching (3000 cm^{-1}). The peaks in the 2300-2200 cm^{-1} area are more evident in the 90 W coating than that obtained in pulsed regime, the shift in the zone of the C=N indicates that the chemical structure is changed and the peak of the CO is no longer recognizable. Other peaks are identifiable in the 90 W spectra profile, the degree of fragmentation is very high. The Yasuda Factor (paragraph 3.5) of the sample obtained at 90 W (continuous regime) is 26.5, the oxazoline ring is broken; the Yasuda Factor of the coating obtained at 10 % (pulsed regime) is 5.5, the oxazoline ring is maintained.

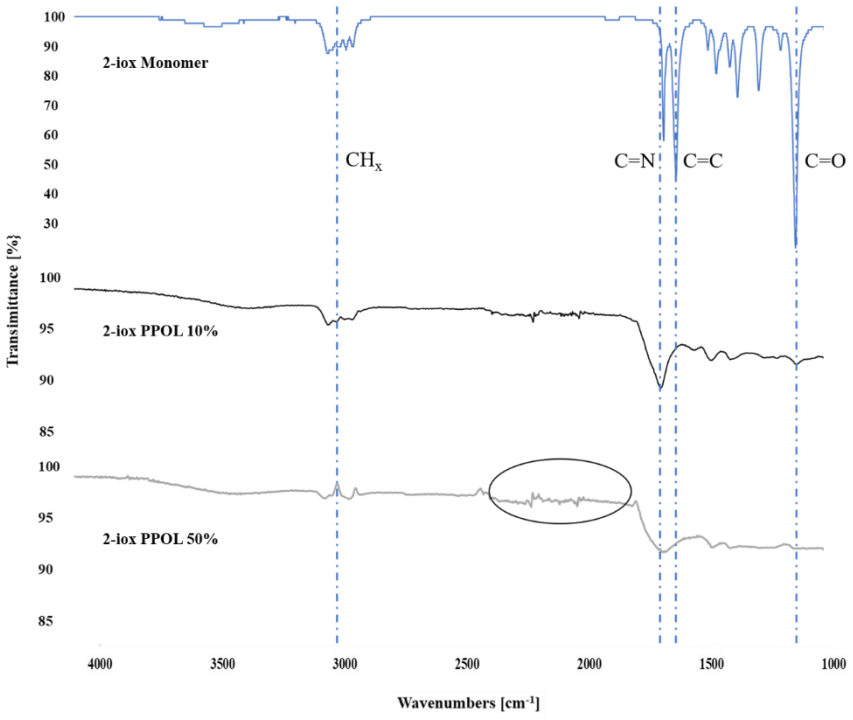

Figure 13 Comparison of spectra of "continuous coating" and "pulsed coating"

ATR-IR characterization was carried on after the annealing of the coating, in order to study the effect of the temperature on the thin films. The annealing happens during the preparation of the samples for the peel test, this process was performed at Sicrem (paragraph 4.6.1). Two examples are proposed in the figure 14, 90 W coating and 10 %

coating, in the figure the spectra are compared before and after the annealing at 230° C for 120 s. The temperature does not seem to have a great influence on the surface composition of the coating.

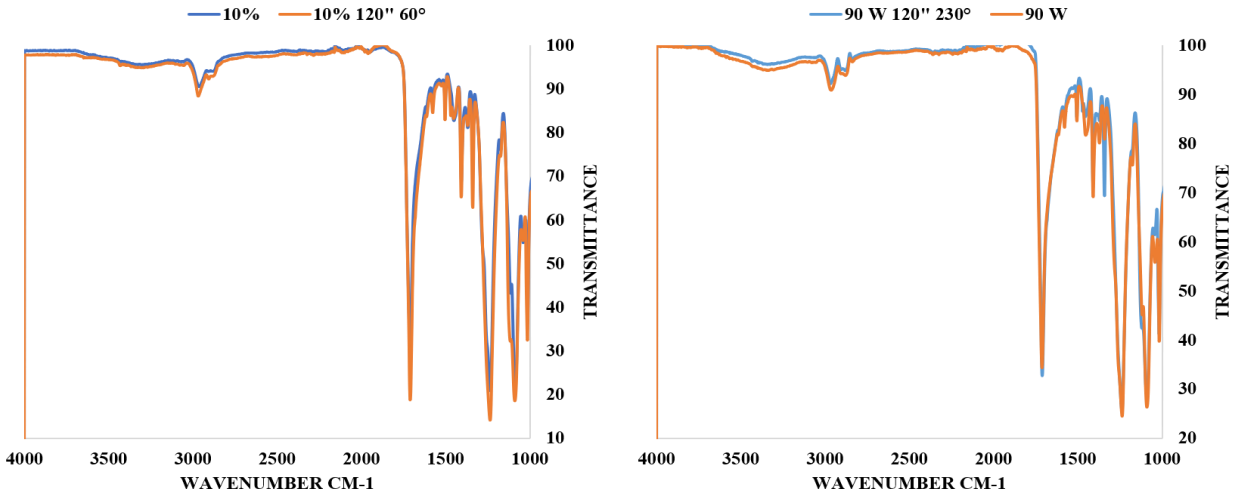

Figure 14 ATR-IR annealing 10% and 90W

4.7.4 XPS

XPS analysis was performed by ICMATE-CNR, the images were taken from the report. The analysis was used to identify the difference between the pristine (PET), the 10 % d.c. coating, the 50 % d.c. coating and the coating obtained in continuous regime at 175 W. The first indication of the analysis was the success of deposition, the Nitrogen was not present in the pristine but was recognized in the other three samples (table 11). The difference between the coatings are not so clear because “the noise” of the substrate where the coating was deposited, the most important indication is the increase of the fragmentation with the increase of the power: the percentage of the carbon increases with the power, the percentage of oxygen and nitrogen decreases with the power. The C-O contribution, characteristic of the oxazoline ring, decrease its percentage with the increment of fragmentation and this aspect is more evident if it’s compared with the contribution of the C element contribution (figure 15).

Table 11 Element %

Element	C			O		N
Sample	**C-C C=C**	**C-O**	**O-C=O**	**C-O-C**	**C=O**	
Pristine	83.4 %			16.6 %		/
	74.1 %	5.7 %	3.6 %	8.4 %	8.2 %	/
10 %	73.9 %			12.5 %		13.6 %
	47.1 %	19.2 %	7.6 %	6.3 %	6.2 %	
50 %	76.7 %			10.7 %		12.6 %
	53.0 %	17.3 %	6.4 %	5.3 %	5.4 %	
175 W	77.9 %			10.2 %		10.9 %
	55.1 %	18.7 %	4.1 %	5.1 %	5.1 %	

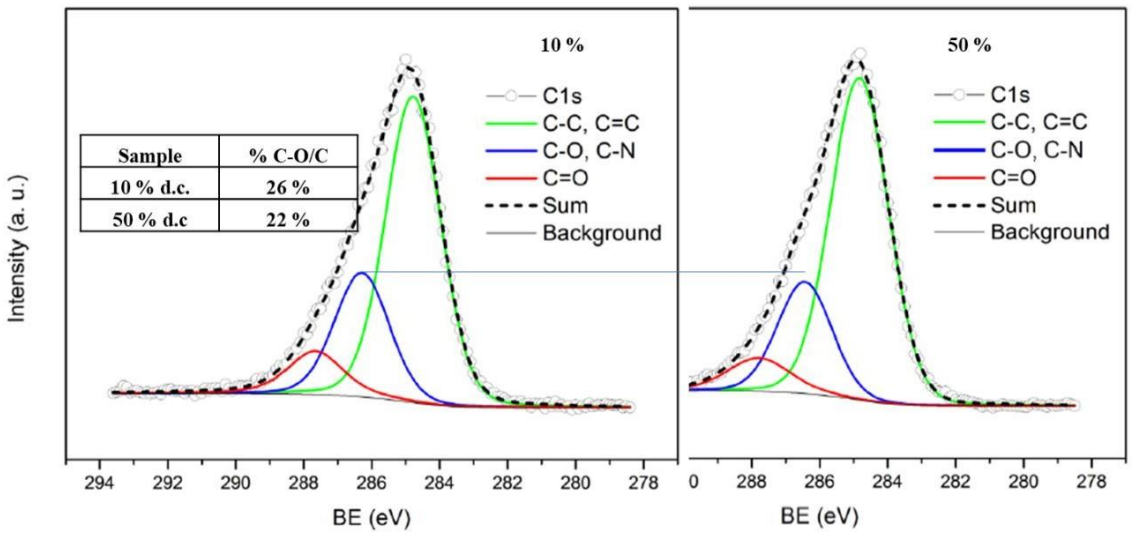

Figure 15 CO vs C %

4.8 Result – Adhesion

In this paragraph the results of the adhesion characterizations are presented. At first Peeling test on different coatings deposited on the PET sheets was carried on to define the best treatment condition to guarantee the adhesion between the reinforcement and the matrix (rubber), then the CRA test was made on the monofilament that suffered the best plasma treatment, defined in the phase 1. In order to observe the different between the plasma coating and the adhesive, TEM images were collected.

4.8.1 Peel test

Peel test was made on the PET sheets as was described in 4.6.1 paragraph, different coatings obtained in different plasma condition were tested; different samples was prepared for each treatments condition in order to study the effect of the temperature on the adhesion and to study the coating also as a pre-dip. The different coating is reported again in the following tables (table 1 and table 2).

Table 1 Tested W

Sample	Tested power (W)	Plasma Act.
PC-1	20	60 s 100 W Argon
PC-2	50	60 s 100 W Argon
PC-3	90	60 s 100 W Argon
PC-4	130	60 s 100 W Argon
PC-5	175	60 s 100 W Argon

Table 2 Tested d.c.

Sample	Tested D.C. (%)	Power
PC-6	10 %	175 W (2-iox+Ar)
PC-7	30 %	175 W (2-iox+Ar)
PC-8	50 %	175 W (2-iox+Ar)
PC-9	70 %	175 W (2-iox+Ar)

Untreated PET and PET sheet treated using the chemical classical treatment (epoxy bath + RFL) were used as references to evaluate the positive or negative effect of different plasma polymer deposited. The results of the adhesion test are presented in this paragraph by means of tables and graph, the adhesion is expressed as average Force and max Force. Max Force (figure 16) refers to the average of the peaks with higher values and it is identified on the graph Force vs deformation.

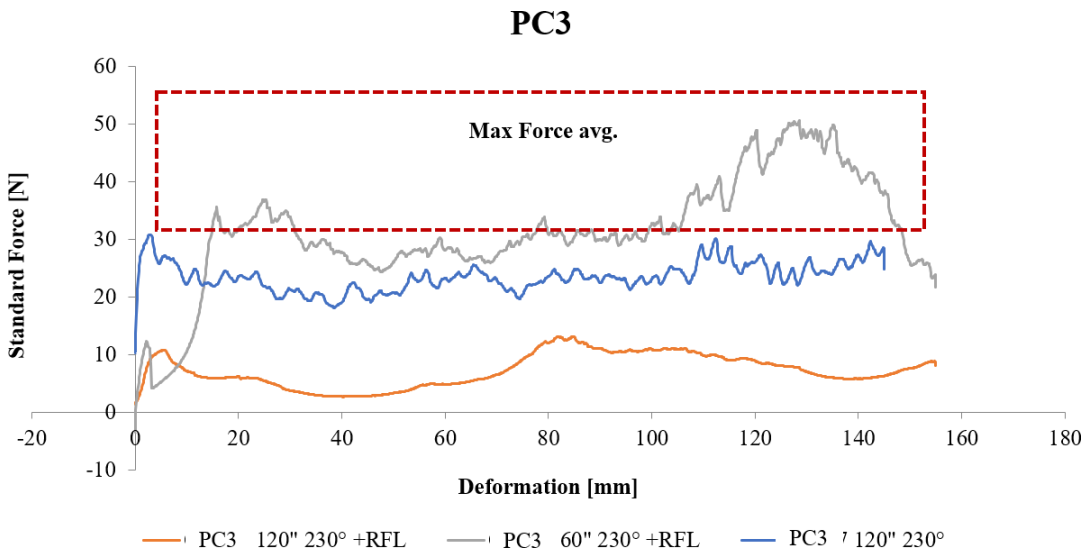

Figure 16 Max Force PC3

The graph in figure 16 is chosen as example to show how the maximum force is identified, the different curves are referred to three different situations tested: coating annealing, application of RFL warmed for 60 s and application of RFL warmed for 120 s. The results of the adhesion test are collected in two different tables: table 12 contains the force values of the coatings obtained in continuous regime, table 13 contains the force values referred to the coatings obtained in pulsed regime.

Table 12 Peel force of W coatings

	Treatment	Avg F (N)	St. Dev	Range	Max F (N)	St. Dev	Range
PC1	20 W	**26.7**	1.8	9.5	**26.7**	1.8	9.5
PC1	20 W 60" 230° +RFL	**18.3**	3.6	18.1	**incalculable**		
PC1	20 W 120" 230° +RFL	**12.9**	1.2	5.6	**14.1**	0.6	3.0
PC2	50 W	**22.9**	1.9	11.8	**22.9**	1.9	11.8
PC2	50 W 60" 230° +RFL	**25.5**	2.2	11.2	**27.5**	2.0	8.2
PC2	50 W 120" 230° +RFL	**36.9**	4.2	21.9	**42.2**	2.1	12.3
PC3	90 W	**23.1**	1.7	12	**23.9**	1.4	10.5
PC3	90 W 60" 230° +RFL	**33.6**	5.8	26.2	**41.1**	5.1	20.2
PC3	90 W 120" 230° +RFL	**7.3**	2.8	10.3	**incalculable**		
PET	EP.BATH+RFL	**52.9**	4.7	/	**65.2**	4.3	
PET	Untreated	**9.3**	2.3	/	**11.3**	2.9	

Three PET sheets were tested for each treatment. The force values of PC4 and PC5 were incalculable, the adhesion is zero both with the rubber and with the pre-dip, high degrees of 2-iox fragmentation have not good reactivity both with the rubber and with RFL. The coatings obtained in continuous regime (excluding PC4 and PC5) improve the adhesion between the PET sheets untreated and the rubber: PC2 and PC3 seem to have a good reactivity with RFL; PC1 coting gives the best result only with the 2-iox plasma treatment and the annealing. None of the coatings, obtained after a plasma treatment with 2-iox as monomer, has values comparable with the PET sheets treated by the classical way (ep.bath + RFL).

Table 13 Peel force of d.c. coatigns

	Treatment	Avg. F (N)	St. Dev	Range	Max F (N)	St. Dev	Range
PC6	10%	**22.2**	1,4	10.4	**23.4**	1.2	7.9
PC6	10% 60" 230° +RFL	**14.8**	3.0	26.6	**Incalculable**		
PC6	10% 120" 230° +RFL	**18.9**	0.8	5.2	**18.9**	0.8	5.2
PC7	30%	**26.0**	1.5	10.2	**26.3**	1.5	8.3
PC7	30% 60" 230° +RFL	**24.6**	2.5	13.3	**25.9**	2.9	12.9
PC7	30% 120" 230° +RFL	**34.1**	2.2	14.4	**36.3**	1.8	11.3
PC8	50%	**40.5**	2.2	13.1	**42.7**	1.6	8.4
PC8	50% 60" 230° +RFL	**15.3**	2.3	11.2	**17.3**	1.3	7.6
PC8	50% 120" 230° +RFL	**20.4**	1.0	6.6	**20.4**	1.0	6.6
PC9	70%	**36.9**	2.3	18.7	**38.2**	2.0	12.8
PC9	70% 60" 230° +RFL	**27.7**	4.6	28.2	**29.9**	3.4	19.0
PC9	70% 120" 230° +RFL	**29.5**	1.8	12.9	**30.3**	1.2	8.7
PET	EP.BATH+RFL	**52.9**	4.7	/	**65.2**	4.3	
PET	Untreated	**9.3**	2.3	/	**11.3**	2.9	

The coatings obtained in pulsed regime improve the adhesion of the PET with the rubber; the samples tested after 2-iox treatment and the annealing show better results without RFL application compared with the adhesion values of the coatings obtained in continuous regime (table 12). The force value that comes closest to the reference is the PC8 (50 % of d.c.). PC6 has the worst adhesion, low levels of 2-iox fragmentation give low reactivity with the rubber and the adhesive. Plasma coatings in pulsed regime are more promising as adhesive without the using of RFL, for this reason the coatings were investigated more: the adhesion of PC6, PC7, PC8 and PC9 were tested after 2-iox plasma treatment, without the annealing, table 14.

Table 14 Coatings (in pulsed regime) adhesion

	Treatment	Avg. F (N)	St. Dev	Range	Max F (N)	St. Dev	Range
PC6	10%	**19.2**	2.3	5.6	**19.2**	2.3	5.6
PC7	30%	**31.2**	5.1	13.1	**35.6**	3.7	10.1
PC8	50%	**55.3**	5.9	14.2	**61.7**	5.1	12
PC9	70 %	**37.1**	4.8	13.4	**41.3**	6.7	16.3
PET	EP.BATH+RFL	**52.9**	4.7	/	**65.2**	4.3	
PET	Untreated	**9.3**	2.3	/	**11.3**	2.9	

Three sheets were tested for each plasma polymer coating. The adhesion test was performed by tensile tester Zwick z/10, the results show how the coating obtained using 50 % of d.c was the closest value to the sheet treated by chemical treatment (epoxy bath + RFL). After the last peel test (table 14) the PE-CVD parameters to apply to the PET monofilament (target material) were defined:

Pow.: 175 W; D.c.:50 %; tTr.: 20 min; 2-iox (Ø= 3.3 sccm) + Ar (Ø= 2.3 mln/min)

4.8.2 CRA and coverage evaluation

After the definition of the treatment that guaranteed the adhesion, the monofilament of PET (diameter 0.40 mm) was inserted in the reactor in its mold (paragraph 4.2 figure 3) and the material was treated. The adhesion was tested by CRA test (paragraph 4.6.2): the extraction strength was measured by tensile tester Zwick z/10 and the coverage was observed by optical microscopy. In table 15 and in the figure 17 the first CRA result are shown and compared with the untreated PET.

Table 15 CRA results

Materials	Sample	PE-CVD 2-iox		Avg F (N)	Min F (N)	Max F (N)	CRA date	Ageing
PET 0,40 mm	n.t		Avg	4.21	2.15	2.83	17/09/2019	
			St. dev	0.24	0.55	0.82		
PET 0,40 mm	60919	x	Avg	4.77	1.99	2.66	17/09/2019	11 days
			St. dev	0.26	0.24	0.15		
PET 0,40 mm	90919	x	Avg	5.30	3.03	3.75	17/09/2019	8 days
			St. dev	0.28	0.35	0.40		
PET 0,40 mm	120919	x	Avg	6.31	4.84	5.95	17/09/2019	5 days
			St. dev	0.45	1.26	1.36		

(Due to technical times, at the begin, it was not possible to carry out CRA immediately after the test)

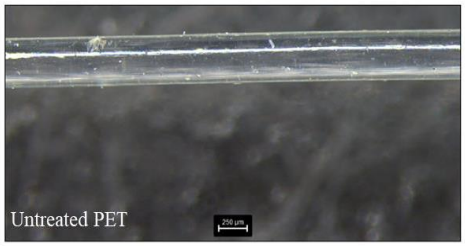

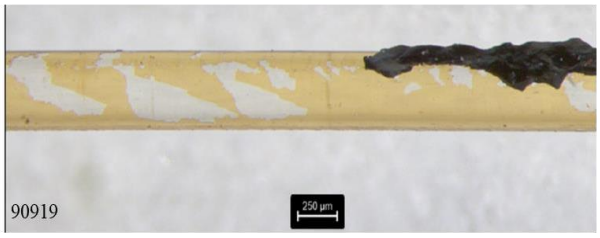

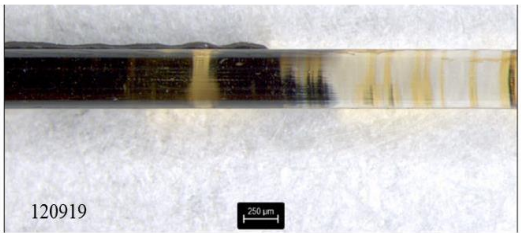

Sample	Coverage
Untreated PET	0
60919	0
90919	1
120919	2

Figure 17 OM and coverage

The treatment improves the extraction strength, even after 11 days the coating has positive effect on the adhesion with the rubber, however the values in Newton decrease as days

go by. The degree of coverage is good only if the CRA is performed earlier than 5 days; thanks to the optical microscope images is possible to observe that the coating was scraped off after the CRA test. In order to avoid the scraping the surface of the PET monofilament was pre-activated, before the PE-CVD with 2-iox as monomer, following two different strategies: Chemical pre-activation and Plasma Argon pre-activation. The chemical pre-activation is operated in Sicrem (Glanzstoff group) using the same epoxy bath (water-soluble polyfunctional epoxies + MDI isocyanate blocked with caprolactam) which is used in the classical treatment with RFL figure 18; the plasma pre-activation was operated in Bicocca laboratories (as the PE-CVD) using a discharge of Argon for 2 minutes using 100 W of power, during this discharge the radical species are formed on the surface, the monofilament pre-activated with argon and treated with 2-iox is shown in figure 19.

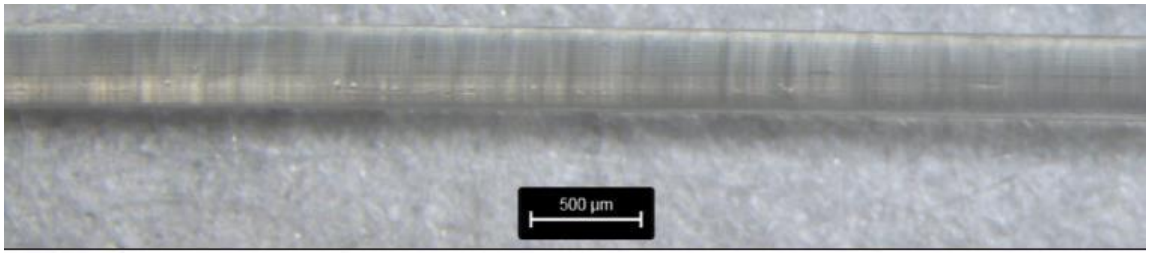

Figure 18 Pre-act. Epoxy

Figure 19 PET mono (0.4 mm) Ar + PE-CVD 2-iox

The surface of the monofilament is completely covered by the coating of 2-iox, the epoxy bath does not appear to completely cover the substrate, but the transparent colour makes the optical evaluation difficult. The sample were vulcanized the same day of the pre-

activation treatments and the CRA test was performed the day before (table 16 and figure 20).

Table 16 pre-activation comparison

Sample	Pre-act		Avg F (N)	Min F (N)	Max F (N)
PET 0.40 mm	**Ar+2-iox**	**Avg.**	**14.3**	**13.5**	**16.1**
		St.dev.	**1.7**	**0.4**	**2.1**
PET 0.40 mm	**Epox+2-iox**	**Avg.-**	**11.0**	**7.8**	**11.8**
		St. dev.	**0.6**	**0.9**	**0.9**

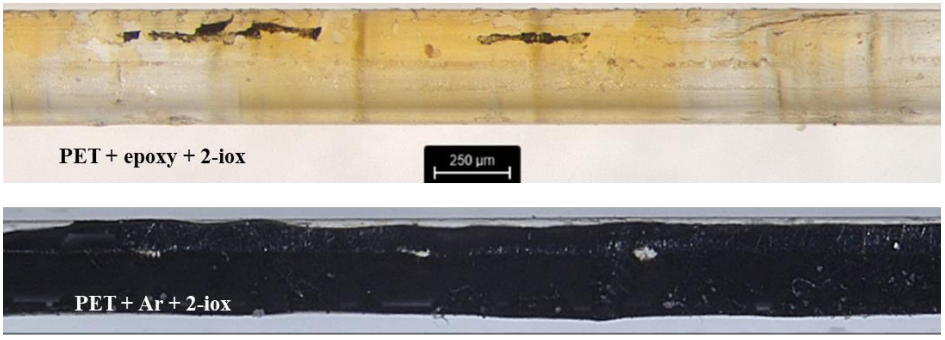

Sample	Coverage
PET + epoxy + 2-iox	0
PET + Ar + 2-iox	4

Figure 20 Coverage evaluation

The obvious difference is due to the pre-activation method, in particular the epoxy bath can't cover uniformly the PET monofilament because the smooth surface of the sample; on other ends after the pre-activation the coating is more stable and more reactive with the rubber during the fragmentation. To compare the PE-CVD deposition with and

without the pre-activation, another CRA test was performed 5 days before the treatment (table 17).

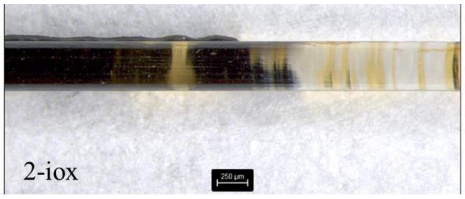

Sample	Treatement		Avg. F (N)	Max F (N)	Min F (N)	Ageing
PET 0.40 mm	2-iox	**Avg.**	6.31	4.84	5.95	5 days
		St.dev	0.45	1.26	1.36	
PET 0.40 mm	Ar+2-iox	**Avg.**	9.07	7.27	9.54	6 days
		St.dev	0,.8	0.65	0.6	

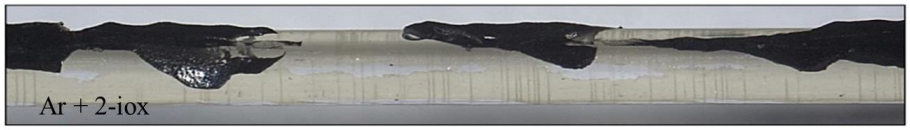

Figure 21 pre-act vs no-act

The results of the CRA indicate that the adhesion of the pre-active PE-CVD coating (table 17) is better, the extraction strength is higher, and the degree of coverage seems similar, but the residues of rubber on the PET monofilament are bigger and more “attached”. The OM images (figure 21) highlight how the pre-activated plasma polymer is more stable than the coating obtained without the Argon pre-activation.

Table 17 Plasma parameter of the alternative treatment

Pre-activation			**PE-CVD**			
W	tT	Gas	W	d.C	tT	Gas
100 W	2 min	Ar	175 W	50 %	20 min	Ar+2-iox

(Ø Ar= 2.3 mln/min; Ø 2-iox= 3.3 sccm)

In order to evaluate how is promising the pre-activated plasma treatment on the PET monofilament cord (table 17), the adhesion test CRA was also performed on the monofilament cord treated by the classical method (epoxy bath + RFL). Before the CRA

test some images, of the dipping on the monofilament, were taken to evaluate the uniformity (figure 22).

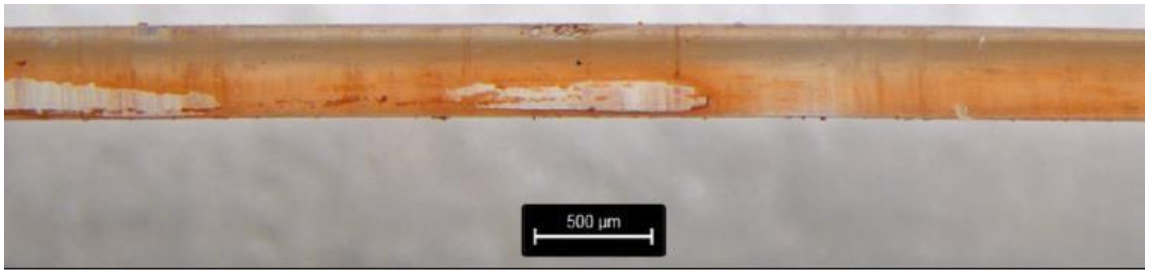

Figure 22 epoxy+RFL dipping on PET monofilament

A PET monofilament covered by the epoxy pre-activator was immersed in a bath of RFL, the distribution of the adhesive is not uniform and compared with the plasma coating (figure 19) the covering is not total. A more complete analysis of the uniformity of two coatings is made in the next paragraph, where the images taken using TEM are collected. The comparison between monoPET + epoxy + RFL and monoPET + Ar + 2-iox PE-CVD is collected and the extraction strength (table 18) and coverage degree (figure 23) are compared.

Table 18 extraction strength comparison

Material	**Treatment**		**Avg. F (N)**	**Max F (N)**	**Min F (N)**
PET 0.40 mm	Ar + 2-iox	Avg	14.3	13.5	16.1
		St.dev	1.7	0.4	2.14
PET 0.40 mm	Epox + RFL	Avg	19.7	16.4	20.0
		St.dev	1.3	1.9	1.9

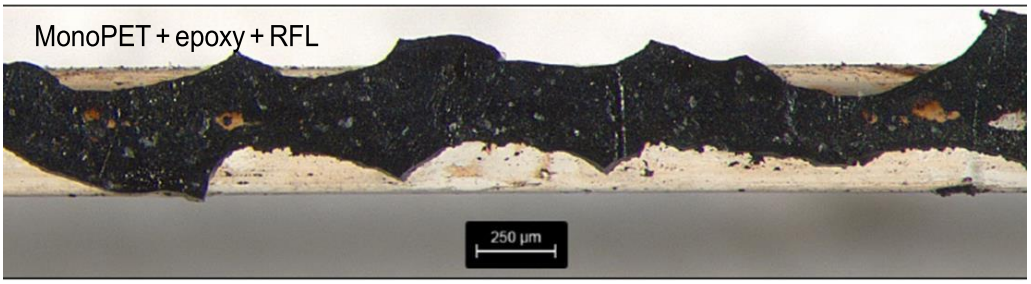

Sample	Coverage
monoPET + Ar + 2-iox	4
monoPET + epoxy + RFL	3

Figure 23 Plasma coating vs RFL coating coverage degree

The extraction force of the sample treated by RFL is higher than that of the sample treated by plasma, but the results are comparable; even the coverage degree is comparable but the coverage of the sample treated with the alternative plasma treatment shows better result. After the extraction the plasma polymer seems more stable in comparison to the RFL system, in this case the covering is more scraped.

4.8.3 TEM

Before to take images using TEM microscopy, the use of SEM microscopy was tried but the compositional contrast it was not detectable (figure 24).

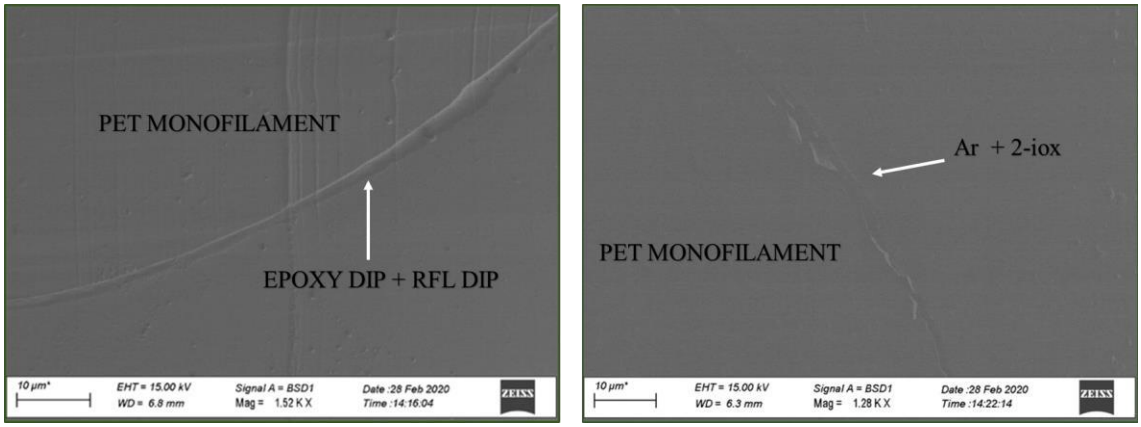

Figure 24 SEM-BSD RFL vs PECVD

The coverings and the monofilament are not distinguishable, but the epoxy + RFL dip seems thicker. To deepen the study TEM images were taken, the "adhesive" and the PET monofilament are recognizable, the measure of the thickness is more precise (figure 25).

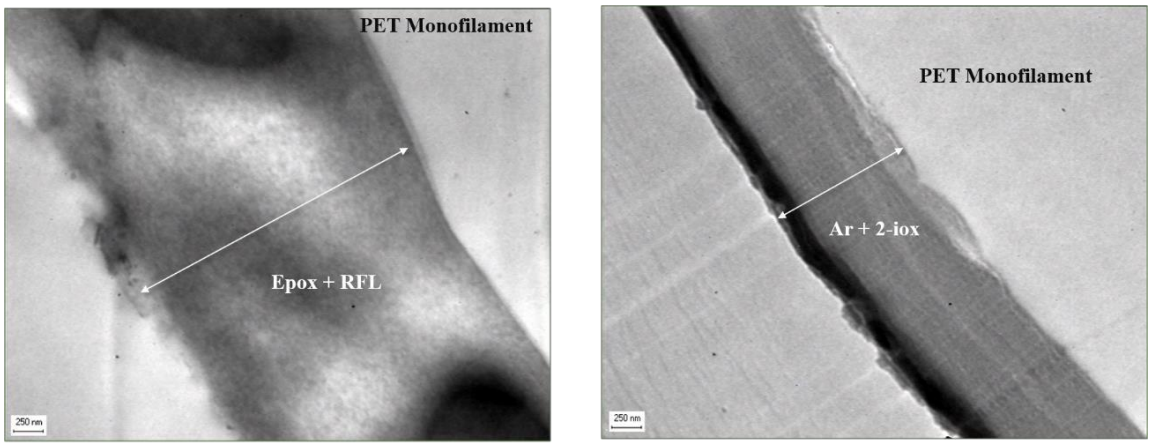

Treatment	Thickness
Epox + RFL	1.1 µm
Ar + 2-iox	1.7 – 2.8 µm

Figure 25 TEM RFL vs PECVD

As how was predicted, the two "adhesives" cover the monofilament in different way, the monofilament covered by the two baths (epoxy and RFL) is not uniform, the thickness is variable between 1.7 µm and 2.8 µ and the sample preparation for the TEM analysis was difficult because the RFL dip makes the filament hard and brittle. The monofilament covered by the plasma polymer, resulting from the Ar pre-activated PE-CVD of 2-iox, is uniform and the thickness of 1.1 µm is constant, the particles on the coating are due to an external contamination.

4.9 Conclusion

In this chapter the aim of the thesis was explained: the goal was to find an alternative method to guarantee the adhesion between a fiber and the rubber matrix. The treatment which is used overall is a chemical treatment with RFL that acts as interface between the reinforcement and the matrix, but the presence of formaldehyde and resorcinol could be restricted in next years due to their toxicity [24]. The real request of the scientific research is to find not only a treatment that gives the same adhesion of the RFL, but this treatment has to be clean. For this reason, the plasma technology was chosen, this technology doesn't need a high quantity of reagents, doesn't need solvent and is performable at room temperature. A plasma treatment could be performed in different condition of pressure, in this work an LPP was chosen, to better control the formation of plasma polymer in different condition, in the reactor a PE-CVD with 2-iox was performed. The resultant coating is deposited on PET monofilament and its adhesion was compared with a PET monofilament treated by a RFL dip, preceded by an epoxy bath using to activate the inert surface of the PET. To find the better plasma parameters, at first different plasma polymer created in different conditions of Power and Duty Cycle was deposited on PET sheets. The surface characterization was carried on the PET sheets; the c.a measurement allowed to understand that already at low Power (20 W) the fragmentation happened, only at low Duty Cycle (10%) the contact angle had values similar to 2-iox not fragmentated. This aspect of this kind of plasma polymer was confirmed by the ATR-IR and XPS characterization. The adhesion was evaluated with a peel test, each sample was tested in different condition (paragraph 4.8.1), the best plasma polymer to guarantee the adhesion was individuated at this condition:

Pow.: 175 W; D.c.:50 %; tTr.: 20 min; 2-iox (Ø= 3.3 sccm) + Ar (Ø= 2.3 mln/min)

The adhesion force of the PE-CVD coating is comparable with the adhesion obtained with the doble baths with epoxy and RFL. At high level of fragmentation, the direct adhesion with the matrix was not good as well as the low level of fragmentation, this means that is more important the plasma polymer structure than the number of functional group present on the surface. The same treatment was applied on the “target material” the PET monofilament; the adhesion was evaluated using a CRA test that indicated that the treatment improves the adhesion of the cord. The more detailed observation highlighted that the plasma coating didn’t cover the surface and its appeared scraped. To improve the stability between the coating and surface two different pre-activation was studied: chemical (epoxy bath) and plasma (100 W for 2’ of Argon). The plasma pre-activation was more efficient as was demonstrated by the values of the extraction force and the degree of coverage. The comparison with the PET monofilament treated by the classical treatment show how the two treatment are comparable and the degree of coverage is higher for the PET monofilament covered by the plasma polymer created in this PhD project. The plasma polymer is obtained using low doses of reagents and without solvent, the treatment was environmentally friendly and guarantees high level of adhesion if compared with the classical treatment use today all over the world.

References

[1] Carlo Gaifami, Polimerizzazione a plasma di 2-etil-2-ossazolina e 2-isopropenil-2-ossazzolina; 2016

[2] Zanini, S., Zoia, L., Della Pergola, R., & Riccardi, C. (2018). Pulsed plasma-polymerized 2-isopropenyl-2-oxazoline coatings: Chemical characterization and reactivity studies. Surface and Coatings Technology, 334, 173–181. https://doi.org/https://doi.org/10.1016/j.surfcoat.2017.11.044

[3] Colombo, A., Tassone, F., Mauri, M., Salerno, D., Delaney, J. K., Palmer, M. R., Rie, R. D. La, & Simonutti, R. (2012). Highly transparent nanocomposite films from water-based poly(2-ethyl-2-oxazoline)/TiO2 dispersions. RSC Advances, 2(16), 6628–6636. https://doi.org/10.1039/C2RA20571H

[4] Judy Chu, James Gregory Gillick, Ohio; The General Tire & Rubber Company, 2004; USOO6703077B1

[5] David B. Wootton, The Application of Textiles in Rubber, 2001, Rapra Technology LTD.

[6] Stefano Zanini, Introduzione alla tecnologia del vuoto; 2015

[7] Biederman, H.: Plasma polymer films. London: Imperial College Press, 2004. ISBN: 1-86094-467-1

[8] Siow, K., Britcher, L., Kumar, S., & Griesser, H.J. (2006). Plasma Methods for the Generation of Chemically Reactive Surfaces for Biomolecule Immobilization and Cell Colonization - A Review. Plasma Processes and Polymers, 3, 392-418.

[9] Bracco, Gianangelo, Holst, Bodil; Surface Science Techniques; Springer 2013, 3-33.

[10] T. Young, Philos. Trans. R. Soc. Lond. 95, 65 (1805)

[11] Stefano Zanini et al 2014 J. Phys. D: Appl. Phys. 47 325202

[12] Olsztyńska-Janus, S., & Czarnecki, M. A. (2020). Effect of elevated temperature and UV radiation on molecular structure of linoleic acid by ATR-IR and two-dimensional correlation spectroscopy. Spectrochimica Acta Part A: Molecular and Biomolecular Spectroscopy, 238, 118436. https://doi.org/https://doi.org/10.1016/j.saa.2020.118436

[13] Vandenbroucke, A. (2015). Abatement of volatile organic compounds by combined use of non-thermal plasma and heterogeneous catalysis.

[14] J.W. Robinson, E.M.S. Frame, G.M. Frame II, "Undergraduate instrumental analysis - Sixth edition", Marcel Dekker, 2005, pag.250, ISBN 0-8247-5359-3

[15] Carlo Gaifami, Modifica della bagnabilità di materiai polimerici mediante trattamenti a plasma; 2014

[16] A.Daccà, G.Gemme, R.Parodi; Tecniche di spettroscopia elettronica per l'analisi di superfici; Istituto nazionale di fisica nucleare 1997

[17] ASTM D1876 - 08(2015)e1; https://www.astm.org/Standards/D1876

[18] David B. Wootton, The Application of Textiles in Rubber, 2001, Rapra Technology LTD.

[19] IUPAC. Compendium of Chemical Terminology, 2nd ed. (the "Gold Book"). Compiled by A. D. McNaught and A. Wilkinson. Blackwell Scientific Publications, Oxford (1997). Online version (2019-) created by S. J. Chalk. ISBN 0-9678550-9-8. https://doi.org/10.1351/goldbook

[20] Savile Bradbury, David C. Joy and Others; Transmission electron microscope; Encyclopædia Britannica, inc.; September 23, 2019

[21] IR Spectrum Table & Chart; https://www.sigmaaldrich.com/technical-documents/articles/biology/ir-spectrum-table.html

[22] Dane K. Parker, Derek Shuttleworth; The Goodyear Tire & Rubber Company, 1996; US5501880

[23] J. Janca, P. Stahel et al.; Plasma Surface Treatment of Polyester Textile Fabrics Used for Reinforcement of Car Tires; Plasmas and Polymers, Vol. 6, Nos. 1/2, June 2001

[24] RAC, European Chemicals Agency (2012); Helsinki, December 2012.

CHAPTER 5

5-PREPARATION OF COMPOSITE MATERIALS REINFROCED WITH NATURAL AND SYNTHETIC FIBERS

In the third year of the Phd the thesis was carried forward at the “Universidad Carlos III de Madrid” in the department of chemical and engineering of materials under the supervision of professor Miguel Angel Martinez Casanova and Doctor Juana Abenojar.

Due to the confidentially reason the work was not focused on the tyre reinforcing material, but on the use of plasma technology, the adhesion and fibers which are three important topics of the thesis. I was integrated in two different works; the projects are focused on the preparation of composite material where the reinforcements were both natural and synthetic fibers and the matrices were biocompatible or biodegradable polymer. The atmospheric pressure plasma and low pressure plasma were performed on the fiber to improve the adhesion with the matrix, the treatments were performed using Atmospheric Pressure Plasma Torch (APPT) and using a plasma generated in a chamber to prevent the fraying of the fibers (LPP). The surface of the fibers was studied after and before the plasma treatment, the contact angle was measured to characterize the materials. Two different equipment were used one "static" and one "dynamic" the wettability was evaluated by placing a drop of different matrices on the different reinforcements. The best treatment condition was found, and the composite materials were prepared using a press. The evaluation of the adhesion was performed also performed on the composite materials by the measure of the tensile properties and the impact test. Due to the COVID-19 emergency the experience was prematurely terminated, not all studies and characterizations were completed. In this chapter are described the fibers and the matrices used, the plasma treatments, the characterization performed and the results

5.1 Fibers as reinforcement

As was described in the paragraph 1.1 a composite material can be reinforced using particles or fibers, in a continuous or discontinuous form. For the preparation of the composite materials carbon and flax fibers were used in form of fabric to reinforce the matrix. Carbon fibers are a middle ground between organic and inorganic fibers, while i.e the glass fibers are completely inorganic, and the flax fibers are natural fibers. The fiber-reinforced composites materials are characterized by a low density, the strength weight ratio and fatigue resistance [1]. In the next paragraphs the different fibers, that were studied and used in the laboratory of the U3CM, are described.

5.1.1 Synthetic fibers

The synthetic fibers used during the experience at "Universidad Carlos III de Madrid" were recycled carbon fibers. Carbon fibers and glass fibers are the most common used

synthetic fibers in the construction of composite materials. The synthetic fiber used in the project is a transition between an organic and inorganic fiber. Carbon fibers (Cf) has reduced price and greater availability, these characteristics make the Cf one of the widely used synthetic fiber [2]. Carbon fibers are made up from the oxidation and pyrolysis of polyacrylonitrile (PAN) which is derivate from the acrylonitrile (figure 1), PAN is heated two times at different temperature to eliminate Hydrogen and to form a derivate with a similar structure of the graphite [3]. Carbon fiber is characterize by high tensile strength (higher than that of Glass fiber) and Young's modulus, moreover this synthetic fiber has high thermal conductivity [5].

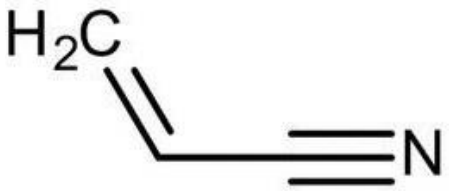

Figure 1 Acrylonitrile

5.1.2 Natural fibers

Natural fibers (NF) are increasingly studied because the attention of the research is now focused on the respect of the environment; the target is to reduce the carbon footprint and the oil-based products as well as a better managing of the waste and the use of low impact material [4]. NF, i.e. Flax Fibers (FF), are also interesting because they own some of the characteristic required by the industry as the lightweight, the lower price, the ease to manufacture, and the availability; for these reasons, from an industrial point of view the NF are good alternative to synthetic fibers [5]. The main drawbacks of the natural fibers concern their heterogeneous composition, because the presence of cavities and defects. The disadvantages of the natural fibers are reflected on their mechanical properties; in general the natural fibers have a higher cellulose content , the flax and hemp are the ones with a higher tensile strength and Young's modulus, between the natural fibers but the cellulose causes an high value of moisture regain [6-7] (table 1). The high level of moisture

regain of the natural fiber has a direct effect on the adhesion with the matrices; for this reason, the surface treatments as plasma treatment are necessary before to build the composite material [8].

Table 1 Mechanical properties of NF [9]

Fiber	Density (g/cm^3)	Elongation (%)	Tensile strength (Mpa)	Young's modulus (Gpa)
Jute	1.3	1.5 – 1.8	393 – 773	26.5
Flax	1.5	2.7 – 3.2	345 – 1035	27.6
Hemp	-	1.6	690	-
Ramie	-	3.6 – 3.8	400 – 938	61.4 – 128
Sisal	1.5	2.0 -2.5	511 - 635	9.4 – 22.0

In the projects the natural fibers which were used was flax fibers. The flax production follows different steps that start with the sowing of the seed and after three months the plant reaches the requested height (80 cm). The flax is pulled out and soaked and then dried for more than one week; the plants are bundled and the fibers are broken down and the final fiber are ready for the use (figure 2).

Figure 2 Flax fibers[9]

The high percentage of cellulose in the flax fibers composition is responsible of the high tensile strength; this fiber doesn't resist at high temperatures and degrades at a temperature above 200 ºC [10], this aspect is crucial to consider in order to choose the matrix. The degradation temperature of the flax fibers suggests that a thermoplastic polymeric matrix is needed for our purpose.

5.2 Matrices

Three different matrices were used during the experience in the U3CM laboratory, all polymers used were thermoplastic. Thermoplastic polymers are formed by linear and non-branching chains, the increasing of the temperature causes the transition to a viscous and mouldable state [11]. In the project titled *"Replacement of carbon fibers by flax fibers in fiber reinforced composites with thermoplastic matrix. Mechanical properties analysis"* the matrix used was a fossil-based product: Polybutylene Succinate (PBS). PBS is considered as bioplastic due to its biodegradability and is synthesised form 1.4-butanediol and succinic acid using a catalyst [12]. The mechanical properties of the PBS are collected in table 2.

Table 2 PBS mechanical properties

	PBS
σ_{max} (MPa)	35-41
Elongation (%)	100-200
Density (g/cm3)	1.26

In the project *"Estudio y ensayo de materiales compuestos de matriz termoplástica reforzada con fibra de carbono reciclada"* two different polyamides were studied as a matrix: Polyamide 11 (PA 11) and Polyamide 12 (PA 12). PA 11 is a thermoplastic material and its environmental impact is low. PA11 is produced from renewable sources (castor oil) and is the only technopolymer that exists in nature The polymer is black and doesn't suffer the effect of the light and the UV. This polyamide is characterized by the resistance against chemical products, high thermal resistance in different condition; the melting point is 189 °C and is density is 1.04 g/cm^3. From the mechanical point of view PA 11 has good elasticity and high impact resistance [13]. PA 12 is produced form the oil [16], its colour is white. The polymer is characterized by good chemical resistance and high stability against the moisture, its melting point is around the 180 °C and the density is 1.02 g/cm^3. PA 12 has high impact resistance [14].

5.3 Replacement of carbon fibers by flax fibers in fiber reinforced composites with thermoplastic matrix. Mechanical properties analysis

The project was born for the necessity to investigate on renewable and recyclable materials in order to fight against the high levels of waste and carbon emission and their impact effect on the environment. The aim of the work is the study and the evaluation of the properties of composite materials, made by PBS matrix and recycled carbon fibers, when some layers of synthetic fibers is replaced by flax fibers. The target is the creation of a composite material environmentally friendly with the similar mechanical properties of the synthetic composite. As was mentioned in the paragraph 5.1.2 the natural fibers do not have good adhesion properties, for this reason an Atmospheric Pressure Plasma Torch (APPT) was performed on the surface of the fibers in order to change the surface energy and the wettability. The surface characteristics were characterized by the measure of the contact angle (C.A.). In order to evaluate the mechanical properties of the composite material, Tensile test, three-point bending test and impact test were performed.

5.3.1 Materials

The recycled Carbon Fibers used in the experiment were provided by Materiales Estructurales Ligeros S.L. (Barcelona, Spain), the fibers was in form of bidirectional fabric. The mass per unit area was of 600 g/m^2; the Flax Fibers was provided by Easy Composites (Staffordshire, United Kingdom) with a weigh of 275 g/m^2 (figure 3).

Figure 3 Flax fibers and carbon fibers

The biodegradable PBS was produced by TNJ Chemical Industry (Hefei, China) from 1.4-butanediol and succinic acid or its anhydride in the presence of a catalyst.

5.3.2 Plasma treatment on flax fibers

The surface of the flax fibers was treated by plasma, the discharge was generated by an Atmospheric Pressure Plasma Torch (Plasma treat GmbH, Steinhgen, Germany) (figure 4). The equipment works at a frequency of 17 kHz and a release tension of 20 kV. The torch rotates at 1900 rpm and the plasma is generated at a pressure of 2 bar; the plasma flow comes out from a hole and hit the sample positioned on a mobile sample holder. The treatment was performed at room temperature with a relative humidity of 35-40%. The parameters that were set in this experiment were the distance between the plasma source and the sample and the speed of the sample holder: the distance was set at 20 mm and the speed at 2.5 m/min.

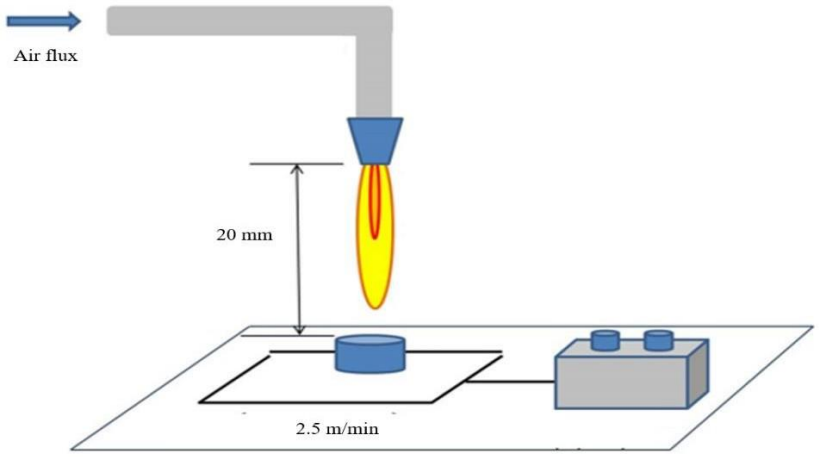

Figure 4 APPT[15]

5.3.3 Surface characterizations

The effect of the plasma treatment on the surface properties was evaluated with the measurement of the C.A (paragraph 4.5.1). The laboratory tools used was a dataphysics OCA15 plus goniometer, the measurement was performed with SCA20 software (DataPhysics Instruments GmbH, Filderstandt, Germany) which permits to quantify the surface energy. The SE was measured before and after plasma treatment, four drops of water, diiodomethane and glycerol (6 µl) were field on the surface and the variation of the Surface energy was calculated by Owens-Wendt-Rable-Kaelble method [16]. The contact angle was measured even between the matrix and the flax fiber, a pellet of PBS was put on the surface and the two phase were inserted in the oven up to the melt of the PBS in order to measure the C.A using the SCA20 software; but the flax absorbed the matrix and the characterization was impossible. To overcome the problem another tool was used for the aim, the C.A of the PBS on the flax fibers was measured by Kruss contact-angle system (GmbH, Germany). The equipment holds an oven and a camera which permits to follow the evolution of the C.A. with the increasing of the temperature.

Two parameters can be set in this equipment: the final temperature (115 °C) and the heating rate (5 °C/min). The characteristic of the carbon fibers permitted to measure the C.A, with the PBS, with the dataphysics OCA15 using SCA20 software. Before the measure the carbon fibers and the PBS were put in a hoven up to melting point of the polymer (155 °C).

5.3.4 Composite preparations

The composite materials were prepared using an equipment which permits to create material sheet at high temperature and high pressure, in this project the PBS sheets were formed by hot plate press FONTUNE PRESSES TP400 s/n P0960010A-02.10/tpb374 (Barendrecht, Netherlands). 20 g of matrix pellets were placed between the two hot presses of the tool for 13 minutes (20 kN), during this period the hot plate press reach the maximum temperature of 130 °C which was chosen in consideration of the degradation of the PBS matrix and the natural fibers of flax. The first step was the preparation of the sheets of PBS, the second step was the assembling of the natural and/or synthetic fibers layers (15x15 cm^2) with the matrix layers, the assembling was performed using the same equipment in the same condition of temperature and pressure. The hot plate press is heated and cooled using water and air (figure 5). To study the effect of the flax fibers on the properties of the composite materials, three different materials were built, these composites differed for the number of natural fibers layers (table 3).

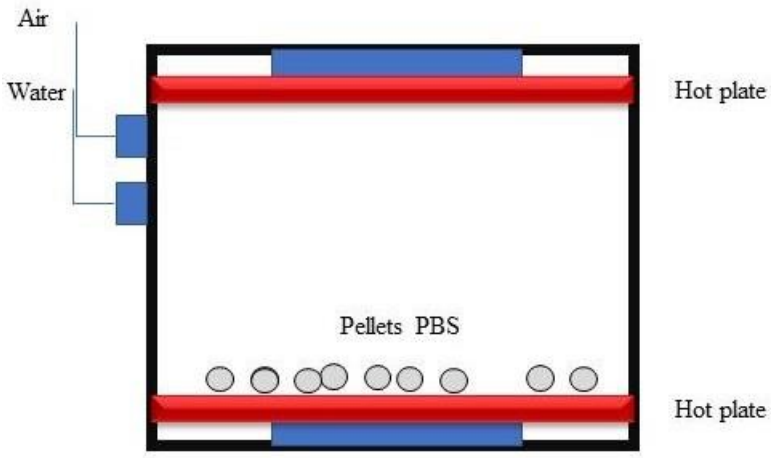

Figure 5 Hot press scheme

Table 3 Three composite materials

Layers n° of Carbon fiber	Layers n° of Flax fiber	Sample
3	0	3cf
2	1	1ff/2ff
2	2	2ff/2cf

(Between every layer of fibers was placed one sheet of PBS)

5.3.5 Tensile and three points bending test

After the creation of the composite materials, samples for the measure of the mechanical properties were prepared cutting a section with a thickness between 1.7 and 2.1 mm and with specific dimension (figure 6).

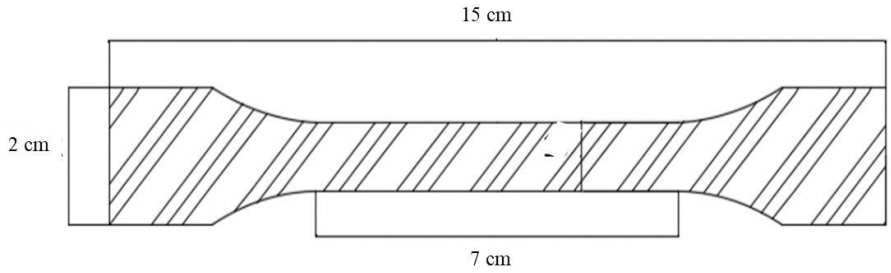

Figure 6 Sample dimension

The tensile and bending test were performed using the same electromechanical test machine Microtest EM2/FR (Madrid, Spain) following the norm UNE-EN ISO 527-1:2012 [17]. The measure of the mechanical properties is possible thanks to a load cell of 50 kN for the tensile test, the samples were blocked in an upper grip and in a lower grip and the sample is pulled using a speed of 5 mm/min until it breaks. The maximum strength is calculated with the equation 5.1.

$$\sigma = \frac{F}{A_0}$$

(Equation 5.1 F is the force and A_0 is the cross section)

For the bending test a 20 kN cell was used and the norm UNE-EN ISO 178:2003 [18] was applicated. The bending happens thanks to three constraints, the samples, of the three different composite materials, used for this test were rectangular dimensioned 80x10 mm and the distance between the three support points was 50 mm (figure 7).

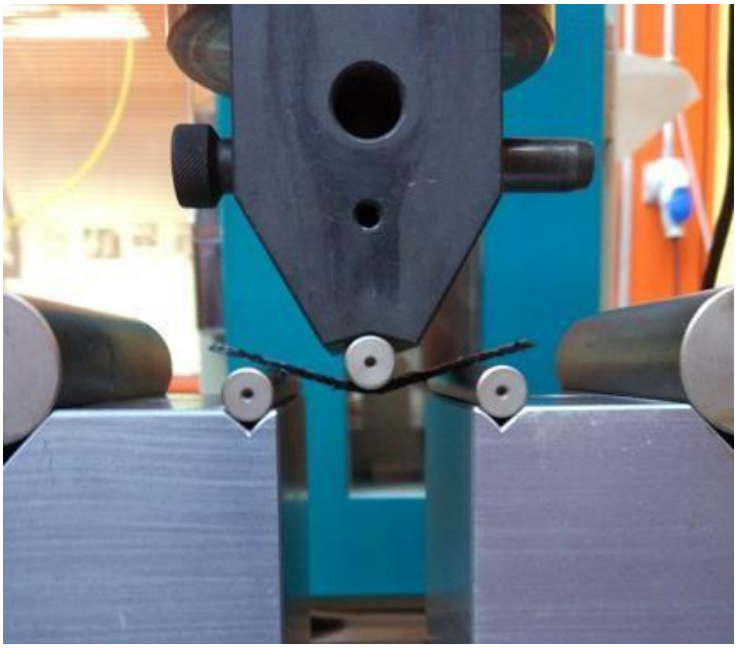

Figure 7 Three points bending test

The stress and elongation were calculated with the equation 5.2 and 5.3.

$$\sigma_f = \frac{3FL}{2bh^2}$$

(Equation 5.2 F is the force, L is the distance between the grips, b is the width, h is the thickness)

$$\varepsilon_f = \frac{6sh}{L^2} 100\ (\%)$$

(Equation 5.3 F is the force, L is the distance between the grips, b is the width, h is the thickness and s is the displacement)

5.3.6 Impact test

A characterization was performed using Charpy pendulum (Instron, Norwood, MA, US), which permits to measure the impact energy. The equipment holds a hammer that impacts the samples when it reaches the lowest point of its trajectory, the energy absorbed by the sample was measured using a pendulum (figure 4). The value of the energy absorbed is obtained from the height at which the pendulum starts its movement and the height which the pendulum reaches after it has impacted the specimen. The height of the pendulum and the weight of the pendulum are used to measure the potential energy, the difference in potential energy of the pendulum, at the start and the end of the test, is the absorbed energy [19].

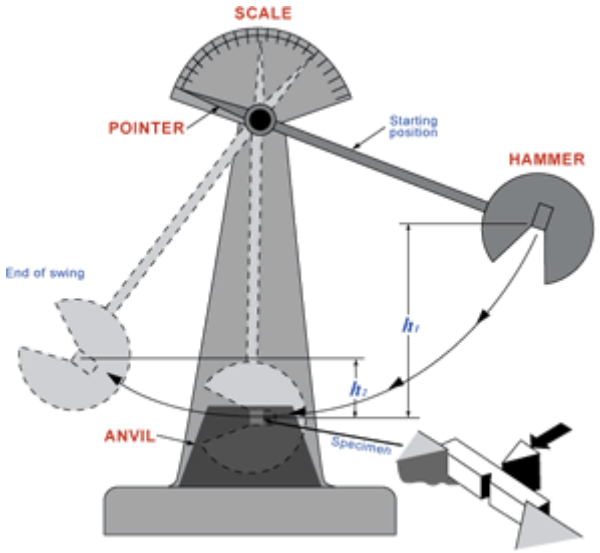

Figure 8 Charpy pendulum[22]

The samples of the composite materials prepared for the impact test measured 80x10 mm, and the test was performed according the ISO 179-A norm [20].

5.3.7 Contact Angle and Surface Energy

Four pellets of PBS matrix were put on a fabric of Carbon fibers, the structure was inserted in oven set at 115 °C, melting point of the matrix, for 45 minutes. After the heating, the fibers and matrix were positioned on the sample holder of the OCA15, the contact angles was measured (figure 9) using the software SCA 20.

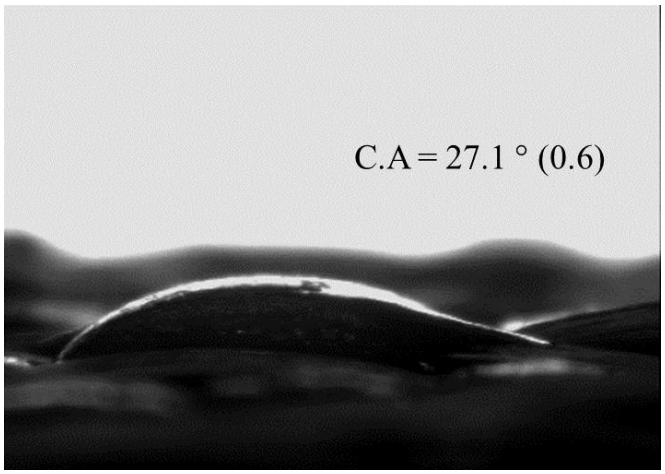

Figure 9 C.A PBS and CF

The "drops" of PBS wet the surface, this means that the matrix has a good ability to adhere with the reinforcement and the surface energy of the CF is pretty high. The contact angle is 27.1 °, the CF had a good reactivity with the PBS because the angle is < 90° (paragraph 4.5.1) and no more treatment are requested to improve the adhesion between the reinforcement and the matrix. The wettability is directly related to the surface energy of the fibers, the higher it is the greater the ability of the "liquid" to adhere [21]. As was mentioned in the paragraph 5.3.3, the wettability between the PBS and flax fibers couldn't measure as for the carbon fiber because the "drops" of PBS penetrated the flax when they reached the melting point. Thanks to Kruss contact-angle system (GmbH, Germany) equipped with oven and a camera, it was possible to measure the C.A and observe the evolution of the wettability from room to melting temperature, using a rate of 5 °C/min

(figure 10). The values of the angles had high standard deviation because the flexion of the fibers with the temperature which complicated the characterization.

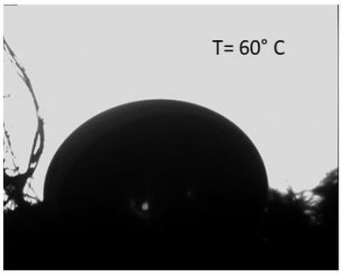

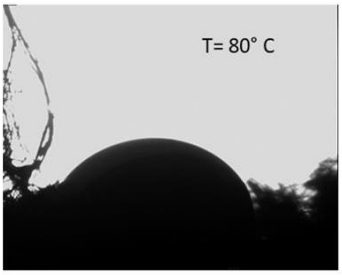

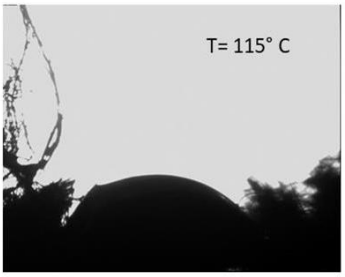

PBS_FF 60 °C	PBS_FF 80 °C	PBS_FF 115 °C
104.8 ° (±2.8)	80.6 (±2.3)	67.5 (±10.6)

Figure 10 C.A PBS and FF

The values of the C.A is the average of four different measurements, the values of the contact angle decrease with the increment of the temperature until to the complete fusion. The values of the contact angle at 115 °C is less than 90° C, the flax fibers were wet by the PBS matrix, but the values is less than that obtained by the measure of the C.A. between the synthetic fibers and the matrix; for this reason, the flax fibers were treated by plasma in order to improve the adhesion. After the APPT treatment, which was performed following the parameters mentioned in the paragraph 5.3.2, the surface energy was measured and compared with the S.E of the natural fibers before the plasma treatment. To evaluate the changes of the surface four drops of water, diiodomethane and glycerol with a volume of 6µl were used to measure the C.A and the different contribution to the SE (table 4 and table 5).

Table 4 C.A of flax fibers after and before APPT

Drop	C.A°	C.A° APPT
Water	123.4 (1.4)	83.5 (0.7)
Diiodomethane	41.5 (4.1)	10.0 (0.5)
Glycerol	114.2 (1.3)	90.1 (2.3)

Table 5 SE after and before APPT

Samples	S.E mN/m	DISP mN/m	POL mN/m
Flax Fabric	44.79	41.74	3.05
Flax Fabric + APPT	30.24	22.71	7.53

The values of the total surface energy decrease after the plasma treatment, this is probably due to removal by the plasma of the finishing treatment that the flax fibers suffered by the producer. The contact angle between the PBS and the plasma treated FF was measured with the same equipment used previously with the same parameters (figure 11).

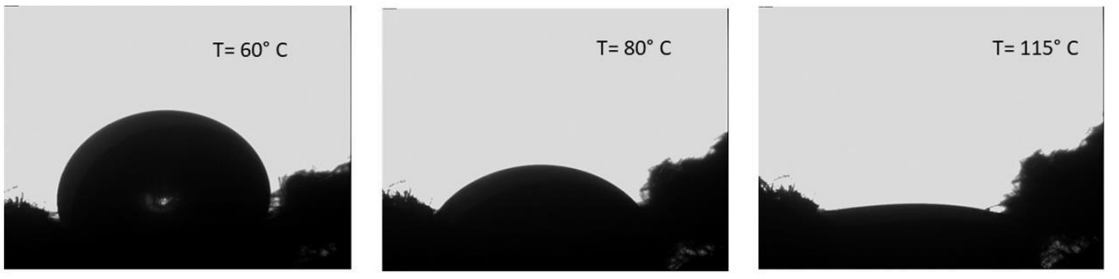

PBS_FF 60 °C	PBS_FF 80 °C	PBS_FF 115 °C
104.9 ° (±1.2)	50.5 (±3.4)	12.4 (±0.1)

Figure 11 C.A PBS and FF

The values of the contact angle between the matrix and the flax fibers indicate that the wettability is improved by the APPT, the grow of the polar contribution to the surface energy contributes to decrease the values of the C.A at 115 °C, << 90°.

5.3.8 Tensile and bending test

The fibers of flax and carbon were weighted before to perform the tensile test, in order to estimate the weight reduction due to the presence of different layers of flax fibers; the thickness was also measured because the tests performed were calculated per unit of area (table 6).

Table 6 Weight and thickness

Fiber	Weight (g/cm^2)	Composite	Thickness (mm)
Flax	0.0274 ± 0.0023	**3cf**	2.0 ± 0.10
Carbon	0.0608 ± 0.0004	**1ff/2cf**	1.7 ± 0.16
		2ff/2cf	2.1 ± 0.08

The composite 2ff/2cf was the thicker because is formed by 4 layers and each layer is separate by matrix layer. The tensile properties were measured as was explained in the paragraph 5.3.5, the test is performed with test machine Microtest EM2/FR (Madrid, Spain) using a load cell of 50 kN with a rate of 5 mm/min. The results of the tensile measurement are presented in the figure 12. The modulus were calculated at 200 MPa.

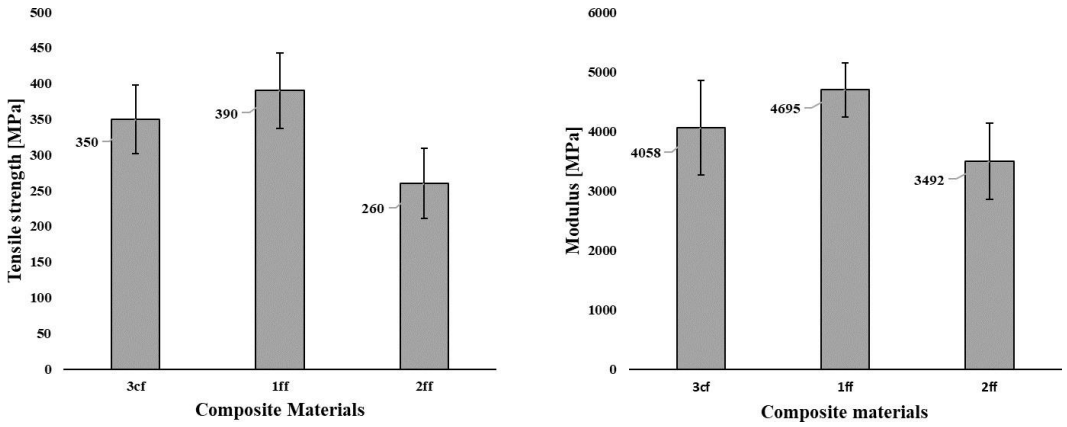

Figure 12 Tensile strength and modulus comparison

The composite material 1ff/2cf has the higher tensile strength and the modulus, is the lightest. The composite 2ff/2cf has the lower values of modulus and strength, is the thickest because is the composite materials with multiple layers of PBS. During the experiment was observed that the matrix broke before the fibers, the tensile strength of the PBS is smaller than that of the fibers. With the same tool the three points bending test was performed, using a load cell of 20 kN and the parameters explained in the paragraph 5.3.5.. The materials weren't break during the test for this reason a deformation of 3.5 %

was chosen to compare the bending strength, in figure 13a the bending strength without fixed deformation is shown and, in the figure, 13b the bending strength with fixed deformation.

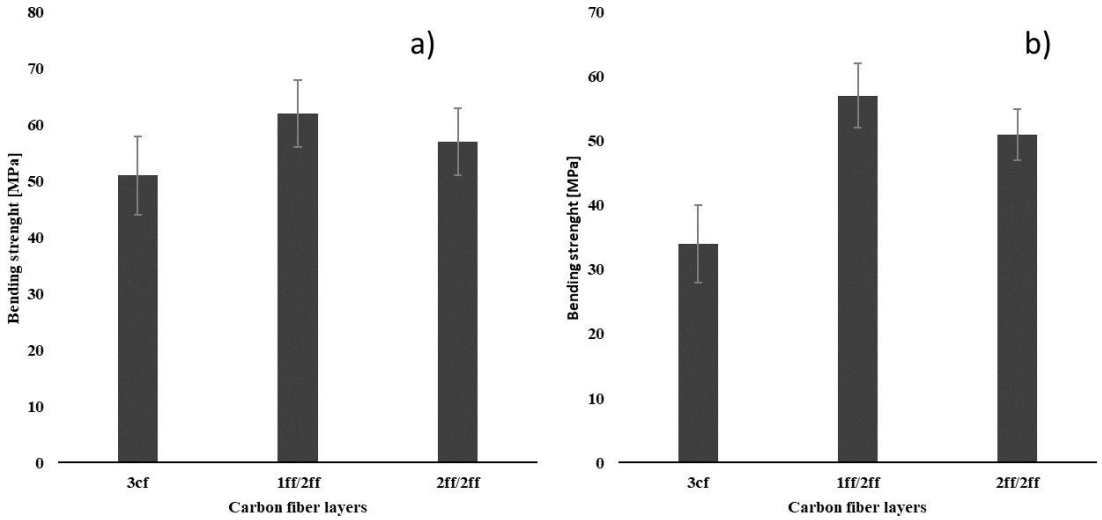

Figure 13 Bending strength

The trend for the two deformation is the same, the flax fibers has an influence on the bending strength. The 1ff/2cf is the composite material with the highest values in MPa, the 3cf and the 2ff/2cf have similar values. The flax fiber instead of one layer of carbon fiber makes that the composite material is more resistant per unit area when the samples suffer a flexion. On the contrary the load per unit area doesn't increase for the 2ff, as could be expected, because not only two layers of natural reinforcement are added but even others matrix layers; the thermoplastic matrix decrease, as mention before, the mechanical strength properties of the composite.

5.3.9 Impact test results

The impact energy was measured with a Charpy pendulum as was described in the paragraph 5.3.6. The graph collects the impact test results, figure 14. The impact energy trend increases with the increment of the natural fiber layers and consequently of the PBS matrix layers. The sample with two layers of flax fiber absorbs more energy per m^2 in comparison to the other; this is due to the fact that the naural fibers are more tenacious

and absorbs more energy, this is confirmed by other experiments that obtained comparable results on hybrid (synthetic and natural reinforcement) composite materials [22-23].

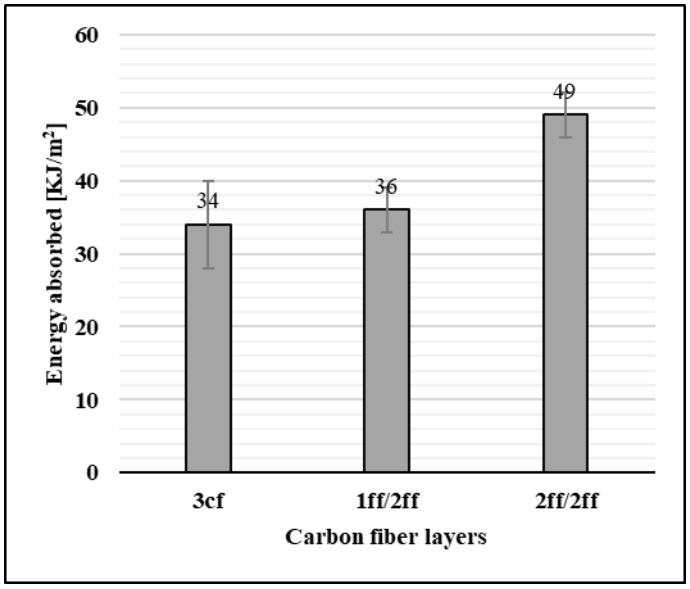

Figure 14 Impact energy absorbed

The substitution of one layer of carbon fibers using two layers of flax fiber improves the values of the impact energy by a 30%.

5.3.10 Conclusion

"Replacement of carbon fibers by flax fibers in fiber reinforced composites with thermoplastic matrix. Mechanical properties analysis" is a project focused on the investigation of different composite materials which were built with different contribution of flax fibers and carbon fibers; the matrix is a thermoplastic polymer: the PBS, a biodegradable matrix. The natural fibers are a good alternative to replace the synthetic fibers, the main advantages are the availability, the price, carbon emissions and recyclability. The plasma technology was used to improve the adhesion between the flax fibers and the matrix, the treatment was performed by APPT. The effectiveness of the treatment was estimated and confirmed by the measure of the

c.a, with a Kruss contact-angle system (GmbH, Germany) equipped with oven and a camera, the C.A. measured after the plasma treatment between the flax fiber and the PBS is << 90°. The measure of the surface energy was performed by the SCA20 software. The plasma treatment didn't increase the total surface energy but removed the finishing treatment that the flax fabric suffered during is production, while the polar contribution increases. After the definition of the plasma treatment, useful for the improvement ofthe adhesion, the three composite materials were built using a FONTUNE PRESSES TP400. One composite is reinforced with three layers of CF separated by matrix layers (3cf), the second composite has instead of one layer of CF one FF layer (1ff/2cf) and the third composite has two layers of FF and two layers of CF (2ff/2cf). The comparison of the composite was made with the measure of some mechanical properties and by the measure of the impact energy absorbed. With the tensile tester and the cell load of 50 kN the maximum strength and the modulus were measured for each composite material, the 1ff/2cf was the composite which has the highest strength and modulus and even the bending test show how the highest bending strength is that of the 1ff/2cf. The presence of the flax fiber improves some mechanical properties of the composite material in comparison to the reference (3cf), but the presence of the flax fibers is balanced by the effect of the PBS layer, in fact the composite material 2ff/2cf does not improve the mechanical properties of the 1 ff/2cf. The impact test highlights how more layers of flax fiber, and PBS matrix, improve the absorbed impact energy of the composite material. The work demonstrates that is possible to prepare a lighter composite material, using natural fibers, i.e. FF, and a biodegradable matrix, i.e. PBS, without compromise the mechanical properties as the maximum strength, the bending strength and the absorbed energy; for these reasons the composite materials proposed in the work are an environmentally friendly option for the applications that needs lightweight and impact resistant materials.

5.4 Study of composite materials with polymer matrix reinforced with recycled carbon fiber

The second project, developed in the U3C de Madrid, was focused on the study of new composite materials that differs for the thermoplastic matrices: PA11 and PA12 (paragraph 5.2). The matrices were reinforced using recycled carbon fibers, these materials were obtained from the Carbodur which is constituted by CF and epoxy; for this

reason, the reinforcement used in the project has epoxy residual. The composite materials were prepared using hot plate press FONTUNE PRESSES TP400. The efficiency of the new composite material was tested using a tensile test; after the traction test was decided to work with PA12 because the matrix is less fragile than the PA11 and the transparent colour allows a better study of the fracture points. The specific research on the composite materials PA12 + CF was performed with the Microtest EM2/FR, the values were collected. During the preparation of the composite materials and the tensile test, the wettability of the polyamides and the CF were studied by the measure of the contact angle (OCA15, paragraph 4.5.1). To improve the adhesion between the reinforcement and the matrix, a plasma treatment in a chamber were performed on the carbon fiber, and a new composite material was prepared to compare it with the untreated PA12 + CF. The treatment performed increases the surface energy, but it was not enough for improve the adhesion and, consequently, the tensile properties. In this project the same tools of the work mentioned in this chapter were used, except for the plasma reactor because the treatment was performed at low pressure Due to the COVID-19 emergency it was not possible to investigate different strategies.

5.4.1 Plasma treatment on carbon fibers

Due to the characteristic of the carbon fibers, which have filaments that could burn during the treatment with APPT, in this project the plasma discharge was generated at low pressure in a chamber. Inside the chamber the sample are placed on the sample holder and the system is sealed ready to be brought in vacuum. A rotary vane pump (paragraph 4.3) is connect to the chamber and generates the vacuum in the reactor to 10^{-5} mbar. When the system reaches the low pressure, atmospheric air is inserted in the system until stabilization at 0.6 mbar, at this pressure the treatment was performed for 1 minute. The chosen gas is air because the presence of species containing oxygen (oxygen, nitrous oxide and water vapour) during the plasma discharge creates new oxygen species that settle on the surface and increase the surface energy [24]. In figure 15 the reactor where the air plasma was generated is schematized, is a Harrick Plasma Cleaner (Ithaca, NY, EE. UU) model PDC-002 (220 V, 50 Hz). The plasma generated in the chamber is a cold plasma and the maximum power of the RF can reach 30 W. The source of plasma is a capacitively coupled plasma (CCP) that exploits the presence of two electrodes.

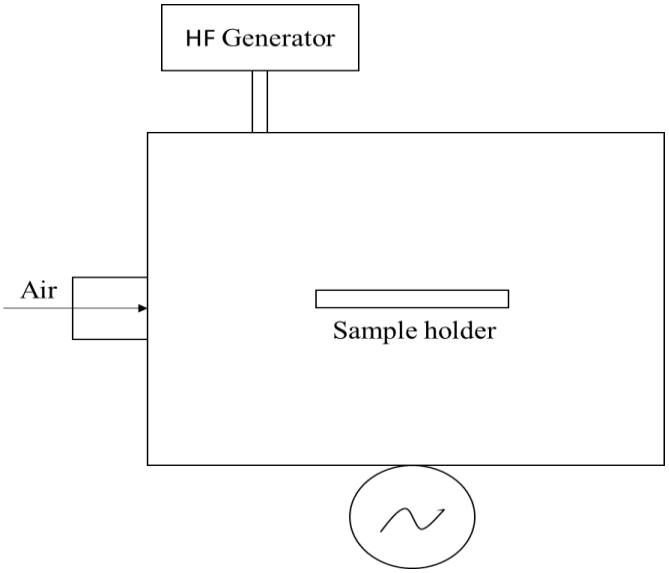

Figure 15 Harrick plasma

5.4.2 Composite materials

The composite materials were prepared using the hot plate FORTUNE PRESS TP400 (paragraph 5.3.4). The first step was the preparation of the sheets of polyamides from pellets of both thermoplastic (figure 16), then the sheets are reinforced with the carbon fibers. Two different cycles of temperature were performed (table 7) depending on the melting point of the two different polyamides: the fusion temperature of PA11 is 189 °C and the fusion temperature of PA12 is 180 °C [13-14]. For the preparation of the polymer sheets the temperature was set higher than the fusion temperature, to be sure the pellets melt.

Figure 16 Pellets of Pa12 in the press

Table 7 Cycles

PA 11			PA 12		
kN	**° C**	**min**	**kN**	**° C**	**min**
0	20	0	0	20	0
20	195	14	20	190	14
20	195	28	20	190	28
0	20	40	0	20	40

Two sheets of both materials were prepared, between the sheets the CF recycled were placed. The fibers, with epoxy residual, were in form of plates but they were cut and disposed in the same direction and arranged in the matrix (figure 17). Then a new cycle for each polyamide were performed and the composite materials were ready (figure 18) to be tested in the tensile tester, the thickness was approximately 2.5 mm.

Figure 17 Composite preparation

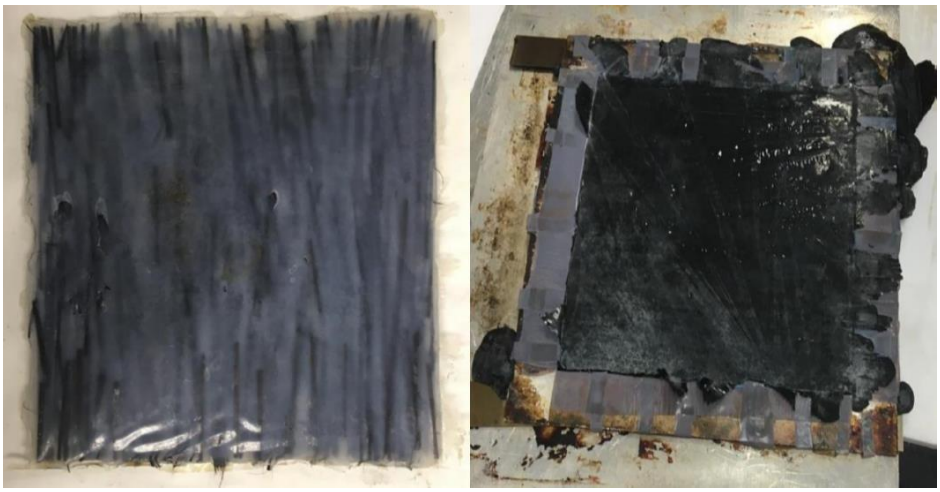

Figure 18 Final products

To evaluate the effect of plasma treatment on the adhesion and the mechanical properties, other composite materials were prepared using plasma treated CF (5.4.1). To study easily the composite reinforced by plasma treated fibers, only PA12 was chosen as a matrix because for its transparency which permits to see were the material breaks.

5.4.3 Contact angle between carbon fibers and polyamides

To evaluate the adhesion between the reinforcement and the matrices the contact angle was measure using OCA15 and the software SCA20. Pellets of the matrices were inserted on the carbon fiber, the structure were put in a preheated oven at the respective melting temperatures -PA11 (189 °C) and PA 12 (180°)- for 45 minutes. For each matrix four pellets were used to measure the C.A (figure 19).

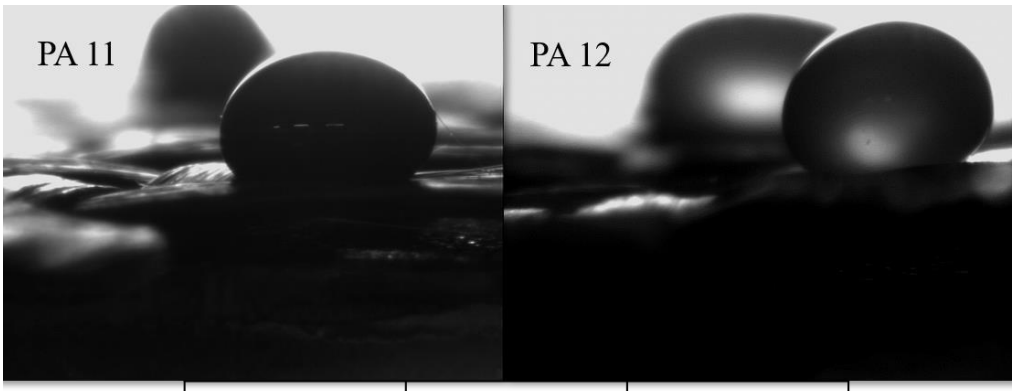

Matrices	C.A. (°)	Dev.st
PA 11	142.2	2.5
PA 12	146.3	4.4

Figure 19 C.A cf with PA11 and PA12

The values collected with the OCA15 indicates how the both matrices do not wet the surface of the carbon fibers, the values of the contact angle are >> 90°, the adhesion between the reinforcement and the polyamides is not good. To investigate the behaviour of the matrix and the CF the Kruss contact-angle system (GmbH, Germany) was used. In the figure 20 the frames shown are referred to PA12.

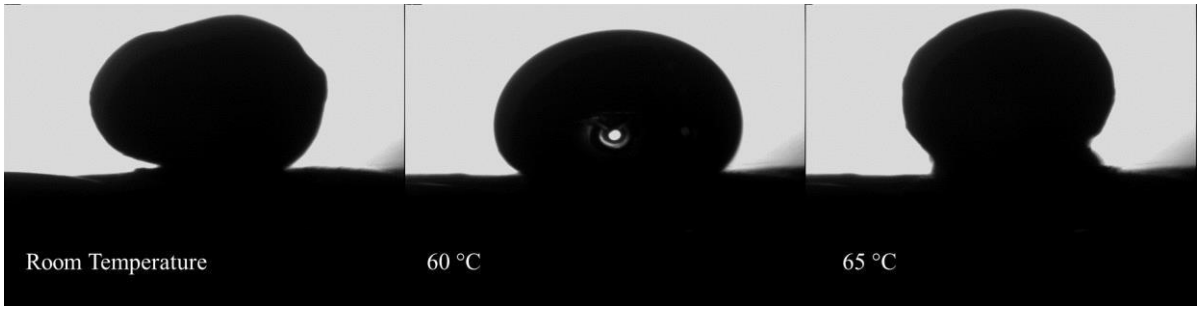

Figure 20 PA12 C.A at different temperature

The different frames are chosen to highlight the behaviour of the thermoplastic matrix that suffers a kind of melt at 60° C which results in a decrease of the C.A, but is evident how the difference of the surface energy of the two materials does not permit the wetting and, at 65°, the contact angle increases again. To improve the surface energy of the carbon fibers, in order to improve the adhesion, plasma treatment was performed (5.4.1). The surface energy was calculated using the by Owens-Wendt-Rable-Kaelble method [16], four drops of water, diiodomethane and glycerol (6 µl) were deposited on the fiber, after and before the LPP, to measure the angle to use for the calculation (table 8 and table 9).

Table 8 CF contact angle after and before LPP

Drop	**C.A°**	**C.A° APPT**
Water	83.4	26.6
Diiodomethane	57.1	11.0
Glycerol	71.2	17.3

Table 9 SE after and before the LPP

Samples	S.E mN/m	DISP mN/m	POL mN/m
Carbon Fiber	22.4	6.1	16.3
Carbon Fiber + LPP	78.0	1.3	77.0

The surface energy increases as the polar contribution, the contact angle was measured again, the value decreases but the wetting still not optimal (figure 21).

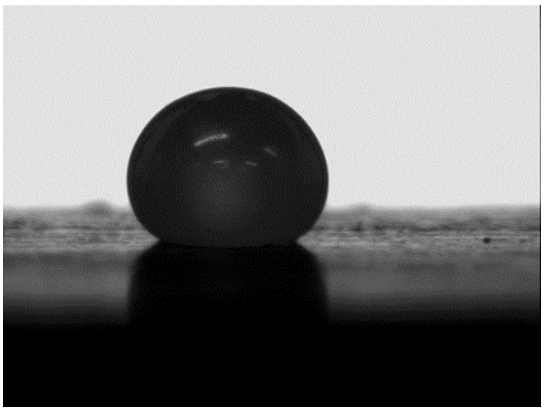

Figure 21 C.A. CF +LPP and PA12

Even if the treatment seems to have no significant effect on the wettability, the composite material with the LPP treated CF was prepared to compare it with the no treated CF PA12 composite material.

5.4.4 Tensile test

The tensile test was performed on different sample (table 10) using the same condition (50 kN, 5 mm/min), the reference were sheets of polyamide 11 and polyamide 12 without the reinforcement but prepared with the same process. For each sample, seven sheets were tested, to prevent the slipping of the composite from the grips sandpaper was placed on the sample (figure 22).

Table 10 Sample for the tensile test

Sample	Matrix	Reinforcement	Plasma
PA11_s	PA11	/	/
PA12_s	PA12	/	/
PA11+CF	PA11	CF	/
PA12+CF	PA12	CF	
PA12+CF_P	PA12	CF	LPP

Figure 22 Sample with sandpaper

The first sample measured was the references (PA11_s and PA12_s) which were compared with the carbon fiber reinforced composite materials (table 11). The samples were compared using the maximum tension (σ_{max} eq 5.2), the deformation (ε eq 5.3) and the elastic modulus:

$$E = \frac{\sigma}{\varepsilon}$$

Equation 5.4

Table 11 Tensile test

Sample	σ_{max} (MPa)	ε (%)	E(GPa)
PA11_s	55.32 ± 23.04	10.29 ± 1.79	0.84 ± 0.28
PA12_s	64.14 ± 4.42	13.72 ± 3.02	0.74 ± 0.06
PA11+CF	28.49 ± 0.06	3.08 ± 0.11	1.33 ± 0.09
PA12+CF	117.5 ± 28.05	7.60 ± 1.18	1.96 ± 1.31

As was expected, the composite materials with PA12 as a matrix, reinforced by the recycled carbon fibers, has a maximum tension strength higher in comparison to the matrix without reinforcement. On the other hand the PA11+CF has no advantages in comparison to the PA11 without reinforcement, this could be due to the colour of the material (black) which doesn't permit to see how the fiber are placed and if some "hole" are present in the composite. The non-uniformity of the material is confirmed how it breaks down (figure 23), there is no fiber in the break point; moreover, the PA11 results more fragile than the PA12 (figure 24) which is ductile. In the figure 24, is it possible to see how the break happens along the fibers: the composite breaks on the polyamide.

Figure 23 PA11+CF

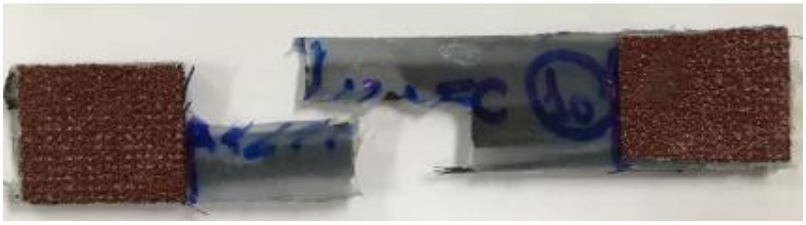

Figure 24 PA12+CF

To prevent the rupture that happens on the matrix, a plasma treatment was performed (5.4.1) to improve the adhesion between the two phases (5.4.3). To evaluate if the treatment was effective on the mechanical properties, the tensile test was performed even on the PA12+CF_P treated as was described (paragraph 5.4.1). The sandpaper was applied to prevent the slipping from the grips, the results are compared with the matrix sheets (PA12) and with the composite reinforced by untreated CF (table 12), for each sample seven sheets were tested.

Table 12 Tensile test PA12

Sample	σ_{max} (MPa)	ε (%)	E(GPa)
PA12_s	64.14 ± 4.42	13.72 ± 3.02	0.74 ± 0.06
PA12+CF	117.5 ± 28.05	7.60 ± 1.18	1.96 ± 1.31
PA12+CF_P	104.88 ± 21.91	7.77 ± 0.32	1.78 ± 0.31

As was expected the plasma treatment does not increase the tensile strength of the composite material, the adhesion between the two phases is not optimal even if the surface energy of the carbon fiber was strongly increased.

5.4.5 SEM

A SEM image of the composite material, with PA12 as a matrix and reinforced by plasma treated CF, was collected thanks to the kindness of U3C de Madrid. In the figure 25 is highlighted how the two phases are not adherent between each other, the analysis with the contact angle was effective as forecasting method.

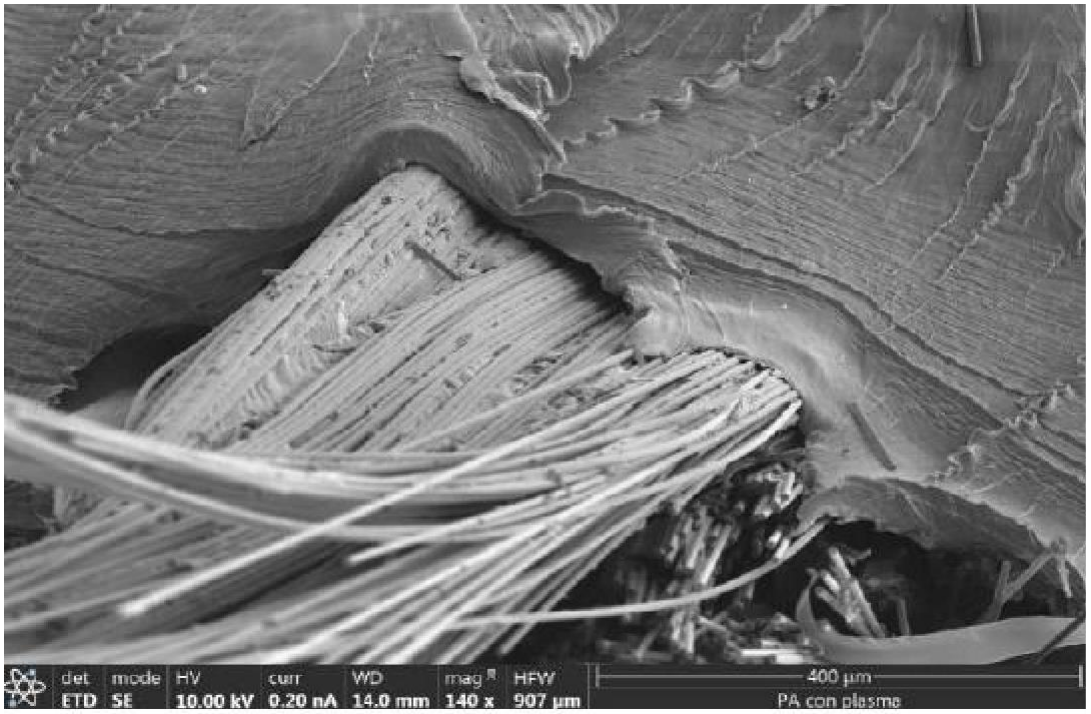

Figure 25 SEM PA12+CF_P

5.4.6 Conclusions

In this project, developed at UC3M, two different thermoplastic matrices were used to build composite materials reinforced by recycled carbon fiber. The polyamides sheets were prepared using the same hot plate press (FONTUNE PRESSES TP400) but with different cycles, the composite materials were prepared with the same press and with the two cycles which differ for the temperature: 195 for PA11 and 190 for the PA12. The reinforcement used in the project were recycled carbon fibers. The tensile properties highlighted how the fibers improve the mechanical properties for the PA12. The sample was broken, the rupture happened on the matrix and along the fiber, this is due to the lower tensile resistance of the PA12 in comparison to the reinforcement, for this reason an LPP treatment was performed on the recycled fibers to increase the adhesion between the CF and the matrix. Before to preparing the new composite material with the treated fibers, the effect of the plasma treatment was estimated by the measure of the surface energy and the measure of the contact angle. The treatment greatly improved the surface energy, but the values of the contact angle between the PA12 and the CF remained greater than 90 °. The high value of the C.A. is due to the high surface energy of the “liquid” phase. To have a good level of the wettability, the surface energy of the solid phase has to be high; in this case the surface energy of the CF was increased but the S.E. of the drop of PA12 remains higher. The composite material with the treated CF and PA12 was

prepared to evaluate if the plasma treatment had any effect and, on the contrary, if the C.A. analysis predicted a situation of no-adhesion between the two phases. As was expected the LPP didn't improve the tensile properties, the SEM image allowed to identify the two different phases and their no- adhesion. For the future development of the project, different conditions of plasma could be tested: the increment of the treatment time and different condition of pressure are explorable strategies, it is also possible to consider another matrix, with lower surface energy. Another promising strategy could be the deposition by PE-CVD of a thin adhesive film.

References

[1] "Types of reinforcements." [Online]. Available: https://ingemecanica.com/tutorialsemanal/tutorialn114.html.

[2] B. D. Agarwal, L. J. Broutman, and K. Chandrashekhara, Analysis and Performance of Fiber Composites Third Edition. 2006.

[3] "How is Carbon Fiber Made?". Zoltek. 2017-08-10. Archived from the original on 2015-03-19.

[4] O. Faruk, A. K. Bledzki, H. P. Fink, and M. Sain, "Progress report on natural fiber reinforced composites," Macromol. Mater. Eng., vol. 299, no. 1, pp. 9–26, 2014

[5] B. D. Agarwal, L. J. Broutman, and K. Chandrashekhara, Analysis and Performance of Fiber Composites Third Edition. 2006.

[6] A. K. Bledzki and J. Gassan, "Composites reinforced with cellulose based fibres," Prog. Polym. Sci., vol. 24, pp. 221–274, 1999.

[7] R. Malkapuram, V. Kumar, and Y. Singh Negi, "Recent development in natural fiber reinforced polypropylene composites," J. Reinf. Plast. Compos., vol. 28, no. 10, pp. 1169–1189, 2009.

[8] T. Khan, M. T. Bin Hameed Sultan, and A. H. Ariffin, "The challenges of natural fiber in manufacturing, material selection, and technology application: A review," J. Reinf. Plast. Compos., vol. 37, no. 11, pp. 770–779, 2018.

[9] http://www.dyeinghousegallery.com/lino-fiore-delicato-si-ricava-una-fibra-tenace/

[10] K. L. Pickering, M. G. A. Efendy, and T. M. Le, "A review of recent developments in natural fibre composites and their mechanical performance," Composites Part A: Applied Science and Manufacturing, vol. 83. pp. 98–112, 2016

[11] Ulf W. Gedde, Polymer physics, Springer, 1995, ISBN 0-412-62640-3.

[12] M. Niaounakis, "1 - Definitions of Terms and Types of Biopolymers," in Biopolymers: Applications and Trends, M. Niaounakis, Ed. Oxford: William Andrew Publishing, 2015, pp. 1–90.

[13] «Plásticos avanzados: PA11 y PA12 para impresión 3D,» Ficeps3. https://ficeps3.com/plasticos-avanzados/.

[14] «TECAMID 12 natural» Ensigner. https://www.ensingerplastics.com/es/semielaborados/plastico/pa12-tecamid-12-natural

[15] M. B. E. Ramos, "Durabilidad y biodeterioro de materiales compuestos de matriz polimerica reforzados con fibras naturales: effecto de tratamiento de plasma" 2018

[16] N. Graupner and J. Müssig, "A comparison of the mechanical characteristics of kenaf and lyocell fibre reinforced poly(lactic acid) (PLA) and poly(3-hydroxybutyrate) (PHB) composites," Compos. Part A Appl. Sci. Manuf., vol. 42, no. 12, pp. 2010–2019, 2011.

[17] "UNE-EN ISO 527-1:2012. 'Plásticos. Determinación de las propiedades en tracción. Parte 1: Principios generales'.," 2012.

[18] "UNE-EN ISO 178:2003. 'Plásticos. Determinación de las propiedades de flexión,'" pp. 0–3, 2003.

[19] "CharpyTester." [Online]. Available: https://www.ndeed.org/EducationResources/CommunityCollege/Materials/Mechanical/ImpactToughness.htm.

.

[21] «Activación con plasma,» Diener. https://www.plasma.com/es/activacion-con-plasma/.

[22] Thermoplastic Composites: Emerging Technology, Uses and Prospects. (2016). http://search.ebscohost.com/login.aspx?direct=true&db=nlebk&AN=1443876&site=eds-live

[23] Z. L. Yan et al., "Reinforcement of polypropylene with hemp fibres," Compos. Part B Eng., vol. 46, pp. 221–226, 2013.

[24] Modification of the PTFE wettability by oxygen plasma treatments: influence of the operating parameters and investigation of the ageing behaviour Stefano Zanini1, Ruggero Barni1, Roberto Della Pergola2 and Claudia Riccardi1 Published 16 July 2014 • © 2014 IOP Publishing Ltd Journal of Physics D: Applied Physics, Volume 47, Number 32

CHAPTER 6

6- GENERAL CONCLUSIONS

The main target of the thesis is the definition of a new environmentally friendly adhesion method to apply on tyre reinforcing materials to guarantee the adhesion to the rubber, efficient adhesion leads to tyre integrity and durability. Nowadays the adhesion between the two phases of the composite materials is allowed by a Resorcinol Formaldehyde Latex (RFL), which acts as interface between the fiber and the compound. The necessary to find an alternative method is due to the toxicity of two components of the RFL system: the Resorcinol and the Formaldehyde. In this thesis plasma technology is chosen as alternative; the creation of plasma in a laboratory permits to perform superficial treatments without the modification of the bulk and doesn't need high doses of reagent and doesn't need solvent, these characteristics make that this technology is considered environmentally friendly.

To find the best plasma treatment to apply to the textile reinforcing materials, the first year was dedicated to the study of the main fibers, used as reinforcements in the tyre, and focused on a bibliography research on the plasma treatments applied on the textile materials. The state of art of the textile materials and their characterizations lead to the creation of new characterization methods for two innovative materials: PET/Aramid commingled yarns and mono/multifilament Nylon cords. A new proceeding for the measurement of the interlacing was defined, the procedure outlines the differences from PET/Aramid commingled yarns built from distinct producers. The most important change in the input was the growth of the trip- force, that permits to count the stronger nodes and the weak nodes which define the interlace. To complete the analysis on the interlace, a number of cords built with different commingling parameters were characterized by a tensile tester in order to study the relationship between the number of nodes and the mechanical properties. The analysis

demonstrates the correlation that the number of nods (interlace) has with the mechanical properties, the overfeeding parameter is the parameters that has maximum impact. The second alternative method proposed is the hysteresis characterization of different nylon cords, which differ for the percentage of monofilament and multifilament. The analysis was performed by a tensile tester, cycles of measure were set with a fix values of elongation and the hysteresis, define as the work loss, was calculated by subtracting from the positive work the negative work. The experiments were performed in three different condition: room temperature, high temperature and on the RFL treated cords at room temperature The no-friction in the 100% monofilament cords permits that the hysteresis of the construction is lower in comparison to the other cords, where the filaments act as constraints.

The study of the fiber, supported by the development of the new characterization methods, and the conclusion of the bibliography research on the plasma treatment, applied to the fibers to improve the adhesion, lead to the preparation of the reactor and the definition of the strategy. Plasma Enhanced Chemical Vapor Deposition was chosen, the interaction between plasma and surface results in a deposition of a plasma polymer on the surface. 2-isoprepenyl-2-oxazoline was the starting monomer, the oxazoline ring and the presence of the doble bond in the isopropenyl group make the molecule reactive with surface and interesting for the high number of functional groups. PET monofilament was chosen as a material to treat, for is peculiar characteristic and its low reactivity. The deposition happened in a vacuum system, continuous plasma and pulsed plasma were tested in the laboratory. At first the plasma polymers were deposited on a PET sheets to facilitate the surface characterization. The measurement of the C.A highlighted how the oxazoline ring was broken even at low values of the power supplied to the system, the retention of the oxazoline ring is verified on the coating obtained at 10% of d.c (175 W). The ATR-IR analysis confirms the conclusion observed by the measure of the wettability, but also informs how in a continuous regime the films were characterized by high number of functional groups. In pulsed system the creation of plasma polymer is more controlled. The peeling test performed on the sheets ends with the definition of the treatment which guarantees adhesion comparable with the classical chemical treatment (RFL system):

Pow.: 175 W; D.c.:50 %; tTr.: 20 min; 2-iox (Ø= 3.3 sccm) + Ar (Ø= 2.3 mln/min)

The results point out how the reaction, between the adhesive and the compound, is more affected by the crosslinking between the plasma polymer (obtained at low level of fragmentation) and the compound. The PE-CVD of 2-isopropenyl-2-oxazoline (2-iox), using the best treatment condition, were replicated on the PET monofilament. The evaluation of the coverage, by optical microscopy after CRA test, highlighted a low stability of the coating with the PET monofilament; in order to increase the stability of the plasma polymer with the surface, different pre-activations were studied. The argon plasma pre-activation permits to improve the stability. The PE-CVD with 2-iox pre-activated by Argon plasma discharge has a coverage degree, on PET monofilament, greater than that measured for the classical chemical method. The studies and the experiments, performed during the PhD, ended with the discovery of a plasma treatment that guaranteed adhesion between PET monofilament reinforcing materials with the rubber. The results are comparable with that obtained by the classical chemical method, the advantage of the plasma technology is the use of low doses of reagent and the non-use of solvent. This environmentally friendly treatment is a valid alternative to the chemical treatment, beacuse the Resorcinol and the Formaldehyde are a dip limit for their toxicity.

The period carried out at the Universidad Carlos III de Madrid was focused, due to confidentially agreement, on the study of composite materials reinforced by synthetic and natural fibers where the plasma was used to improve the adhesion between the reinforcements and the matrix. In the first project the surface energy of a flax fabric was modified by an Atmospheric Pressure Plasma Torch (APPT), even if the surface energy didn’t increase after the APPT, the matrix (poly butyl succinate, PBS) completely wet the natural fiber fabric. Two composite materials, which differ for the number of the layers of flax fiber and PBS, were compared with a carbon fiber reinforced composite material because the aim of the project is the construction of a new lightweight and sustainable composite material that guaranteed the same performance of a synthetic composite. The evaluation was performed by the measurement of some mechanical properties, the presence of the flax fabric instead of the carbon fiber does not affected the mechanical properties but even increase the energy absorbed by the lightweight composite. The second project started with the preparation of two composite materials reinforced by recycled carbon fiber. The two composites differ for the polyamide used as matrix: polyamide 11 (PA11) and polyamide 12 (PA12). The first step was the evaluation of the effective improvement that the reinforcements give to the material, this evaluation was

carried out with the measure of the tensile properties. The PA12 reinforced by carbon fibers had higher maximum tension in comparison to the PA12 not reinforced, the composite broke on the polyamide. The PA11 is to fragile and the colour of the matrix does not permit a complete analysis. To increase the adhesion between the reinforcement and the PA12 a Low-Pressure Plasma (LPP) was performed on the carbon fiber, the LPP increase the surface energy. The LPP treatment change the surface energy but does not increase the wettability, this is due to the high surface energy of the PA12 (liquid phase). The non-effect of the plasma treatment is confirmed by the measure of the tensile properties, no improvement is observed, and the rupture happens on the polyamide 12.

(Due to the Covid-19 emergency the experience at the Universidad Carlos III de Madrid was prematurely interrupted)